

Matter-enhanced transition probabilities in quantum field theory

Kenzo Ishikawa and Yutaka Tobita

*Department of Physics, Faculty of Science,
Hokkaido University, Sapporo 060-0810, Japan*

Abstract

The relativistic quantum field theory is the unique theory that combines the relativity and quantum theory and is invariant under the Poincaré transformation. The ground state, vacuum, is singlet and one particle states are transformed as elements of irreducible representation of the group. The covariant one particles are momentum eigenstates expressed by plane waves and extended in space. Although the S-matrix defined with initial and final states of these states hold the symmetries and are applied to isolated states, out-going states for the amplitude of the event that they are detected at a finite-time interval T in experiments are expressed by microscopic states that they interact with, and are surrounded by matters in detectors and are not plane waves. These matter-induced effects modify the probabilities observed in realistic situations. The transition amplitudes and probabilities of the events are studied with the S-matrix, $S[T]$, that satisfies the boundary condition at T . Using $S[T]$, the finite-size corrections of the form of $1/T$ are found. The corrections to the Fermi's golden rule become larger than the original values in some situations for light particles. They break Lorentz invariance even in high energy region of short de Broglie wave lengths.

arXiv:1206.2593v3 [hep-ph] 7 May 2014

I. INTRODUCTION

In high energy scattering experiments, initial states formed in accelerator are approximately plane waves of finite spatial sizes, and final states identified through their reactions with atoms or nucleus in detector have the microscopic sizes of these objects. Hence the S-matrix for in- or out-going states of wave functions of finite sizes, wave packets, are necessary for the realistic experiments [1, 2]. The ordinary S-matrix is defined at the infinite-time interval, which is denoted by $S[\infty]$, and the total probability from $S[\infty]$ defined with the wave packets agrees with that defined with plane waves. As far as they form complete sets, the probability is unique and independent from the base functions. Computation is easiest with the planes waves. Accordingly, the transition probability at $T = \infty$ has been computed with plane waves, and compared with the experiment. Measurements are made with large-time intervals of macroscopic lengths, which were approximated with ∞ . The approximation was considered very good, because that is much larger than both of de Broglie wave length and Compton wave length, $\frac{\hbar}{p}$ and $\frac{\hbar}{mc}$, for a particle of the mass and momentum m and p . In a previous paper, it was studied if this approximation is always verified using an S-matrix of satisfying boundary conditions at finite-time interval T , denoted as $S[T]$, [3]. It was found that the probabilities of the events that the decay products are detected at T are different from those at $T \rightarrow \infty$ in various situations, and that the deviation is determined by a new length $(\frac{\hbar}{mc}) \times (\frac{E}{mc^2})$, which becomes large for light particles or at high energy. Transition probability P of these events at T then has the form,

$$P = T\Gamma + P^{(d)}, \quad (1)$$

where Γ is computed with Fermi's golden rule and fulfills the conservation law of kinetic energy and Poincaré invariance. Γ from $S[T]$ agrees with that from $S[\infty]$, and for $\Gamma \neq 0$ and $T \rightarrow \infty$, the first term is dominant and the second term is negligible. Now in a situation where the second term is not negligible, P behaves differently. Especially $\Gamma \approx 0$ or $T \leq \tau$, where $\tau = \frac{\hbar}{\Gamma}$ is the average life-time of parent, are such cases. Because the state is described by a superposition of the parent and daughters, they have a finite interaction energy, if they overlap. Then kinetic energy becomes different from that of the initial state. The rate and other physical quantities in this region which have been unclear [4], are affected by $P^{(d)}$. Thus the probability at T deviates from the value at $T = \infty$, which we call a finite-size correction, by an amount that is proportional to $1/T$ in $T < \tau$. The corrections depend on

the particles that are detected, and are large for light particles but small for heavy particles. They were found extremely large in

$$\pi \rightarrow l + \nu, \quad (2)$$

$$\mu \rightarrow e + \gamma, \quad (3)$$

and violate Poincaré invariance [3]. The present paper clarifies the reasons and presents quantitative analysis of the process Eq. (2). The detailed study of process Eq. (3) and others will be given elsewhere.

At $T \leq \tau$, the wave functions of the parent and daughters retain the wave nature of the probability wave, which can not be studied with $S[\infty]$ [4], but with the $S[T]$. $S[T]$ satisfies

$$[S[T], H_0] \neq 0, \quad (4)$$

and couples with the states of non-conserving the kinetic energy. The kinetic-energy conserving states give Γ and non-conserving states give $P^{(d)}$. A state that starts from an eigenstate of H_0 of an eigenvalue E_0 evolves with $H_0 + H_{int}$ to become a superposition of waves of kinetic energies E_β that includes $\omega_\beta = E_\beta - E_0 \neq 0$ at a finite t , which is similar to diffraction of classical wave. The amplitude and probability show a diffraction pattern. Diffraction in classical physics, appears in its intensity in systems of disorder of violating a translational symmetry. Now the diffraction in the probability amplitude is caused by non-constant kinetic energy at a finite time, and appears in the system without disorder even in vacuum, hence depends on the physical constants of Lagrangian. From Eq. (4), $P^{(d)}$ necessarily violates Poincaré invariance.

A complete set of wave functions are necessary to compute the probability correctly. A complete set is constructed with those functions that are translated in space and having position coordinates [5], and the $S[T]$ is formulated as an extension of LSZ [1] formula. LSZ and textbooks on scattering [6–9], quantum field theory including axiomatic field theory [10, 11] have given $S[\infty]$ with the large wave packets in Poincaré invariant manner. These works have solved of obtaining scattering amplitudes in general manners, and proved Poincaré invariance. Finite T corrections are not Poincaré invariant, although the asymptotic values are Poincaré invariant. The infinitely large wave packets combined with Poincaré invariance are not suitable to find if the observed quantities in experiments are subject to the finite-size corrections. So in this paper we do not assume the Poincaré invariance in ad hoc manner but compute the corrections from Schrödinger equation.

Weak decays mainly have been studied with massive particles. For the probabilities of the events that the charged leptons are detected [1, 2, 12–14], theoretical values of decay rates, average life times, and various distributions have agreed with experiments [15]. Thus they do not have finite-size corrections. Neutrinos are extremely light and show large $P^{(d)}$ at near detectors of much shorter distance than the flavor oscillation length. Flavor oscillations are observed at $T \gg \tau$ and are computed with $S[\infty]$. Neutrino's mass squared differences were determined from experiments [16–21] of using neutrinos from the sun, accelerators, reactors, and atmosphere as [22],

$$\Delta m_{21}^2 = m_2^2 - m_1^2 = (7.58_{-0.26}^{+0.22}) \times 10^{-5} \text{ [eV}^2/\text{c}^4], \quad (5)$$

$$|\Delta m_{32}^2| = |m_3^2 - m_2^2| = (2.35_{-0.09}^{+0.12}) \times 10^{-3} \text{ [eV}^2/\text{c}^4], \quad (6)$$

where m_i ($i = 1 - 3$) are mass values. Oscillation experiments are useless for determining absolute masses, and tritium beta decays [23] have been used but an existing upper bound for an effective electron neutrino mass-squared is of the order of 2 [eV²/c⁴]. The mass is 0.3 – 1.3 [eV/c²] from cosmological observations [24]. The neutrino spectrum at $T \leq \tau$ is irrelevant to flavor oscillations due to such small Δm^2 of Eqs. (5) and (6). It will be shown that $P^{(d)}$ is directly connected with the absolute neutrino masses.

$P^{(d)}$ is connected with scattering-into-cones theorem [25]. The amplitude and probability of the event that the particle of a certain momentum is detected at a certain position, \vec{X} , are computed in field theory [3, 5], using the small wave packets. It is found that \vec{X} dependence of the probability per unit time, $C(\vec{X}, \vec{p})$, is written in the form,

$$C^{(0)} + C^{(1)} \frac{2l_0}{|\vec{X} - \vec{X}^{(i)}|}, \text{ for large } |\vec{X} - \vec{X}^{(i)}|, \quad (7)$$

where $\vec{X}^{(i)}$ is the position of the initial state, $C^{(0)}$ and $C^{(1)}$ correspond to Γ and $P^{(d)}$ and

$$l_0 = \left(\frac{2|\vec{p}|\hbar c}{m_o^2} \right). \quad (8)$$

l_0 determines a typical length that the finite-size correction remains and is called a coherence length of the process. For a pion and an electron of energy 1 [GeV], they are

$$l_0^{pion} = \frac{2\hbar c}{0.13^2} [\text{GeV}^{-1}] = 2 \times 10^{-14} [\text{m}], \quad (9)$$

$$l_0^{electron} = \frac{2\hbar c}{0.5^2} [\text{GeV}^{-1}] = 1.6 \times 10^{-9} [\text{m}]. \quad (10)$$

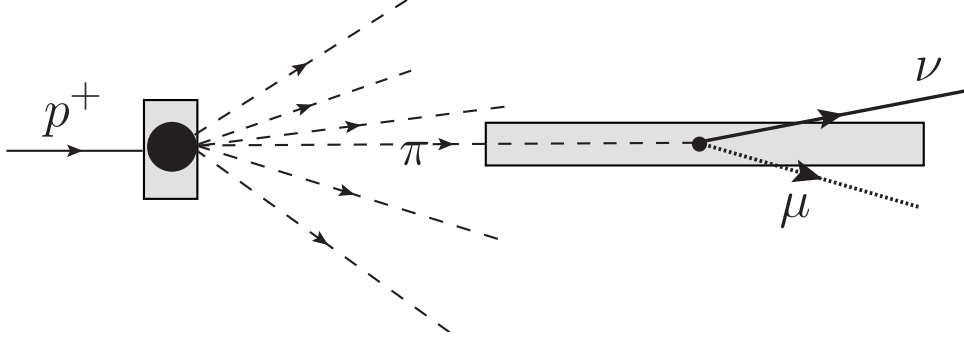


FIG. 1. The whole process in a high-energy neutrino experiment is illustrated. By a collision of a proton with a target, a pion is produced. The pion propagates a macroscopic distance and decays in a decay tunnel. A neutrino is produced and is detected.

Other hadrons are heavier and have shorter lengths than that of the pion. Thus l_0 for hadrons and charged leptons are microscopic lengths. The coherence length for a neutrino of mass 1 [eV/ c^2] and energy 1 [GeV] is

$$l_0^{neutrino} = \frac{2\hbar c}{1^2} \times 10^{18} [\text{GeV}^{-1}] = 10^2 - 10^3 [\text{m}], \quad (11)$$

and is macroscopic length of a few hundred meters. The details of the derivation of Eq. (7) will be presented in Section 5.

In a spatial region where $C(X, \vec{p})$ is independent of \vec{X} , particle-zone, the probability shows particle-like behavior, and its flux follows that of classical particles. The particle is treated as a classical particle of a flux determined by the distribution functions of the decay process. From Eq. (10), ordinary scattering experiments of the charged leptons and hadrons belong the particle-zone, and are treated with the ordinary S-matrix, $S[\infty]$. From the delta function of an energy and momentum conservation, a total probability becomes proportional to T, and the decay rate becomes constant.

Now in the region $|\vec{X} - \vec{X}^{(i)}| \leq l_0$, where $C(X, \vec{p})$ depends on \vec{X} and disagrees with the asymptotic value, the final state behaves like a correlated wave [26].

The whole process expressed in Fig.1 is studied. We study first the probabilities of the events that the pion is detected, and second that of the event that the decay products of the pion are detected, in regions, $|\vec{X} - \vec{X}^{(i)}| < l_0$. A pion has short l_0^{pion} , and retains wave nature only in microscopic region and the ordinary experiments are treated with $S[\infty]$. The neutrino has long $l_0^{neutrino}$, and retains wave nature in a macroscopic region and is treated with $S[\text{T}]$.

The finite-size correction depends on the neutrino energy and size of wave packet, and is not invariant under Lorentz transformation. The large finite-size correction in a macroscopic area can be used to test quantum mechanics and must be included for comparisons of the theory with experiments in this region.

The spectrum of neutrino reveals an unusual macroscopic behavior of an interference pattern determined by the wave function of entire decay process. Quantum mechanics has been verified from many tests with the electron, photon, and other elements and most of them are restricted to microscopic areas. In electron bi-prism experiments by Tonomura et al [27], single quantum interference becomes visible as a total number of events becomes significant. Even though initial electrons are created randomly, a clear single quantum interference is seen when a signal exceeds a statistical fluctuation, and can be used as a new test in macroscopic area.

This paper is organized in the following manner. In section 2, S-matrix of a finite-time interval, $S[\mathbf{T}]$, is introduced. In section 3, pions in hadron reactions are studied. In section 4, we study an amplitude of the event that a neutrino is detected in a pion decay and compute a position-dependent probability in section 5. For a rigorous calculation of the position-dependent probability, a correlation function is introduced. Using an expression with the correlation function and its singular structure at a light-cone region, the finite-size correction is computed in section 6. Implication to neutrino experiments, features of the finite-size corrections, and summary and prospects are given in section 7, 8, and 9. Various properties of wave packets including the size, shape, and completeness are studied in Appendix A.

II. S-MATRIX IN THE OVERLAPPING REGION: $S[\mathbf{T}]$

Poincaré invariant system described by the action integral

$$\mathcal{S} = \int d^4x \mathcal{L}[\varphi(x), \psi(x)] \quad (12)$$

with the Lagrangian density

$$\mathcal{L} = \mathcal{L}_0 + \mathcal{L}_{int}, \quad (13)$$

where \mathcal{L}_0 is a free part and \mathcal{L}_{int} is an interaction part has conserved tensors,

$$\mathcal{T}_{\mu\nu}, M_{\mu\nu\lambda}, \quad (14)$$

$$\partial^\mu \mathcal{T}_{\mu\nu} = 0, \partial^\mu M_{\mu\nu\lambda} = 0, \quad (15)$$

and conserved charges

$$\mathcal{P}_\mu = \int d\vec{x} \mathcal{T}_{0\mu}, \quad (16)$$

$$\mathcal{L}_{\mu\nu} = \int d\vec{x} M_{0\mu\nu}. \quad (17)$$

Thus the physical system is invariant under Poincaré transformation, the symmetry generated by \mathcal{P}_μ and $\mathcal{L}_{\mu\nu}$.

A. Wave function at a finite time

1. Wave functions at a finite time

A time evolution of the state vector $|\Psi(t)\rangle$ is described with H composed of a free and interaction parts, H_0 and H_{int} , derived from \mathcal{L}_0 and \mathcal{L}_{int} of Eq. (13)

$$H = H_0 + H_{int}, \quad (18)$$

as [28, 29],

$$i\frac{\partial}{\partial t}|\Psi(t)\rangle = (H_0 + H_{int})|\Psi(t)\rangle, \quad (19)$$

in a unit of $\hbar = 1$. Unitary operators

$$U(t) = e^{-iHt}, U_0(t) = e^{-iH_0t}, \quad (20)$$

give time evolutions of the state vectors. A state vector in the interaction representation defined by

$$|\tilde{\Psi}(t)\rangle = U_0|\Psi(t)\rangle, \tilde{H}_{int}(t) = U_0(t)H_{int}U_0^\dagger(t), \quad (21)$$

satisfies

$$i\frac{\partial}{\partial t}|\tilde{\Psi}(t)\rangle = \tilde{H}_{int}(t)|\tilde{\Psi}(t)\rangle, \quad (22)$$

and a solution is given by a time-ordered product,

$$|\tilde{\Psi}(t)\rangle = \mathbf{T} \int_0^t dt' e^{\tilde{H}_{int}(t')t'/i} |\Psi(0)\rangle = |\Psi(0)\rangle + \int_0^t dt' \tilde{A}(t') |\Psi(0)\rangle, \quad (23)$$

where

$$\tilde{A}(t') = \tilde{H}_{int}(t')/i + \int_0^{t'} dt'' (\tilde{H}_{int}(t')/i) (\tilde{H}_{int}(t'')/i + \dots). \quad (24)$$

Divergences due to ultraviolet components in higher order corrections are controlled with the methods of Refs. [28, 29]. In the first order in H_{int} and in tree levels, there is no ambiguity in the computations. The solution in the first order is

$$\begin{aligned} |\tilde{\Psi}(t)\rangle &= \left\{ 1 + \int_0^t dt' \tilde{H}_{int}(t')/i \right\} |\Psi(0)\rangle \\ &= |\Psi(0)\rangle + \int d\beta \frac{e^{i\omega t} - 1}{\omega} |\beta\rangle \langle \beta | \tilde{H}_{int}(0) | \Psi(0)\rangle, \end{aligned} \quad (25)$$

where

$$\begin{aligned} H_0 |\Psi(0)\rangle &= E_0 |\Psi(0)\rangle, \quad H_0 |\beta\rangle = E_\beta |\beta\rangle, \\ \omega &= E_\beta - E_0. \end{aligned} \quad (26)$$

At $t \rightarrow \infty$, the formula

$$\frac{e^{i\omega t} - 1}{\omega} = 2ie^{i\frac{\omega t}{2}} \left(\frac{\sin(\omega t/2)}{\omega} \right) \approx 2\pi i \delta(\omega), \quad (27)$$

is substituted into Eq. (25), and the state becomes

$$\begin{aligned} |\tilde{\Psi}(t)_\infty\rangle &= |\Psi(0)\rangle + 2\pi i \int d\beta |\beta\rangle \langle \beta | \tilde{H}_{int}(0) | \Psi(0)\rangle |\delta(E_\beta - E_0)\rangle, \\ H |\tilde{\Psi}(t)\rangle &= E_0 |\Psi(t)\rangle, \\ H_0 |\tilde{\Psi}(t)_\infty\rangle &= E_0 |\Psi(t)_\infty\rangle. \end{aligned} \quad (28)$$

At a finite t , the function has a finite peak at $\omega = 0$ and a tail $\omega \neq 0$.

Thus $E_\beta = E_0$ at $t = \infty$ in Eq. (28) and the kinetic energy is constant, and the physical quantities at the asymptotic regions such as the cross section and decay rate are computed within this space. Now, at a finite t , $E_\beta \neq E_0$ in Eq. (25), and the kinetic energy is not constant, and the state, Eq. (25), is a superposition of waves of different kinetic energies.

A transition rate at a finite T is computed from Eq. (25) [30]. A probability of the event that β is detected is given in the form,

$$|F_{0,\beta}|^2 \frac{4 \sin^2 [(E_\beta - E_0)T/2]}{(E_\beta - E_0)^2}, \quad (29)$$

$$F_{0,\beta} = \langle \beta | \tilde{H}_{int}(0) | \Psi(0) \rangle.$$

For continuous E_β , a formula

$$\lim_{T \rightarrow \infty} \frac{4 \sin^2 [(E_\beta - E_0)T/2]}{(E_\beta - E_0)^2} = \lim_{T \rightarrow \infty} 2\pi T \delta(E_\beta - E_0) \quad (30)$$

is used normally [31, 32]. At a finite T , however, the tail at $|E_\beta - E_0| \neq 0$ gives a correction proportional to $1/T$ [33]. The correction is computed from Eqs. (27) and (30). Taylor expansion of $g(\omega) = |F_{0,\beta}|^2$ leads

$$\int d\omega g(\omega) \left(\frac{2 \sin[\omega T/2]}{\omega} \right)^2$$

$$= 2\pi T g(0) \left\{ 1 + \frac{1}{T} \frac{2g'(0)}{\pi g(0)} \int dx x \left(\frac{2 \sin x}{x} \right)^2 + O(1/T^2) \right\}, \quad (31)$$

and the integral over $x = \frac{\omega T}{2}$ of the second term of the right-hand side in Eq. (31) diverges. So the tail gives the $1/T$ correction of the diverging coefficient. The divergence suggests a proper method is necessary, which we find in the following.

B. Scattering operator of a finite-time interval

The state, Eq. (25), is a superposition of waves of different kinetic energies, so is non-uniform in space. H_{int} which initially makes a transition of a particle to many particles gives an interaction energy at a finite t of Eq. (25). Accordingly, the wave Eq. (25) shows diffraction that is characteristic of a sum of waves of different wave lengths and reveals a position dependent probability. The diffractive pattern depends upon the spectrum and states at all E_β , even though this is the phenomenon of tree level.

1. Boundary conditions

The scattering process of the finite-time interval T is computed with an S-matrix $S[T]$ that satisfies the boundary conditions at T . For a scattering of a scalar field from an initial

state $|\alpha\rangle$ to a final state $|\beta\rangle$, the coefficients $\varphi^f(t)$ [1] given in the form,

$$\varphi^f(t) = i \int d^3x f^*(\vec{x}, t) \overleftrightarrow{\partial}_0 \varphi(\vec{x}, t), \quad (32)$$

and $\varphi_{in}^f(x)$ and $\varphi_{out}^f(x)$ defined in the equivalent manner, where $f(\vec{x}, t)$ is a set of normalized solutions of the free wave equation, are used. Operators, $\varphi(x)$, $\varphi_{in}(x)$, and $\varphi_{out}(x)$ stand interacting and free fields. The boundary conditions

$$\lim_{t \rightarrow -T/2} \langle \alpha | \varphi^f(t) | \beta \rangle = \langle \alpha | \varphi_{in}^f | \beta \rangle, \quad (33)$$

$$\lim_{t \rightarrow +T/2} \langle \alpha | \varphi^f(t) | \beta \rangle = \langle \alpha | \varphi_{out}^f | \beta \rangle. \quad (34)$$

The states $|\alpha\rangle$ and $|\beta\rangle$ are defined with $\varphi_{in}(x)$ and $\varphi_{out}(x)$. Since the wave packets have finite spatial sizes and decrease fast at large $|\vec{x} - \vec{x}_0|$ around a center \vec{x}_0 , they ensure the boundary conditions at a finite T . The complete set formed as

$$f(\vec{x} - \vec{X}, t) = |\vec{p}, \vec{X}, \beta\rangle; \text{ all } \vec{X}, \quad (35)$$

of the center coordinates of position and momentum, although this is not covariant under Poincaré transformation, is used.

A covariant wave packet defined as

$$|\vec{p}, \vec{X}, T; \text{cov.}\rangle = U_L(\Lambda) U_T(\vec{X}, T) |\vec{p} = \vec{0}, \vec{X} = \vec{0}, T = 0; \text{cov.}\rangle, \quad (36)$$

with unitary operators $U_L(\Lambda)$ and $U_T(\vec{X}, T)$ defined from generators $\mathcal{L}_{\mu\nu}$ and \mathcal{P}_μ and c-number values Λ, \vec{X}, T , is not convenient for practical calculation of experimentally observed quantities. This $|\vec{0}, \vec{X}, T; \text{cov.}\rangle$ is located at \vec{X} , and the momentum and position of $|\vec{p}, \vec{X}, T; \text{cov.}\rangle$ are defined by the following Lorentz transformation, and are located at the four-dimensional position

$$X'_i = \Lambda_{i0} T + \Lambda_{ij} X_j, \quad (37)$$

$$T' = \Lambda_{00} T + \Lambda_{0j} X_j, \quad (38)$$

where $\Lambda_{\mu\nu}$ are defined by

$$P'_i = \Lambda_{i0} M + \Lambda_{ij} P_j, \quad (39)$$

and depend on \vec{P} . Thus the positions are changed depending on the momentum.

In experiments, the positions of the events are not measured. The probabilities of the events that the particles are detected within detectors are given normally. These positions are independent from their momenta. Thus the states defined with Eq. (35) are appropriate but those of Eq. (36) are not for those states of the experiments. Equation (35) are used here.

For the large wave packet $\sigma = \infty$, coordinates are un-necessary and $S[\infty]$ is constructed with

$$|\vec{p}; \text{cov.}\rangle = U_L(\Lambda)|\vec{p} = \vec{0}; \text{cov.}\rangle. \quad (40)$$

The positions do not appear, and the position-independent analysis is made with Eq. (40).

2. Properties of $S[T]$

$S[T]$ satisfies various unique properties and is defined by Møller operators, $\Omega_{\pm}(T)$ [34]. $\Omega_{\pm}(T)$ are defined from $U(t)$ and $U_0(t)$ of Eq. (20) in the form

$$\Omega_{\pm}(T) = \lim_{t \rightarrow \mp T/2} U^{\dagger}(t)U_0(t), \quad (41)$$

and satisfy

$$e^{iH\epsilon t}\Omega_{\mp}(T) = \Omega_{\mp}(T \pm \epsilon t)e^{iH_0\epsilon t}. \quad (42)$$

Scattering operator of a finite-time interval T is the product

$$S(T) = \Omega_{-}^{\dagger}(T)\Omega_{+}(T), \quad (43)$$

and satisfies, from Eq. (42),

$$[S(T), H_0] = i \left(\frac{\partial}{\partial T} \Omega_{-}(T) \right)^{\dagger} \Omega_{+}(T) - i \Omega_{-}^{\dagger}(T) \frac{\partial}{\partial T} \Omega_{+}(T). \quad (44)$$

Hence, $S(T)$ does not commute with H_0 and has two components,

$$S[T] = S^{(0)}[\infty] + S^{(1)}[T], \quad (45)$$

where

$$[S^{(0)}[\infty], H_0] = 0, \quad [S^{(1)}[T], H_0] \neq 0. \quad (46)$$

Matrix elements of $S^{(0)}[\infty]$ for the states defined by the boundary conditions Eqs. (32), (33), and (34) are equivalent to those of momentum states,

$$\langle \beta | S^{(0)}[\infty] | \alpha \rangle = \langle \beta | p_f \rangle \langle p_f | S^{(0)}[\infty] | p_i \rangle \langle p_i | \alpha \rangle, \quad (47)$$

$$\langle p_f | S^{(0)}[\infty] | p_i \rangle = \delta_{p_f, p_i} + (2\pi)^4 \delta^{(4)}(p_f - p_i) f_{p_f, p_i}, \quad (48)$$

where $|p_f\rangle$ and $|p_i\rangle$ are initial and final states of plane waves and f_{p_f, p_i} is the matrix element. The matrix element of $S^{(1)}[T]$ is not equivalent to the standard one and written as,

$$\langle \beta | S^{(1)}[T] | \alpha \rangle = \delta f(T). \quad (49)$$

Since the kinetic energy E_β of $S^{(1)}[T]$ is different from that of $S^{(0)}[\infty]$, the total transition probability becomes a sum of T-independent and dependent probabilities. A magnitude of δf depends on a dynamics of the system and satisfies for the states of energies E_α and E_β , $|\alpha\rangle$ and $|\beta\rangle$,

$$(E_\alpha - E_\beta) \langle \beta | S^{(1)}(T) | \alpha \rangle = \langle \beta | O(T) | \alpha \rangle, \quad (50)$$

$$O(T) = i \left(\frac{\partial}{\partial T} \Omega_-(T) \right)^\dagger \Omega_+(T) - i \Omega_-^\dagger \frac{\partial}{\partial T} \Omega_+(T). \quad (51)$$

Hence

$$\delta f(T) = \frac{1}{E_\alpha - E_\beta} \langle \beta | O(T) | \alpha \rangle. \quad (52)$$

We have the probability,

$$P = P^{(0)} + P^{(1)}, \quad (53)$$

$$P^{(0)} = VT(2\pi)^4 \int dp_f \delta^4(p_f - p_i) |f|^2, \quad (54)$$

$$P^{(1)} = \int d\beta |\delta f(T)|^2, \quad (55)$$

and $P^{(1)}$ is written as,

$$\int d\beta |\delta f|^2 = \int d\beta \left(\frac{1}{E_\alpha - E_\beta} \right)^2 |\langle \beta | O(T) | \alpha \rangle|^2 \geq 0, \quad (56)$$

where the equality is satisfied at $T \rightarrow \infty$. Thus $S^{(1)}[T]$ and states of $E_\beta \neq E_0$ give the finite-size corrections of $1/T$.

The whole set of wave packets forms a complete set [5],

$$\sum_{\vec{p}, \vec{X}} |\vec{p}, \vec{X}, \beta\rangle \langle \vec{p}, \vec{X}, \beta| = 1, \quad (57)$$

hence an expectation value of the physical quantity \mathcal{O} ,

$$\sum |\langle \alpha | \mathcal{O} | \vec{p}, \vec{X}, \beta \rangle|^2 \quad (58)$$

is independent of a choice of the set, if the operator is defined uniquely independent of the set. Normal physical quantities of microscopic physics obtained from $S[\infty]$ are independent from the used basis and the probabilities agree. Now $S[\mathbf{T}]$ is defined according to the boundary conditions Eqs. (32), (33), and (34) which depend on the wave packets, and is not independent of the wave packets. Hence the matrix elements of non-invariant component, $S^{(1)}[\mathbf{T}]$, accordingly the probability depend on the choice of the basis, and the finite-size correction depends on the wave packet size σ .

C. Symmetry of $S[\mathbf{T}]$

1. Poincaré invariance

The wave packets reflect the boundary conditions of experiments and are defined in laboratory frame. The wave packet for out-state shows a wave function of minimum physical system which an outgoing particle makes reactions in a detector, and that for in-state shows a wave function of beam. The former part gives data and both are not symmetric. The wave packets, hence, are not necessary Poincaré invariant. Accordingly $S[\mathbf{T}]$ defined with non-invariant wave packets is not Poincaré invariant even in the invariant system.

$S[\infty]$ has no explicit space-time parameter and is manifestly covariant and can be used for computing the asymptotic values. The probability and matrix elements are connected

$$\sum_{f,i} |\langle \vec{p}_f; cov | S[\infty] | \vec{p}_i; cov \rangle|^2 = \sum_{f,i} |\langle \vec{p}_f, \vec{X}_f; \sigma_f | S[\infty] | \vec{p}_i, \vec{X}_i; \sigma_i \rangle|^2, \quad (59)$$

$$\begin{aligned} \langle \vec{p}_f; cov | S[\infty] | \vec{p}_i; cov \rangle &= \langle \vec{p}_f; cov | \vec{p}_f, \vec{X}_f; \sigma_f \rangle \langle \vec{p}_f, \vec{X}_f; \sigma_f | S[\infty] | \vec{p}_i, \vec{X}_i; \sigma_i \rangle \\ &\quad \times \langle \vec{p}_i, \vec{X}_i; \sigma_i | \vec{p}_i; cov \rangle, \end{aligned} \quad (60)$$

$$\begin{aligned} \langle \vec{p}_f, \vec{X}_f; \sigma_f | S[\infty] | \vec{p}_i, \vec{X}_i; \sigma_i \rangle &= \langle \vec{p}_f, \vec{X}_f; \sigma_f | \vec{p}_f; cov \rangle \langle \vec{p}_f; cov | S[\infty] | \vec{p}_i; cov \rangle \\ &\quad \times \langle \vec{p}_i; cov | \vec{p}_i, \vec{X}_i; \sigma_i \rangle, \end{aligned} \quad (61)$$

where the final states are summed over and the same average are taken for the initial states in Eq. (59), from the completeness of the states.

2. Space-time symmetry

The generators of Poincaré transformations

$$\mathcal{P}_\mu (\mathcal{P}_0 = H), \mathcal{L}_{\mu\nu} \quad (62)$$

are conserved charges and $S^{(0)}[\infty]$ satisfy commutation relations

$$[S^{(0)}[\infty], H_0] = 0, [S^{(0)}[\infty], \vec{\mathcal{P}}] = 0, \quad (63)$$

$$[S^{(0)}[\infty], \mathcal{L}_{\mu\nu}] = 0. \quad (64)$$

$S^{(1)}[\mathbb{T}]$, from its definition, Eqs. (45) and (46), satisfy

$$[S^{(1)}[\mathbb{T}], H_0] \neq 0, [S^{(1)}[\mathbb{T}], \vec{\mathcal{P}}] \neq 0, \quad (65)$$

$$[S^{(1)}[\mathbb{T}], \mathcal{L}_{\mu\nu}] \neq 0. \quad (66)$$

$S[\mathbb{T}]$ does not conserve the kinetic energy, momentum, and angular momentum, so shows different properties from those of $S[\infty]$. The finite-size corrections to transition rates are computable with $S[\mathbb{T}]$, but not with $S[\infty]$. They are necessary to find if the experimental values are subject to the finite-size corrections.

Inversion

Space inversion

$$I_{space} : \vec{x} \rightarrow -\vec{x}, \quad (67)$$

and time inversion,

$$I_{time} : t \rightarrow -t \quad (68)$$

are defined at a finite \mathbb{T} . Hence $S[\mathbb{T}]$ of invariant system such as electromagnetic and strong interactions defined in symmetric region of space and time satisfies

$$[S[\mathbb{T}], I_{space}] = 0, [S[\mathbb{T}], I_{time}] = 0. \quad (69)$$

I_{space} is a linear operator and I_{time} is an anti-linear operator.

3. Internal symmetry

Exact symmetry

A charge Q of internal symmetry satisfies

$$[Q, H] = 0, \quad (70)$$

$$[Q, H_0] = 0, \quad (71)$$

and

$$[Q, S(\mathbf{T})] = 0. \quad (72)$$

Hence Q is conserved in $S(\mathbf{T})$, and a state $|\psi\rangle$ and $S[\mathbf{T}]|\psi\rangle$ have a same charge

$$Q|\psi\rangle = q|\psi\rangle, \quad (73)$$

$$QS[\mathbf{T}]|\psi\rangle = qS[\mathbf{T}]|\psi\rangle. \quad (74)$$

If Q is a charge of non-compact group, its eigenvalue

$$Q|q\rangle = q|q\rangle, \quad (75)$$

is continuous and the eigenstates are normalized with Dirac delta function,

$$\langle q_1 | q_2 \rangle = 2\pi\delta(q_1 - q_2). \quad (76)$$

Then the matrix element is written in the diagonal form in q ,

$$\langle q_2 | S[\mathbf{T}] | q_1 \rangle = 2\pi\delta(q_1 - q_2)\tilde{S}[\mathbf{T}](q_1), \quad (77)$$

and the matrix element between any states is written with the reduced matrix $\tilde{S}[\mathbf{T}]$

$$\int dq_2 dq_1 F(q_2) \langle q_2 | S[\mathbf{T}] | q_1 \rangle G(q_1) = 2\pi \int dq_1 F(q_1) \tilde{S}[\mathbf{T}](q_1) G(q_1). \quad (78)$$

Approximate symmetry

For an approximate symmetry of satisfying

$$[S[\mathbf{T}], Q] \neq 0, \quad (79)$$

the finite-size correction is non-invariant. Because the correction depends on the mass, mass difference causes a large symmetry breaking. The masses are very different in neutrinos and charged leptons, hence they have different finite-size corrections.

D. Unitarity

The $S[\mathbb{T}]$ is defined with Møller operators, Eq. (43), and satisfies a unitarity relation,

$$S^\dagger[\mathbb{T}]S[\mathbb{T}] = S[\mathbb{T}]S^\dagger[\mathbb{T}] = 1, \quad (80)$$

and an optical theorem

$$i(\mathcal{T}[\mathbb{T}] - \mathcal{T}[\mathbb{T}]^\dagger) = \mathcal{T}[\mathbb{T}]\mathcal{T}^\dagger[\mathbb{T}], \quad (81)$$

$$S[\mathbb{T}] = 1 + i\mathcal{T}[\mathbb{T}]. \quad (82)$$

The probability is preserved in $S[\mathbb{T}]$ and the imaginary part of the amplitude at \mathbb{T} is determined by the total probability measured at \mathbb{T} .

$S[\mathbb{T}]$ is decomposed into the energy conserving term $\mathcal{T}_1[\mathbb{T}]$ and non-conserving term $\mathcal{T}_2[\mathbb{T}]$

$$S[\mathbb{T}] = 1 + i(\mathcal{T}_1[\mathbb{T}] + \mathcal{T}_2[\mathbb{T}]), \quad (83)$$

then the unitarity Eq. (80) is written in the form,

$$(1 + i(\mathcal{T}_1[\mathbb{T}] + \mathcal{T}_2[\mathbb{T}]))(1 - i(\mathcal{T}_1^\dagger[\mathbb{T}] + \mathcal{T}_2^\dagger[\mathbb{T}])) = 1. \quad (84)$$

Hence we have

$$\begin{aligned} -i(\mathcal{T}_1[\mathbb{T}] - \mathcal{T}_1^\dagger[\mathbb{T}]) - i(\mathcal{T}_2[\mathbb{T}] - \mathcal{T}_2^\dagger[\mathbb{T}]) &= \mathcal{T}_1[\mathbb{T}]\mathcal{T}_1^\dagger[\mathbb{T}] + \mathcal{T}_2[\mathbb{T}]\mathcal{T}_2^\dagger[\mathbb{T}] \\ &\quad + \mathcal{T}_1[\mathbb{T}]\mathcal{T}_2^\dagger[\mathbb{T}] + \mathcal{T}_2[\mathbb{T}]\mathcal{T}_1^\dagger[\mathbb{T}], \end{aligned} \quad (85)$$

and

$$-i(\mathcal{T}_1[\mathbb{T}] - \mathcal{T}_1^\dagger[\mathbb{T}]) = \mathcal{T}_1[\mathbb{T}]\mathcal{T}_1^\dagger[\mathbb{T}], \quad (86)$$

$$-i(\mathcal{T}_2[\mathbb{T}] - \mathcal{T}_2^\dagger[\mathbb{T}]) = \mathcal{T}_2[\mathbb{T}]\mathcal{T}_2^\dagger[\mathbb{T}] + \mathcal{T}_1[\mathbb{T}]\mathcal{T}_2^\dagger[\mathbb{T}] + \mathcal{T}_2[\mathbb{T}]\mathcal{T}_1^\dagger[\mathbb{T}]. \quad (87)$$

The total transition probability from a state α is

$$P = \sum_{E_\beta \approx E_\alpha} |\langle \beta | \mathcal{T}_1 | \alpha \rangle|^2 + \sum_{E_\beta \neq E_\alpha} |\langle \beta | \mathcal{T}_2 | \alpha \rangle|^2, \quad (88)$$

where the energy conserving term is proportional to \mathbb{T} .

It is noted that the unitarity connects physical quantities measured at \mathbb{T} . Optical theorem proves that the imaginary part of forward amplitude at \mathbb{T} is written by the total probability at \mathbb{T} . Hence the life time at \mathbb{T} , depends on \mathbb{T} if the finite-size correction to the total probability is finite. The unitarity does not connect the probability at \mathbb{T} with those at a different \mathbb{T} .

III. PION IN NN COLLISIONS

Applying $S[T]$, we study pions in nucleon reactions in this section. It is found that the finite-size correction is negligibly small because the pion's mass is not small. Iso-triplet pions and doublet nucleons are expressed with fields $\vec{\varphi}(x)$ and $\psi_N(x)$, and this system is described in term of the renormalizable Lagrangian,

$$\mathcal{L} = \bar{\psi}_N(\not{p} - m_N)N + g\bar{\psi}_N\gamma_5\vec{\tau} \cdot \vec{\varphi}(x)\psi_N + \frac{1}{2}(\partial_\mu\vec{\varphi})^2 - \frac{1}{2}m_\pi^2\vec{\varphi}^2(x), \quad (89)$$

where m_N and m_π are masses of the nucleons and pions. A mass difference between a proton and a neutron and that of neutral and charged pions are ignored and $SU(2)$ symmetry is assumed in most places. Second term in the right-hand side shows an interaction between a nucleon and a pion. Due to this interaction, a nucleon emits and absorbs a pion in intermediate states. These physical processes are treated by a renormalization prescription in a nucleon self-energy and others.

A. Relativistic wave packets

Wave packets are normalizable solutions of free wave equations, and those of Dirac equation are similar to that of non-relativistic Schrödinger equation.

1. Nucleon

Plane waves of the Dirac equation,

$$(\not{p} - m_N)\psi_N(x) = 0, \quad (90)$$

are

$$u(p, s)e^{ip \cdot x}; (\bar{u}(p, s_1), u(p, s_2)) = \delta_{s_1 s_2}, \quad (91)$$

$$v(p, s)e^{ip \cdot x}; (\bar{v}(p, s_1), v(p, s_2)) = -\delta_{s_1 s_2}, \quad (92)$$

$$\sum_s u_\alpha(p, s)\bar{u}_\beta(p, s) = \left(\frac{\not{p} + m_N}{2m_N}\right)_{\alpha\beta}, \quad (93)$$

$$\sum_s v_\alpha(p, s)\bar{v}_\beta(p, s) = \left(\frac{\not{p} - m_N}{2m_N}\right)_{\alpha\beta}. \quad (94)$$

The nucleon field operator is expanded with annihilation and creation operators as

$$\psi_N(x) = \sum_i \int \frac{d\vec{p}}{(2\pi)^{\frac{3}{2}}} \left(\frac{m_N}{E(\vec{p})} \right)^{\frac{1}{2}} \{u(p, s)b(\vec{p}, s)e^{-ip \cdot x} + v(p, s)d^\dagger(\vec{p}, s)e^{ip \cdot x}\}, \quad (95)$$

$$\{b(\vec{p}_1, s_1), b^\dagger(\vec{p}_2, s_2)\} = \delta(\vec{p}_1 - \vec{p}_2)\delta_{s_1, s_2}, \quad (96)$$

and one particle states are constructed from creation operators

$$b^\dagger(\vec{p}, i)|0\rangle, \quad (97)$$

$$d^\dagger(\vec{p}, i)|0\rangle. \quad (98)$$

They satisfy

$$\mathcal{P}_\mu b^\dagger(\vec{p}, i)|0\rangle = p_\mu b^\dagger(\vec{p}, i)|0\rangle, \quad (99)$$

$$\mathcal{P}_\mu d^\dagger(\vec{p}, i)|0\rangle = p_\mu d^\dagger(\vec{p}, i)|0\rangle, \quad (100)$$

and are expressed as

$$b^\dagger(\vec{p}, i)|0\rangle = U(\Lambda)b^\dagger(\vec{0}, i)|0\rangle, \quad (101)$$

$$d^\dagger(\vec{p}, i)|0\rangle = U(\Lambda)d^\dagger(\vec{0}, i)|0\rangle, \quad (102)$$

with a unitary operator of transforming the state $\vec{p} = 0$ to that of \vec{p} .

One particle states of wave packets are constructed with c-number functions as

$$|\vec{p}, \vec{X}, \mathbb{T}\rangle = \int d\vec{k} e^{i(\vec{k} \cdot \vec{X} - E(\vec{k})\mathbb{T})} f(\vec{k} - \vec{p}; i) b^\dagger(\vec{k}, i)|0\rangle, \quad (103)$$

$$|\vec{p}', \vec{X}, \mathbb{T}\rangle = \int d\vec{k} e^{i(\vec{k} \cdot \vec{X} - E(\vec{k})\mathbb{T})} g(\vec{k} - \vec{p}'; j) d^\dagger(\vec{k}, j)|0\rangle. \quad (104)$$

The functions Eqs. (103) and (104) satisfy the normalization conditions,

$$\int d\vec{k} f^*(\vec{k}, i) f(\vec{k}, j) = \delta_{i, j}, \quad (105)$$

$$\int d\vec{k} g^*(\vec{k}, i) g(\vec{k}, j) = \delta_{i, j}, \quad (106)$$

and the states form a complete set [5],

$$\begin{aligned} & \int \frac{d\vec{p} d\vec{X}}{(2\pi)^3} |\vec{p}, \vec{X}, \mathbb{T}\rangle \langle \vec{p}, \vec{X}, \mathbb{T}| \\ &= \int d\vec{p} \sum_{i, j} \int d\vec{k} f^*(\vec{k} - \vec{p}; i) f(\vec{k} - \vec{p}; j) b^\dagger(\vec{p}, j)|0\rangle \langle 0| b(\vec{p}, i) \\ &= \sum_i \int d\vec{p} b^\dagger(\vec{p}, i)|0\rangle \langle 0| b(\vec{p}, i) = 1, \end{aligned} \quad (107)$$

within one particle states. Many particle states constructed as direct products of one particle states of wave packets form a complete set.

Invariant wave packets under space-time inversions are expressed by those that satisfy

$$I_{space} : f(\vec{k} - \vec{p}, i) = f(-\vec{k} + \vec{p}, i), \quad (108)$$

$$I_{time} : f(\vec{k} - \vec{p}, i) = f^*(-\vec{k} + \vec{p}, -i). \quad (109)$$

A spin independent Gaussian wave packet,

$$f(\vec{k} - \vec{p}; i) = N e^{-\frac{\sigma}{2}(\vec{k} - \vec{p})^2}, \quad (110)$$

satisfies these conditions and used here. That gives

$$\begin{aligned} \langle 0 | \psi_N(x) | \vec{p}, \vec{X}, T \rangle &= \sum \int \frac{d\vec{p}'}{(2\pi)^{\frac{3}{2}}} \sqrt{\frac{m}{E(\vec{p}')}} e^{i\vec{p}' \cdot x} u(\vec{p}') d\vec{k} f(\vec{k} - \vec{p}) e^{-i\vec{k} \cdot \vec{X}} \delta(\vec{k} - \vec{p}') \\ &= \sum \int \frac{d\vec{p}'}{(2\pi)^{\frac{3}{2}}} \sqrt{\frac{m}{E(\vec{p}')}} e^{i\vec{p}' \cdot (x - X)} u(\vec{p}') f(\vec{p}' - \vec{p}) \\ &\approx \tilde{N} \frac{1}{(2\pi)^{\frac{3}{2}}} \sqrt{\frac{m}{E(\vec{p})}} e^{-\frac{1}{2\sigma}(\vec{x} - \vec{v}(t - T) - \vec{X})^2 + i\vec{p} \cdot (x - X)} u(\vec{p}), \end{aligned} \quad (111)$$

where $\tilde{N} = N(2\pi/\sigma)^{\frac{3}{2}}$. Thus the state is the approximate eigenstate of \mathcal{P}_μ of average value \vec{p} and its center moves with a constant velocity \vec{v} as

$$\vec{x} = \vec{v}(t - T) + \vec{X}, \quad (112)$$

$$\vec{v} = \frac{\vec{p}}{E(\vec{p})}. \quad (113)$$

2. Pion

Klein-Gordon equation,

$$(p^2 - m_\pi^2)\varphi(x) = 0 \quad (114)$$

has solutions

$$e^{i(E(\vec{p})t - \vec{p} \cdot \vec{x})}, \quad E(\vec{p}) = \sqrt{\vec{p}^2 + m_\pi^2}, \quad (115)$$

and the field is expanded as

$$\varphi(x) = \int d\vec{p} \left(\frac{1}{2E(\vec{p})(2\pi)^3} \right)^{\frac{1}{2}} (a(\vec{p})e^{ip \cdot x} + a^\dagger(\vec{p})e^{-ip \cdot x}), \quad (116)$$

$$[a(\vec{p}_1), a^\dagger(\vec{p}_2)] = \delta(\vec{p}_1 - \vec{p}_2). \quad (117)$$

B. Pion emitted from a nucleon

1. Fluctuations

Fluctuations of a relativistic field is expressed by the Green's function $\Delta(x_1 - x_2)$,

$$\Delta(x_1 - x_2) = \frac{1}{(2\pi)^4} \int d^4p e^{ip \cdot (x_1 - x_2)} \frac{1}{p^2 - m^2}, \quad (118)$$

where m is a particle's mass. From the pole of positive frequency, we have a component of on-mass shell waves of positive frequency

$$\Delta_0(x_1 - x_2) = \frac{1}{(2\pi)^3} \int \frac{d\vec{p}}{2E(\vec{p})} e^{ip \cdot (x_1 - x_2)}, \quad E(\vec{p}) = \sqrt{\vec{p}^2 + m^2}. \quad (119)$$

$\Delta_0(x_1 - x_2)$ is composed of a singular part and Bessel functions [35],

$$\Delta_0(x_1 - x_2) = i \left[\frac{1}{4\pi} \delta(\lambda) \epsilon(\delta t) + f_{short} \right], \quad (120)$$

$$f_{short} = - \frac{im}{8\pi\sqrt{-\lambda}} \theta(-\lambda) \left\{ N_1 \left(m\sqrt{-\lambda} \right) - i\epsilon(\delta t) J_1 \left(m\sqrt{-\lambda} \right) \right\} \\ - \theta(\lambda) \frac{im}{4\pi^2\sqrt{\lambda}} K_1 \left(m\sqrt{\lambda} \right), \quad \lambda = (x_1 - x_2)^2, \delta t = \delta x^0, \quad (121)$$

where N_1 , J_1 , and K_1 are Bessel functions. The latter damp or oscillate rapidly and are short range functions of order Compton wave length $L_{cw} = \hbar/(mc)$. $L_{cw} = \hbar/(mc)$ becomes

$$L_{cw} \geq \begin{cases} 2 \times 10^{-15} \text{ [m]} & \text{pion,} \\ 2 \times 10^{-16} \text{ [m]} & \text{proton,} \end{cases} \quad (122)$$

and de Broglie wave length for 1 [GeV/c] is

$$\lambda_{dB} = 2 \times 10^{-16}. \quad (123)$$

Lengths become, 2×10^{-7} [m], 4×10^{-13} [m], and 1×10^{-15} [m] for neutrino ($m_\nu \leq 1\text{eV}/c^2$), electron, and muon, respectively. The first term in the right-hand side of Eq. (120) is called the light-cone singularity and is long-range in $|t_1 - t_2|$ or $|\vec{x}_1 - \vec{x}_2|$. This singularity reflects relativistic invariance, i.e., an energy of a mass m and a momentum \vec{p} is $E(\vec{p}) = \sqrt{\vec{p}^2 + m^2}$ and approaches $E(\vec{p}) \rightarrow |\vec{p}|$ at $|\vec{p}| \rightarrow \infty$. Hence the phase in Eq. (119), $p \cdot (x_1 - x_2)$, cancels at a light-cone, $|t_1 - t_2| = |\vec{x}_1 - \vec{x}_2|$ in the direction \vec{p} then. Consequently the wave becomes singular and real along the light cone.

If m is pure imaginary in Eq. (120), the behaviors at $\lambda > 0$ and $\lambda < 0$ are interchanged, but the light-cone singularity is the same. It is shown that correlation functions of many particle states also have the light-cone singularity.

C. Position-dependent amplitude from $S[\mathbf{T}]$

We study the amplitude of a charged pion produced in a hadron reaction with $S[\mathbf{T}]$. The position-dependent amplitude of a pion is expressed with a wave packet.

A nucleon of a momentum \vec{p}_{N_i} is prepared at time $t = T_{N_i}$, and makes a transition to a pion of average values of the momentum \vec{p}_π at a four dimensional position (T_π, \vec{X}_π) and other particles [5]. The amplitude from this nucleon to a nucleon of \vec{p}_{N_f} and a pion is,

$$\mathcal{M} = \int d^4x \langle N_f, pion | H_{int}(x) | N_i \rangle, \quad H_{int} = g \bar{\psi}_N \gamma_5 \vec{\tau} \cdot \vec{\varphi}(x) \psi_N, \quad (124)$$

where the time and space are integrated over the region $T_{N_i} \leq x^0 \leq T_\pi, X_{N_i}^j \leq x^j \leq X_\pi^j$. The initial and final states are either plane waves or the wave packet,

$$|N_i\rangle = |\vec{p}_{N_i}, T_{N_i}\rangle, \quad |N_f, pion\rangle = |N_f, \vec{p}_{N_f}; pion, \vec{p}_{pion}, \vec{X}_{pion}, T_{pion}\rangle. \quad (125)$$

The matrix elements of these states are defined in the forms,

$$\begin{aligned} \langle \vec{p}_\pi, \vec{X}_\pi, T_\pi | \varphi(x) | 0 \rangle &= N_\pi \rho_\pi \int d\vec{k}_\pi e^{-\frac{\sigma_\pi}{2}(\vec{k}_\pi - \vec{p}_\pi)^2} e^{i(E(\vec{k}_\pi)(t - T_\pi) - i\vec{k}_\pi \cdot (\vec{x} - \vec{X}_\pi))} \\ &\approx N_\pi \rho_\pi \left(\frac{2\pi}{\sigma_\pi} \right)^{\frac{3}{2}} e^{-\frac{1}{2\sigma_\pi}(\vec{x} - \vec{X}_\pi - \vec{v}_\pi(t - T_\pi))^2} e^{i(E(\vec{p}_\pi)(t - T_\pi) - \vec{p}_\pi \cdot (\vec{x} - \vec{X}_\pi))}, \end{aligned} \quad (126)$$

$$\begin{aligned} \langle N_f, \vec{p}_{N_f} | \bar{u}(x) \gamma_5 u(x) | N_i, \vec{p}_{N_i}, T_{N_i} \rangle &= \frac{1}{(2\pi)^3} \left(\frac{m_N}{E(\vec{p}_{N_f})} \right)^{\frac{1}{2}} \left(\frac{m_N}{E(\vec{p}_{N_i})} \right)^{\frac{1}{2}} \frac{1}{\sqrt{V_i}} \\ &\times \bar{u}(\vec{p}_{N_f}) \gamma_5 u(\vec{p}_{N_i}) e^{i((E(\vec{p}_{N_f}) - E(\vec{p}_{N_i}))t - (\vec{p}_{N_f} - \vec{p}_{N_i}) \cdot \vec{x} + E(\vec{p}_{N_i})T_{N_i})}, \end{aligned} \quad (127)$$

where

$$N_\pi = \left(\frac{\sigma_\pi}{\pi} \right)^{\frac{3}{4}}, \quad \rho_\pi = \left(\frac{1}{2E_\pi(2\pi)^3} \right)^{\frac{1}{2}},$$

and V_i is normalization volume for initial state. In this paper, the spinor's normalization is

$$\sum_s u(p, s) \bar{u}(p, s) = \frac{\not{p} + m}{2m}. \quad (128)$$

In the above equation the pion life time is ignored.

Substituting Eqs. (126) and (127), we have the amplitude for the pion detected at the space-time position (\vec{X}_π, T_π) , which satisfies the boundary condition at \mathbf{T} . It is important that the \vec{k}_π was integrated in Eq. (126). If the integration over \vec{x} is made prior to the

integration over \vec{k}_π , the amplitude does not satisfy the boundary condition. That becomes,

$$\begin{aligned}
& N \int dt d\vec{x} d\vec{k}_\pi e^{-i(\vec{p}_{N_i} - \vec{p}_{N_f} - \vec{k}_\pi) \cdot \vec{x}} e^{i(E(\vec{p}_{N_f}) - E(\vec{p}_{N_i}) + E(\vec{k}_\pi))t + iE(\vec{p}_{N_i})T_{N_i}} \\
& \quad \times \bar{u}(\vec{p}_{N_f}) \gamma_5 u(\vec{p}_{N_i}) e^{-\frac{\sigma_\pi}{2}(\vec{k}_\pi - \vec{p}_\pi)^2} e^{-i(E(\vec{k}_\pi)T_\pi - \vec{k}_\pi \cdot \vec{X}_\pi)} \\
& = N \int dt d\vec{k}_\pi (2\pi)^3 \delta_L(\vec{p}_{N_i} - \vec{p}_{N_f} - \vec{k}_\pi) e^{i(E(\vec{p}_{N_f}) - E(\vec{p}_{N_i}) + E(\vec{k}))t + iE(\vec{p}_{N_i})T_{N_i}} \\
& \quad \times \bar{u}(\vec{p}_{N_f}) \gamma_5 u(\vec{p}_{N_i}) e^{-\frac{\sigma_\pi}{2}(\vec{k}_\pi - \vec{p}_\pi)^2} e^{-i(E(\vec{k}_\pi)T_\pi - \vec{k}_\pi \cdot \vec{X}_\pi)}, \tag{129}
\end{aligned}$$

$$N = N_\pi \rho_\pi \left(\frac{m_N}{(2\pi)^3 E(\vec{p}_{N_f})} \frac{m_N}{(2\pi)^3 E(\vec{p}_{N_i})} \frac{1}{\sqrt{V_i}} \right)^{\frac{1}{2}}, \tag{130}$$

where $\delta_L(x)$ is an approximate delta function of a finite size L, where $L = |\vec{X}_\pi - \vec{X}_{N_i}|$. In the above expression, \vec{x} was integrated over whole region at any t , hence Eq. (129) does not satisfy the boundary condition at T. This is not suitable and is not used here. However this amplitude shows some features of the phenomenon, and its feature is analyzed hereafter.

The integrand in Eq. (129) has two stationary momenta, one is that of the real part and the other is that of the imaginary part of the exponent. The stationary momentum from the real part,

$$\vec{k}_\pi = \vec{p}_\pi \tag{131}$$

gives

$$\vec{p}_{N_f} \approx \vec{p}_{N_i} - \vec{p}_\pi, \tag{132}$$

which gives a finite contribution to Eq. (129). The momentum is conserved approximately within uncertainty $1/\sqrt{\sigma_\pi}$, so the probability from this kinematical region is regarded as an energy-conserving term, which agrees with that computed in the standard method of plane waves and asymptotic boundary conditions. Another stationary momentum obtained from the imaginary part of the exponent satisfies

$$\frac{\partial}{\partial \vec{k}_\pi} \xi = 0, \quad \xi = ((E(\vec{p}_{N_f}) - E(\vec{p}_{N_i}) + E(\vec{k}))t - E(\vec{k})T_\pi + \vec{k} \cdot \vec{X}_\pi)|_{\vec{k}=\vec{p}_{N_i}-\vec{p}_{N_f}}, \tag{133}$$

and is important at large $T_\pi - T_{N_i}$ and $|\vec{X}_\pi - \vec{X}_{N_i}|$. The solution is,

$$\vec{v}_{N_f} t - \vec{v}_\pi t + \vec{v}_\pi T_\pi - \vec{X}_\pi = 0, \tag{134}$$

$$\vec{v}_{N_f} = \frac{\vec{p}_{N_f}}{E(\vec{p}_{N_f})}, \quad \vec{v}_\pi = \frac{\vec{p}_{N_i} - \vec{p}_{N_f}}{E(\vec{p}_{N_i} - \vec{p}_{N_f})}, \tag{135}$$

and is determined with the space-time position. The latter gives a new contribution of violating the kinetic-energy conservation. Thus two stationary momenta have different properties.

The first one corresponds to the normal term of Eq. (49) and the second one corresponds to the finite-size correction δf of Eq. (49). The finite-size correction is computed rigorously next.

D. Expressing probability with correlation function

The total probability is expressed in the form

$$P = \int \frac{d\vec{X}_\pi}{(2\pi)^3} d\vec{p}_\pi d\vec{p}_{N_f} |\mathcal{M}|^2 = \int \frac{d\vec{X}_\pi}{(2\pi)^3} \frac{1}{V_i} \frac{1}{E_{N_i}} \frac{1}{(2\pi)^3} \frac{d\vec{p}_\pi}{E_\pi (2\pi)^3} \tilde{P}, \quad (136)$$

$$\tilde{P} = \int dx_1 dx_2 \Delta(x_1, x_2) e^{-\sum_i \frac{1}{2\sigma_\pi} (\vec{x}_i - \vec{X}_\pi - \vec{v}(t_i - T_\pi))^2} e^{iE_\pi(\vec{p}_\pi)(t_1 - t_2) - i\vec{p}_\pi \cdot (\vec{x}_1 - \vec{x}_2)}, \quad (137)$$

where

$$\Delta(x_1, x_2) = \int N d\vec{p}_{N_f} d(\vec{p}_{N_f}, \vec{p}_{N_i}) e^{-i(p_{N_i} - p_{N_f}) \cdot (x_1 - x_2)}, \quad (138)$$

$$d(\vec{p}_{N_f}, \vec{p}_{N_i}) = \frac{1}{2} \sum_{spin} (\bar{u}(\vec{p}_{N_f}) \gamma_5 u(\vec{p}_{N_i}))^* \bar{u}(\vec{p}_{N_f}) \gamma_5 u(\vec{p}_{N_i}), \quad (139)$$

$$N = \frac{m_N^2}{(2\pi)^3 E_{N_f}}. \quad (140)$$

Taking a sum over the final spins and an average over the initial spin, we have

$$d(\vec{p}_{N_i}, \vec{p}_{N_f}) = \frac{p_{N_i} \cdot p_{N_f} + m_N^2}{2m_N^2}, \quad (141)$$

$$\begin{aligned} \Delta(x_1, x_2) &= \frac{1}{(2\pi)^3} \int \frac{d\vec{p}_{N_f}}{E_{N_f}} (m_N^2 + p_{N_i} \cdot p_{N_f}) e^{-i(p_{N_i} - p_{N_f}) \cdot (x_1 - x_2)} \\ &= \int d^4 p \theta(p^0) \text{Im} \left[\frac{1}{p^2 - m_N^2 + i\epsilon} \right] (m_N^2 + p_{N_i} \cdot p) e^{-i(p_{N_i} - p) \cdot (x_1 - x_2)} \\ &= e^{-ip_{N_i} \cdot (x_1 - x_2)} \int d^4 p \theta(p^0) \text{Im} \left[\frac{1}{p^2 - m_N^2 + i\epsilon} \right] (m_N^2 + p_{N_i} \cdot p) e^{ip \cdot (x_1 - x_2)}. \end{aligned} \quad (142)$$

The integral over \vec{X}_π in Eq. (136) gives

$$\int d\vec{X}_\pi \frac{1}{V_i} = 1. \quad (143)$$

1. Symmetry of probability

\tilde{P} is written in the form,

$$\begin{aligned} \tilde{P} &= \int dx_1 dx_2 \Delta(x_1, x_2) e^{-\frac{1}{4\sigma_\pi} (\vec{x}_1 - \vec{x}_2 - \vec{v}(t_1 - t_2))^2} e^{iE_\pi(\vec{p}_\pi)(t_1 - t_2) - i\vec{p}_\pi \cdot (\vec{x}_1 - \vec{x}_2)} \\ &\quad \times e^{-\frac{1}{\sigma_\pi} (\frac{\vec{x}_1 + \vec{x}_2}{2} - \vec{X}_\pi - \vec{v}_\pi (\frac{t_1 + t_2}{2} - T_\pi))^2}. \end{aligned} \quad (144)$$

The short-range part $\Delta_s(x_1, x_2)$ in $\Delta(x_1, x_2)$ becomes non-vanishing at

$$(x_1^0 - x_2^0, \vec{x}_1 - \vec{x}_2) \approx (0, \vec{0}), \quad (145)$$

and \tilde{P}_s becomes the product of factorized integrals

$$\tilde{P}_s = N_s \int d(x_1 - x_2) \Delta_s(x_1 - x_2) e^{-\frac{1}{4\sigma_\pi}(\vec{x}_1 - \vec{x}_2 - \vec{v}(t_1 - t_2))^2} e^{iE_\pi(\vec{p}_\pi)(t_1 - t_2) - i\vec{p}_\pi \cdot (\vec{x}_1 - \vec{x}_2)}, \quad (146)$$

$$N_s = \int d\left(\frac{x_1 + x_2}{2}\right) e^{-\frac{1}{\sigma_\pi}\left(\frac{\vec{x}_1 + \vec{x}_2}{2} - \vec{X}_\pi - \vec{v}_\pi\left(\frac{t_1 + t_2}{2} - T_\pi\right)\right)^2}, \quad (147)$$

where N_s is a constant. P_s is equivalent to that of $\sigma_\pi = \infty$ and Lorentz invariant.

The long-range part $\Delta_l(x_1, x_2)$ in $\Delta(x_1, x_2)$ becomes non-vanishing at large

$$x_1 - x_2, \quad (148)$$

and \tilde{P}_l becomes

$$\begin{aligned} \tilde{P}_l &= \int d(x_1 - x_2) \Delta_l(x_1 - x_2) e^{-\frac{1}{4\sigma_\pi}(\vec{x}_1 - \vec{x}_2 - \vec{v}(t_1 - t_2))^2} e^{iE_\pi(\vec{p}_\pi)(t_1 - t_2) - i\vec{p}_\pi \cdot (\vec{x}_1 - \vec{x}_2)} \\ &\quad \times \int d\left(\frac{x_1 + x_2}{2}\right) e^{-\frac{1}{\sigma_\pi}\left(\frac{\vec{x}_1 + \vec{x}_2}{2} - \vec{X}_\pi - \vec{v}_\pi\left(\frac{t_1 + t_2}{2} - T_\pi\right)\right)^2}. \end{aligned} \quad (149)$$

In \tilde{P}_l , two integrals are not factorized. Accordingly \tilde{P}_l is not Lorentz invariant and depends on σ_π .

2. light-cone singularity 1

Here the formula for a relativistic field Eq. (120) is substituted into Eq. (142), and we have

$$\begin{aligned} \Delta(x_1, x_2) &= e^{-ip_{N_i} \cdot (x_1 - x_2)} i \left(\frac{1}{4\pi} \delta(\lambda) \epsilon(t_1 - t_2) + \text{Bessel functions} \right) \\ &= e^{-i\bar{\phi}_{N_i}(\delta t)} \frac{i}{4\pi} \delta(\lambda) \epsilon(\delta t) + \text{Bessel functions}, \\ \bar{\phi}_{N_i} &= (E_{N_i} - |\vec{p}_{N_i}|) \delta t, \quad \delta t = t_1 - t_2. \end{aligned} \quad (150)$$

The first term in the right hand side of Eq. (120) is the most singular term and the second and third terms have singularity of the form $1/\lambda$ around $\lambda = 0$ and decrease as $e^{-\tilde{m}\sqrt{|\lambda|}}$ or oscillates as $e^{i\tilde{m}\sqrt{|\lambda|}}$. The singular functions and regular functions behave differently. The singular functions are non-vanishing in narrow regions around the light cone and the regular functions have finite values in a small area around the origin. Since the light cone

singularity is extended and decreases slowly as $\frac{1}{|t_1-t_2|}$, the correlation function has long-range component. The correlation function from other terms decreases exponentially or oscillates rapidly. In the above equation, ‘‘Bessel functions’’ are oscillating or decreasing fast with λ and this property is sufficient to know a large T behavior of the probability. In latter sections, concrete forms of these functions are obtained and their properties are studied.

Equation (150) is substituted into Eq. (137) and after a tedious calculation the probability is written as the sum,

$$\tilde{P} = \int_{T_{N_i}}^{T_\pi} dt_1 dt_2 (\sigma_\pi)^{\frac{3}{2}} \frac{\sigma_\pi}{2} \frac{1}{|\delta t|} \epsilon(\delta t) e^{i(\bar{\phi}_\pi(\delta t) - \bar{\phi}_{N_i}(\delta t))} + \tilde{P}^{(0)}, \quad (151)$$

$$\bar{\phi}_\pi = \omega_\pi \delta t, \quad \omega_\pi = (E_\pi - |\vec{p}_\pi|), \quad (152)$$

where we use the notation $t = x^0$, and the first and second terms in right-hand side are derived from the long and short range parts. The first term is proportional to the following function of ωT ,

$$Tg(T, \omega) = i \int_0^T dt_1 dt_2 \frac{e^{i\omega\delta t}}{|\delta t|} \epsilon(\delta t) = -2 \left(\text{Sin } x - \frac{1 - \cos x}{x} \right), \quad (153)$$

$$x = \omega T, \quad \text{Sin } x = \int_0^x dy \frac{\sin y}{y},$$

which satisfies

$$\frac{\partial}{\partial T} g(T, \omega) |_{T=0} = -\omega, \quad (154)$$

$$g(\infty, \omega) = -\pi. \quad (155)$$

Subtracting the asymptotic value, we define $\tilde{g}(T, \omega_\nu)$

$$g(T, \omega) = \tilde{g}(T, \omega) + g(\infty, \omega), \quad (156)$$

which satisfies

$$\frac{d}{dx} \tilde{g}(x) = -4 \left(\frac{\sin(x/2)}{x} \right)^2, \quad (157)$$

and oscillates rapidly at large x with an average

$$\tilde{g}(x) = \frac{2}{x}. \quad (158)$$

Thus $\tilde{g}(T, \omega)$ behaves as

$$\tilde{g}(T, \omega) \approx \frac{T_0}{T}, \quad T_0 = \frac{2}{\omega}, \quad (159)$$

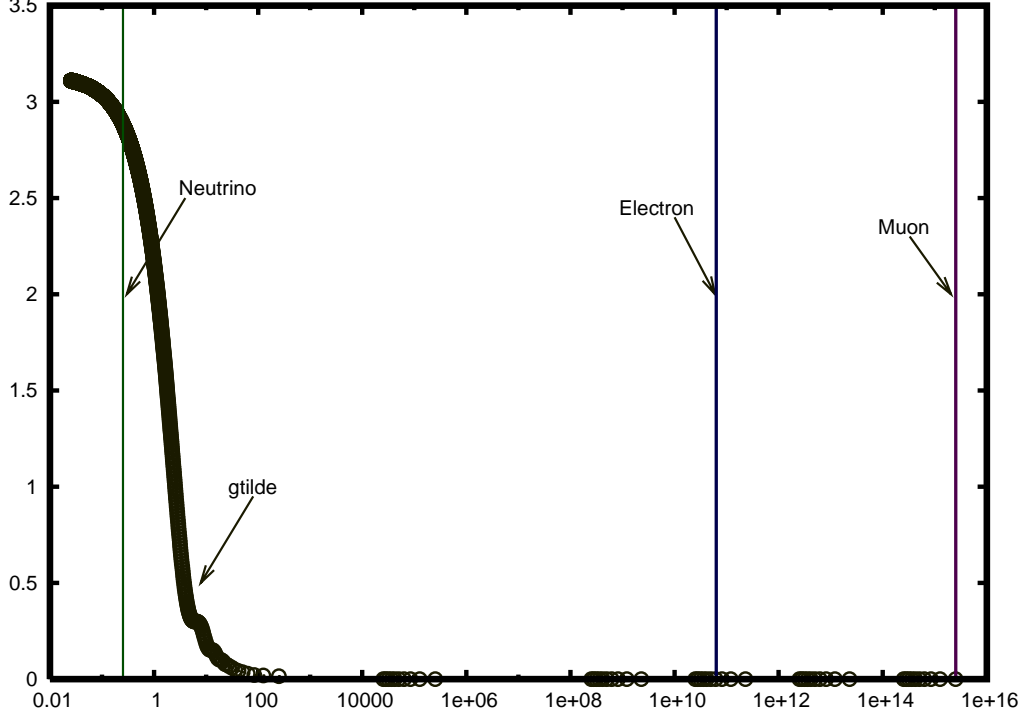


FIG. 2. The function $\tilde{g}(T, \omega)$ is given as a function of ωT . The value of ωT for various particles of the energy 1 [GeV] and $cT = 100[M]$ are expressed in solid lines. The vertical line shows the magnitude of $\tilde{g}(T, \omega)$ and the horizontal line shows ωT . The mass $m_\nu = 1$ [eV] is used for the neutrino in this Figure. Since the electron and muon are massive, $\tilde{g}(T, \omega)$ are negligibly small. The values for the pion and other hadrons are smaller than that of muon.

and is given in Fig. 2 as a function of x . For particles of 1 [GeV] and $cT = 100$ [m]. ω is large and $\tilde{g}(T, \omega)$ is extremely small for the electron and muon, but the value becomes around 1 for the neutrino.

The probability derived from the second term of Eq. (151) is a constant. Thus the probability is expressed in the form

$$\tilde{P} = C_0(\sigma_\pi)\tilde{g}(T, \omega) + \tilde{P}^{(0)}, \quad (160)$$

$$\omega = (E_\pi - |\vec{p}_\pi|) - (E_{N_i} - |\vec{p}_{N_i}|), \quad T = T_\pi - T_{N_i}, \quad (161)$$

$$C_0(\sigma_\pi) = T(\sigma_\pi)^{5/2}/2, \quad \tilde{P}^{(0)} = \tilde{P}^{(0)} + T(\sigma_\pi)^{5/2}/2g(0), \quad (162)$$

$\tilde{g}(\omega, T)$ is a function of ωT and is inversely proportional to ωT at a large ωT . Here ω is determined by the pion's mass and energy and the nucleon's mass and energy and is not very small. Hence, $\tilde{g}(\omega T)$ vanishes at a macroscopic T . The integrand of the probability in

Eq. (151) oscillates rapidly in δt with a non-small angular velocity ω , and the probability becomes constant fast.

3. light-cone singularity 2

The integrand of Eq. (142) around a momentum of $(p_{N_f} - p_{N_i})^2 = 0$ does not oscillate at $\lambda = 0$ and becomes real. A sum of these waves becomes real and singular at $\lambda = 0$ due to constructive interference and forms the light-cone singularity. Especially this function does not accompany the oscillating function $e^{-i\bar{\phi}_{N_i}(\delta t)}$, hence gives different probability. This singularity is extracted with a suitable expression of the integral. Changing the variable from p to $q = p_{N_f} - p$, we write

$$\begin{aligned} \Delta(x_1, x_2) = & \int d^4 q \theta(p_{N_i}^0 - q^0) \text{Im} \left[\frac{1}{(q - p_{N_i})^2 - m_N^2 + i\epsilon} \right] \\ & \times (2m_N^2 - p_{N_i} \cdot q) e^{-iq \cdot (x_1 - x_2)}. \end{aligned} \quad (163)$$

Next we have the expression of the denominator in the form,

$$\frac{1}{(q - p_{N_i})^2 - m_{N_f}^2 + i\epsilon} = \sum_l \left(2q \cdot p_{N_i} \frac{\partial}{\partial \delta m_N^2} \right)^l \frac{1}{q^2 + \delta m_N^2 + i\epsilon}, \quad (164)$$

where a small difference between m_{N_i} and m_{N_f} which has been ignored so far is included here and $\delta m_N^2 = m_{N_i}^2 - m_{N_f}^2$ is the mass-squared difference between a proton and a neutron. Then $\Delta(x_1, x_2)$ is written as

$$\Delta(x_1, x_2) = i \frac{\epsilon(\delta t)}{4\pi} \delta(\lambda) + \text{Bessel functions} + \text{regular function}, \quad (165)$$

where the light-cone singular term is derived from $l = 0$, and the others are from $l \neq 0$. The second and third terms of Eq. (165) are not studied in detail here, but the first term, which gives the large $|\delta t|$ behavior of $\Delta(x_1, x_2)$ is studied hereafter. The regular terms are from $0 < q^0$. This method of applying the Taylor expansion is valid when the infinite series converges. The integrations of the series in the expansion of the denominator converge in the kinematical region,

$$2p_{N_i} \cdot p_\pi \leq \delta m_N^2. \quad (166)$$

Hence the present method is valid and the light-cone singularity exists in this narrow kinematical region. The convergence of the series will be studied later in detail.

Equation (165) is substituted into Eq. (137) and after tedious calculations, we have the probability in the form,

$$\begin{aligned}\tilde{P} &= \int_{\mathbb{T}_{N_i}}^{\mathbb{T}_\pi} dt_1 dt_2 (\sigma_\pi)^{\frac{3}{2}} \frac{\sigma_\pi \epsilon(\delta t)}{2 |\delta t|} e^{i\bar{\phi}_\pi(\delta t)} + \tilde{P}^{(0)}, \\ &= C_0(\sigma_\pi) \tilde{g}(\mathbb{T}, \omega_\pi) + \tilde{P}^{(0)}.\end{aligned}\tag{167}$$

In Eq. (167), $\tilde{P}^{(0)}$ is the asymptotic value, and the first term vanishes at $\mathbb{T} \rightarrow \infty$ and is the finite-size correction. The correction is the product of the universal function $\tilde{g}(\mathbb{T}, \omega_\pi,)$ that is independent of the wave packet and $C_0(\sigma_\pi)$.

Equation (167) has almost the same form as Eq. (160) but a different angular velocity ω_π is used. ω_π is smaller than ω of Eq. (160). Hence this is more convenient to study the large \mathbb{T} behavior than the former one since it has the slowest oscillation. At large $|\delta t|$ region, the frequency in time is given from

$$\bar{\phi}(\delta t) = (E_\pi - |\vec{p}_\pi|)\delta t = \frac{m_\pi^2}{2E_\pi}\delta t.\tag{168}$$

In the last calculation, the large momentum expansion $E(\vec{p}) = |\vec{p}| + \frac{m^2}{2|\vec{p}|}$ was made. The pion's mass m_π , 139 [MeV/ c^2], makes the angular velocity $m_\pi^2/(2E_\pi)$ small only in an extreme high-energy region. Thus a coherence length of a pion emitted from a nucleon is $l_0 = 2cE_\pi/m_\pi^2$, which is microscopic due to the large mass, and the pion in the kinematical region, Eq. (166) can be observed inside this length. If the pion's mass m_π were 1 [eV/ c^2], then l_0 would have been macroscopic.

E. Pion from NN collisions

A probability of the event that one pion produced in NN collision is detected is studied in this section. In the Feynman diagram Fig. 4, the dot line shows the pion that is detected at a position X^μ and other particles are momentum eigen states. $\mathcal{M}(p_{N_f}, \dots, p_n; X_T)$ is the amplitude of the event that one pion of a momentum \vec{p}_π is detected,

$$\mathcal{M} = \int d^4x w(\vec{x}_\pi - \vec{v}_\pi(t - \mathbb{T}_\pi); X_\pi) e^{i(p_{N_f} + p_\pi - p_{N_i}) \cdot x} \mathcal{M}(p_{N_i}, \dots, p_n; X_T),\tag{169}$$

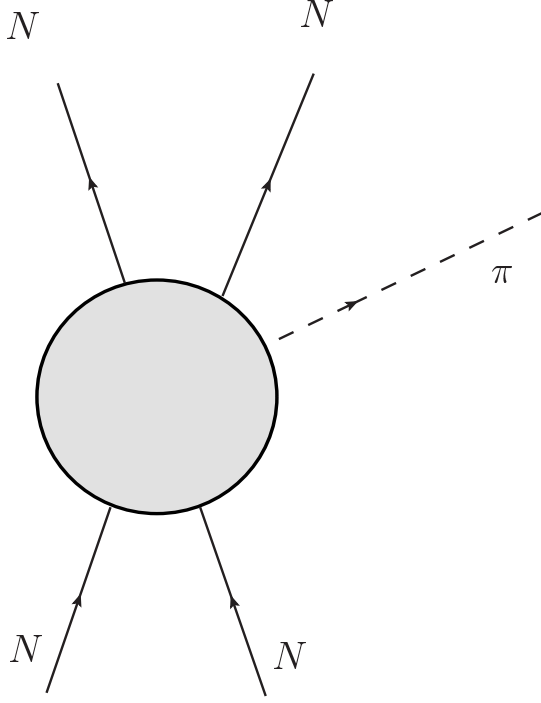


FIG. 3. A Feynman diagram of a pion production in NN scattering. The amplitude for one pion is computed in the text.

where p_{N_i} and p_1, p_2, \dots are momenta of the initial and final state, and X_T is the position of the target, Using \mathcal{M} , the probability of the event is expressed in the form,

$$C(X_\pi, \vec{p}_\pi) = \int d^4x_1 d^4x_2 w(\vec{x}_1 - \vec{v}_\pi(t_1 - T_\pi); X_\pi) w^*(\vec{x}_2 - \vec{v}_\pi(t_2 - T_\pi); X_\pi) \times e^{i(p_{N_f} - p_{N_i}) \cdot (x_1 - x_2)} e^{ip_\pi \cdot (x_1 - x_2)} |\mathcal{M}(p_{N_i}, \dots, p_n; X_T)|^2 d\vec{p}_{N_f}. \quad (170)$$

A sum of the final states is decomposed to a light-cone singularity and regular term,

$$\int \sum d\vec{p}_{N_f} e^{i(p_{N_f} - p_{N_i}) \cdot (x_1 - x_2)} |\mathcal{M}(p_{N_i}, \dots, p_n; X_T)|^2 = D\delta(\lambda)\epsilon(\delta t) + \text{regular term}, \quad (171)$$

where D is the coefficient. Substituting Eq. (171) to Eq. (170) we have

$$C(X_\pi, \vec{p}_\pi) = DC_0(\sigma_\pi) \tilde{g}(T, \omega_\pi), \quad (172)$$

which is equivalent to that of $\tilde{P}(X_\pi, p_\pi; p_{N_i})$ of Eq. (167) and has a length l_0 of Eq. (9). The length $l_0 = c\hbar E_\pi/m_\pi^2$ is much longer than the de Broglie wave length, $\lambda = h/|\vec{p}|$, but is microscopic in ordinary high-energy experiments.

Thus, the pion's coherence length l_0 is of microscopic size and the probability of the event that the pion is detected in the region $|\vec{X}_\pi - \vec{X}_T| \gg l_0$ agrees with that of $S[\infty]$ of σ , hence that of $S[\infty]$ of $\sigma = \infty$ from Eq. (58). The probability of the event that the pion is detected at a macroscopic T agrees with the asymptotic value. The finite-size correction is negligible.

IV. PROBABILITY OF THE EVENT THAT THE NEUTRINO IS DETECTED

The pion decays to a neutrino and lepton by weak interaction. Hereafter, the event that this neutrino is detected is studied.

A. Pion decays

The correction of probability of the event that the neutrino is detected becomes large due to tiny neutrino mass. Particularly a large correction is induced in the electron and electron neutrino mode that is suppressed in the asymptotic region due to kinetic energy and angular momentum conservations. Since a neutrino, charged lepton, and pion are described by a many-body wave function that follows Schrödinger equation, the kinetic energy of the final state at a finite time deviates from that of the initial energy. That is not a constant and takes a wide range of values. If the initial pion is expressed by a wave function of large size, the neutrino wave overlaps with the pion in wide area [4], and $S[T]$ that satisfies boundary conditions of experiments is appropriate [1, 2] and are used here [5, 36, 37]. The entire processes is analyzed with $S[T]$ expressed by wave packets.

A neutrino propagates with almost constant velocity. In an event that a neutrino is detected at one position, the position where the neutrino is produced varies, and a neutrino wave at the detector is a superposition of those waves that are produced at different space-time positions. When these space-time positions is extended in the wide area, as in Fig. 4, the neutrino waves keep their coherence, and the probability amplitude and probability reveal interference patterns. A condition for the interference phenomenon to occur for the pion expressed by a wave function of the size $\sqrt{\sigma_\pi}$ and a velocity \vec{v}_π is easily obtained for one dimensional motion. Let a neutrino be produced either at time t_1 or t_2 from the pion prepared at T_π and travel for some period and be finally detected at T_ν , then the waves

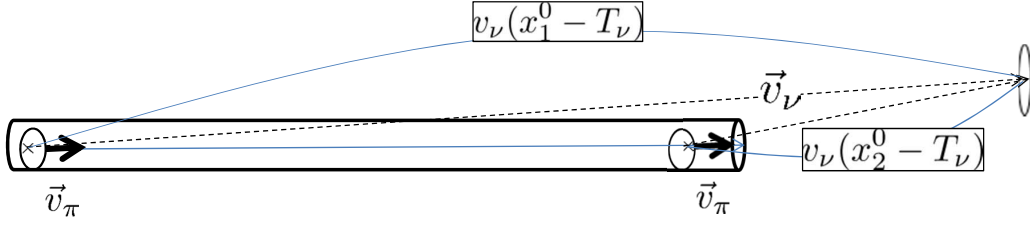


FIG. 4. The geometry of the event that the neutrino is detected. The neutrino is produced in the pion decay and is detected by the detector. Since the decay occurs between the position of the initial pion and that of the detector, the amplitude of the event is the overlap between the superposed initial wave and a final state expressed by the wave packet of the small size. The probability measured by the detector at T_ν shows an interference pattern.

overlap if

$$|(c(T_\nu - t_1) + v_\pi(t_1 - T_\pi)) - (c(T_\nu - t_2) + v_\pi(t_2 - T_\pi))| \leq \sqrt{\sigma_\pi}, \quad (173)$$

is fulfilled, where the speed of light is used for the speed of neutrino $v_\nu = c$. So Eq. (173) is one of the necessary conditions for the neutrino interference to occur in the one-dimensional space. For a plane wave of pion $\sigma_\pi = \infty$ and the above condition is satisfied. For a high-energy pion of a finite σ_π , its speed is close to the speed of light and the left hand side of Eq. (173) becomes $c(m_\pi^2/2E_\pi^2)(t_1 - t_2)$. Hence this condition Eq. (173) is written in the form, $c(t_1 - t_2) \leq \sqrt{\sigma_\pi}(2E_\pi^2/m_\pi^2)$. When this length $c(t_1 - t_2)$ is a macroscopic size, the interference phenomenon occurs at a macroscopic length. We estimate the lengths of these particles in Appendix A and confirm that this condition in three-dimensional space is fulfilled even in a macroscopic distance. It is noted that $\sqrt{\sigma_\pi}$ is the size of pion wave function in laboratory frame and is not related with l_0 of the pion discussed in the previous section.

B. Amplitude of the event that the neutrino is detected at \mathbf{T}

Probabilities of the events that a neutrino and a charged lepton are detected at \mathbf{T} are computed with $S[\mathbf{T}]$. When the wave functions of pion and daughters overlap, they have a finite interaction energy. Consequently, the kinetic energy of daughters deviates from that of the pion.

1. *Leptonic decay of the pion*

A leptonic decay of a pion is described with the weak Hamiltonian

$$H_{int} = g \int d\vec{x} \partial_\mu \varphi(x) J_{V-A}^\mu(x) = -igm_\mu \int d\vec{x} \varphi(x) J_5(x) + \delta L_{int}, \quad (174)$$

$$J_{V-A}^\mu(x) = \bar{\mu}(x) \gamma^\mu (1 - \gamma_5) \nu(x), \quad J_5(x) = \bar{\mu}(x) (1 - \gamma_5) \nu(x), \quad (175)$$

where $\varphi(x)$, $\mu(x)$, and $\nu(x)$ are the pion field, muon field, and neutrino field. In Eq. (174), g is the coupling strength, $J_{V-A}^\mu(x)$, and $J_5(x)$ are a leptonic charged $V - A$ current, and a leptonic pseudoscalar. G_F is Fermi constant and f_π is a pion decay constant, and

$$g = \frac{G_F}{\sqrt{2}} f_\pi. \quad (176)$$

Here

$$\delta L_{int} = \frac{\partial}{\partial x_\mu} G^\mu, \quad G^\mu = g \varphi(x) J_{V-A}^\mu(x), \quad (177)$$

is a total derivative and does not give bulk effects. The equation of motion and Γ are kept intact. Nevertheless, this contributes to the non-bulk probability $P^{(d)}$. Especially $P^{(d)}$ becomes important for the electron mode, because $m_{electron} \ll m_\mu$. A computation will be made later for the electron mode using the $(V - A) \times (V - A)$ form of interaction.

A pion and decay products are expressed by the Schrödinger equation

$$i\hbar \frac{\partial}{\partial t} |\Psi(t)\rangle = H |\Psi(t)\rangle, \quad H = H_0 + H_{int}, \quad (178)$$

and the solution of satisfying the initial condition

$$|\Psi(t)\rangle|_{t=\Gamma_\pi} = |\text{pion}(t)\rangle|_{t=\Gamma_\pi} = e^{-i\frac{E_\pi}{\hbar}\Gamma_\pi} |\vec{p}_\pi, \Gamma_\pi\rangle, \quad (179)$$

in the first order in H_{int} is

$$|\Psi(t)\rangle = |\text{pion}(t)\rangle + |\text{muon, neutrino}(t)\rangle, \quad (180)$$

where

$$|\text{pion}(t)\rangle = a(t) |\text{pion}, \vec{p}_\pi(t)\rangle, \quad a(t) = 1 + O(g^2) \quad (181)$$

$$|\text{muon, neutrino}(t)\rangle = \int_{\Gamma_\pi}^t \frac{dt'}{i\hbar} H_{int}(t') |\text{pion}(t')\rangle. \quad (182)$$

The state is written as

$$\begin{aligned}
|\text{muon, neutrino}(t)\rangle = & g e^{-i\frac{E_\pi}{\hbar}t} \int d\vec{p}_\mu d\vec{p}_\nu \sqrt{\frac{m_\mu m_\nu}{E_\mu(\vec{p}_\mu) E_\nu(\vec{p}_\nu)}} \frac{e^{-i\omega t/\hbar} - 1}{\omega} \\
& \times \delta^{(3)}(\vec{p}_\pi - \vec{p}_\mu - \vec{p}_\nu) (p_\pi)_\mu \bar{\mu}(\vec{p}_\mu) \gamma^\mu (1 - \gamma_5) \nu(\vec{p}_\nu) |\vec{p}_\mu, \vec{p}_\nu\rangle, \quad (183)
\end{aligned}$$

where $\omega = E_\mu + E_\nu - E_\pi$ and $|\vec{p}_\mu, \vec{p}_\nu\rangle$ is a two-particle state composed of the muon and neutrino of momenta \vec{p}_μ and \vec{p}_ν .

At $t = \infty$,

$$\begin{aligned}
|\text{muon, neutrino}(t)\rangle = & -i g e^{-i\frac{E_\pi}{\hbar}t} \int d\vec{p}_\mu d\vec{p}_\nu \sqrt{\frac{m_\mu m_\nu}{E_\mu(\vec{p}_\mu) E_\nu(\vec{p}_\nu)}} (2\pi) \delta^{(4)}(p_\pi - p_\mu - p_\nu) \\
& \times (p_\pi)_\mu \bar{\mu}(\vec{p}_\mu) \gamma^\mu (1 - \gamma_5) \nu(\vec{p}_\nu) |\vec{p}_\mu, \vec{p}_\nu\rangle, \quad (184)
\end{aligned}$$

and the norm of this state is given by,

$$\langle \text{muon, neutrino}(T) | \text{muon, neutrino}(T) \rangle = T\Gamma, \quad (185)$$

where Γ is the average decay rate [31, 32]. A neutrino and muon are produced simultaneously, but they propagate differently. The neutrino propagates long distance with the speed of light and is detected afterward. Hence the probability for the neutrino is affected by a retarded effect similar to the classical electric field caused by a moving charge, and is different from the probability of the events that the muon is detected.

The events of neutrino are identified in experiments with its reaction products with nucleus in detector, hence the wave function of the final states is the one of the nuclei. The simplest form of Gaussian function of the size σ of nuclear wave function is used. Using them, we express $S[T]$ following the formula of Ref. [1]. In Ref. [1], $S[\infty]$ was computed, and the wave functions were replaced with plane waves. Here $S[T]$ is computed with the amplitude of finite σ .

Previous works studied flavor oscillations with $S[\infty]$ [38–45] described with large wave packets in Poincaré invariant manner, where the position dependence is ignorable and non-computable. Now $S[T]$ depends on the position and T , and the finite-size corrections are computable. For the small wave packets, wave packets of different positions [5] are necessary from the completeness.

The element of $S[T]$ is defined with a wave function of an initial pion located at a position \vec{X}_π , a neutrino at a position \vec{X}_ν and a muon as

$$\mathcal{M} = \int d^4x \langle \mu, \nu | H_{int}(x) | \pi \rangle, \quad (186)$$

where the pion and neutrino are expressed in the form

$$|\pi\rangle = |\vec{p}_\pi, \vec{X}_\pi, T_\pi\rangle, \quad |\mu, \nu\rangle = |\mu, \vec{p}_\mu; \nu, \vec{p}_\nu, \vec{X}_\nu, T_\nu\rangle, \quad (187)$$

and with the matrix elements,

$$\langle 0|\varphi(x)|\vec{p}_\pi, \vec{X}_\pi, T_\pi\rangle \approx N_\pi \rho_\pi \left(\frac{2\pi}{\sigma_\pi}\right)^{\frac{3}{2}} e^{-\frac{1}{2\sigma_\pi}(\vec{x}-\vec{X}_\pi-\vec{v}_\pi(t-T_\pi))^2 - i(E(\vec{p}_\pi)(t-T_\pi) - \vec{p}_\pi \cdot (\vec{x}-\vec{X}_\pi))}, \quad (188)$$

$$\begin{aligned} & \langle \mu, \vec{p}_\mu; \nu, \vec{p}_\nu, \vec{X}_\nu, T_\nu | \bar{\mu}(x)(1-\gamma_5)\nu(x) | 0 \rangle \\ &= \frac{N_\nu}{(2\pi)^3} \left(\frac{2\pi}{\sigma_\nu}\right)^{3/2} e^{-\frac{1}{2\sigma_\nu}(\vec{x}-\vec{X}_\nu-\vec{v}_\nu(t-T_\nu))^2} \left(\frac{m_\mu}{E(\vec{p}_\mu)}\right)^{\frac{1}{2}} \left(\frac{m_\nu}{E(\vec{p}_\nu)}\right)^{\frac{1}{2}} \bar{u}(\vec{p}_\mu)(1-\gamma_5)\nu(\vec{p}_\nu) \\ & \times e^{i(E(\vec{p}_\mu)t - \vec{p}_\mu \cdot \vec{x}) + i(E(\vec{p}_\nu)(t-T_\nu) - \vec{p}_\nu \cdot (\vec{x}-\vec{X}_\nu))}, \end{aligned} \quad (189)$$

where

$$N_\pi = \left(\frac{\sigma_\pi}{\pi}\right)^{\frac{3}{4}}, \quad N_\nu = \left(\frac{\sigma_\nu}{\pi}\right)^{\frac{3}{4}}, \quad \rho_\pi = \left(\frac{1}{2E_\pi(2\pi)^3}\right)^{\frac{1}{2}}. \quad (190)$$

In the above equation, the pion's life time is ignored but that is easily introduced and its effect is included later. σ_π and σ_ν , in Eqs. (188) and (189) are sizes of the pion and neutrino wave packets. Minimum wave packets are used in majorities of the present paper but non-minimum wave packets are studied and it is shown that main results are the same¹. From the result of Appendix, the pion produced in proton nucleon collision can be regarded as a free particle. The effect due to a mean free path estimated in the Appendix is used as a size of wave packet. The size of pion wave packet is of the order of 0.5 – 1.0 [m] and a momentum spreading is small. So \vec{k}_π is integrated easily, and is replaced with its central value \vec{p}_π and the final expression of Eq. (188) is obtained. We use the nuclear size for σ_ν .

¹ For non-minimal wave packets which have larger uncertainties, Hermite polynomials of $\vec{k}_\nu - \vec{p}_\nu$ are multiplied to the right-hand side of Eq. (189). A completeness of the wave packet states is also satisfied for the non-minimum case [5] and the probabilities are the same as far as the wave packet is almost symmetric. This condition is guaranteed in the high energy neutrino which this paper studies, but may not be so in the low energy neutrino. We will confirm in the text and appendix that the universal long-range correlation is independent of the wave packet shape as far as the wave packet is invariant under the time inversions. Low energy neutrinos such as solar or reactor neutrinos will be presented in the next paper.

C. Wave of observed neutrino: small angular velocity of a center motion

We have

$$\begin{aligned} \langle \mu, \nu | H_{int}(x) | \pi \rangle &= igm_\mu \tilde{N} e^{-\frac{1}{2\sigma_\pi}(\vec{x} - \vec{X}_\pi - \vec{v}_\pi(t - T_\pi))^2 - iE(\vec{p}_\pi)(t - T_\pi) + i\vec{p}_\pi \cdot (\vec{x} - \vec{X}_\pi) + iE(\vec{p}_\mu)t - i\vec{p}_\mu \cdot \vec{x}} \\ &\times \bar{u}(\vec{p}_\mu)(1 - \gamma_5)\nu(\vec{p}_\nu) e^{i\phi(x)} e^{-\frac{1}{2\sigma_\nu}(\vec{x} - \vec{X}_\nu - \vec{v}_\nu(t - T_\nu))^2}, \end{aligned} \quad (191)$$

$$\tilde{N} = N_\pi N_\nu \left(\frac{2\pi}{\sigma_\pi}\right)^{\frac{3}{2}} \left(\frac{2\pi}{\sigma_\nu}\right)^{\frac{3}{2}} N_0, \quad N_0 = \rho_\pi \frac{1}{(2\pi)^3} \left(\frac{m_\mu m_\nu}{E_\mu E_\nu}\right)^{1/2}, \quad (192)$$

$$\phi(x) = E(\vec{p}_\nu)(t - T_\nu) - \vec{p}_\nu \cdot (\vec{x} - \vec{X}_\nu). \quad (193)$$

where \vec{v}_ν is a neutrino velocity. It is important to notice that the integration over \vec{k}_ν is made prior to the integration over (t, \vec{x}) in order to satisfy the boundary condition of $S[T]$.

The neutrino wave function evolves with time in a specific manner. At $t = T_\nu$,

$$\psi_\nu(T_\nu, \vec{x}) = e^{i\phi(x) - \frac{1}{2\sigma_\nu}(\vec{x} - \vec{X}_\nu)^2}, \quad (194)$$

which is localized around the position \vec{X}_ν and has the phase $\phi = -\vec{p}_\nu \cdot (\vec{x} - \vec{X}_\nu)$. At a time $t < T_\nu$,

$$\psi_\nu(t, \vec{x}) = e^{i\phi(x) - \frac{1}{2\sigma_\nu}(\vec{x} - \vec{X}_\nu - \vec{v}_\nu(t - T_\nu))^2}, \quad (195)$$

which is localized around the position

$$\vec{x}_G = \vec{X}_\nu + \vec{v}_\nu(t - T_\nu), \quad (196)$$

and has the phase $\phi(x)$. $\phi(x)$ is written at a position $\vec{r} = \vec{x} - \vec{x}_G$ in the form,

$$\phi(x) = \bar{\phi}_G + \phi(\vec{r}), \quad (197)$$

where

$$\begin{aligned} \bar{\phi}_G &= E(\vec{p}_\nu)(t - T_\nu) - \vec{p}_\nu \cdot \vec{v}_\nu(t - T_\nu) \\ &= \frac{E_\nu^2(\vec{p}_\nu) - \vec{p}_\nu^2}{E_\nu(\vec{p}_\nu)}(t - T_\nu) = \frac{m_\nu^2}{E_\nu(\vec{p}_\nu)}(t - T_\nu), \end{aligned} \quad (198)$$

$$\phi(\vec{r}) = -\vec{p}_\nu \cdot \vec{r}. \quad (199)$$

A phase at the center, $\bar{\phi}_G$, has a typical form of the relativistic particle. Since the position is moving with the velocity \vec{v}_ν , the time-dependent phase is almost cancelled with the space-dependent phase.

When the position is moving with the light velocity in the parallel direction to the momentum \vec{p}_ν , instead of Eq. (196),

$$\vec{x} = \vec{X}_\nu + \vec{c}(t - T_\nu), \vec{c} = \frac{\vec{p}_\nu}{p_\nu}, \quad (200)$$

the phase is given by

$$\bar{\phi}_c(t - T_\nu) = E(\vec{p}_\nu)(t - T_\nu) - \vec{p}_\nu \cdot \vec{c}(t - T_\nu) = \frac{m_\nu^2}{2E_\nu(\vec{p}_\nu)}(t - T_\nu), \quad (201)$$

and becomes a half of $\bar{\phi}_G$. We will see that this phase plays the important role later.

The coordinate \vec{r} is integrated in the amplitude Eq. (186), where the rapidly changing phase $\phi(\vec{r})$ is combined with those phases of the pion and muon fields, and the slow phase $\bar{\phi}_c$ remains and gives a characteristic behavior to the transition amplitude. The emergence of slow phase occurs independently of the detail of wave packet.

The phase in the longitudinal direction is not affected by a spreading of the wave packet, and does not change the behavior of the amplitude. So the spreading effect has been ignored for simplicity in this section and will be studied in the latter section and Appendix. It will be shown there that the spreading in the transverse direction modifies the \vec{k}_ν integration but the final result turns actually into the same.

A neutrino velocity is slightly smaller than the speed of light. A neutrino of energy 1 [GeV] and a mass 1 [eV/c²] has a velocity

$$v/c = 1 - 2\epsilon, \quad \epsilon = \left(\frac{m_\nu c^2}{E_\nu}\right)^2 = 5 \times 10^{-19}, \quad (202)$$

hence the neutrino propagates a distance l , where

$$l = l_0(1 - \epsilon) = l_0 - \delta l, \quad \delta l = \epsilon l_0, \quad (203)$$

while the light propagates a distance l_0 . This difference of distances, δl , becomes

$$\delta l = 5 \times 10^{-17} \text{ [m]}; \quad l_0 = 100 \text{ [m]}, \quad (204)$$

$$\delta l = 5 \times 10^{-16} \text{ [m]}; \quad l_0 = 1000 \text{ [m]}, \quad (205)$$

which are much smaller than the sizes of the neutrino wave packets. Since the difference of velocities is small, the neutrino amplitude at the nuclear or atom targets show interference. The geometry of the neutrino interference is shown in Fig. 4. The neutrino wave produced at a time t_1 arrives at one nucleus or atom in the detector and is superposed to the wave produced at t_2 and arrives to the same nucleus or atom same time. A constructive interference of waves is shown in the text.

V. POSITION-DEPENDENT PROBABILITY

The probability of the event that the neutrino is detected at a finite-distance is computed and its deviation from the asymptotic value, the finite-size correction, is found. The correction has a universal property unique to the relativistically invariant system and is determined by the absolute neutrino mass.

A. Transition probability

The case of $\sigma_\pi = \infty$ is studied first, and that of large σ_π is later.

In Eq. (191), the integrand is a Gaussian function around the center $\vec{x}_0(t) = \vec{v}_\nu(t - T_\nu) + \vec{X}_\nu$ and is invariant under

$$\vec{x} \rightarrow \vec{x} + \vec{v}_\nu \delta t, \quad (206)$$

$$t \rightarrow t + \delta t. \quad (207)$$

Thus a shifted energy given by

$$H_0 - \vec{v}_\nu \cdot \vec{\mathcal{P}}, \quad (208)$$

satisfies

$$\left[S, H_0 - \vec{v}_\nu \cdot \vec{\mathcal{P}} \right] = 0, \quad (209)$$

and is conserved.

Integrating over \vec{x} in Eq. (191), we have the amplitude,

$$\mathcal{M} = C e^{i\phi_0} \bar{u}(p_\mu) (1 - \gamma_5) u(p_\nu) e^{-\frac{\sigma_\nu}{2} \delta \vec{p}^2} e^{-i\omega T/2} 2 \frac{\sin(\omega T/2)}{\omega}, \quad (210)$$

$$\omega = \delta E - \vec{v}_\nu \cdot \delta \vec{p}, \quad \delta \vec{p} = \vec{p}_\pi - \vec{p}_\mu - \vec{p}_\nu, \quad \delta E = E(\vec{p}_\pi) - E(\vec{p}_\mu) - E(\vec{p}_\nu),$$

where ϕ_0 is a constant. Because the modulus of wave function does not vanish in the finite space-time region around the moving center $\vec{x}_0(t)$ of velocity \vec{v}_ν , the angular velocity in Eq. (210), $\omega = E - \vec{v}_\nu \cdot \delta \vec{p}$, is different from the energy difference δE of the rest system. This causes the unusual properties of transition amplitude.

In Eq. (210), due to the Gaussian factor $e^{-\frac{\sigma_\nu}{2} \delta \vec{p}^2}$, $|\delta \vec{p}|$ has a finite uncertainty. Hence ω generally deviates from δE . At $\delta \vec{p} = 0$, $\omega = 0$ is the same as $\delta E = 0$, whereas at $\delta \vec{p} \neq 0$,

$\omega = 0$ gives the relation $\delta E = \vec{v}_\nu \cdot \delta \vec{p} \neq 0$. Kinetic energy takes broad range and the amplitude at a finite T reflects this. A configuration of the momentum satisfying $\omega = 0$ is a large ellipse, on which the normal solution of $\delta \vec{p} = 0$, and the new solution of large $|\delta \vec{p}|$ are. ω varies rapidly with the change of momentum around the former solution and $2\frac{\sin(\omega T/2)}{\omega} = 2\pi\delta(\omega)$ [30] can be applied. This gives the asymptotic term which satisfies the energy-momentum conservation. On the other hand, ω varies extremely slowly around the latter momentum, and the states of $\omega \approx 0$ lead the slow convergence at large T and give the finite-size correction. Since $|\delta \vec{p}|$ and δE are not small, the spectrum at the ultraviolet region, which exists in the wave function at a finite time, gives a contribution to the finite-size correction.

For computing the probability in a consistent manner with Lorentz invariance, it is convenient to write $|\mathcal{M}|^2$ with a correlation function. A transition probability of a pion of a momentum \vec{p}_π located at a space-time position (T_π, \vec{X}_π) , decaying to the neutrino of the momentum \vec{p}_ν at a space-time position (T_ν, \vec{X}_ν) and a muon of momentum \vec{p}_μ , is expressed in the form

$$\begin{aligned}
|\mathcal{M}|^2 &= g^2 m_\mu^2 |\tilde{N}|^2 \int d^4 x_1 d^4 x_2 S_5(s_1, s_2) \\
&\times e^{i(\phi(x_1) - \phi(x_2))} e^{-\frac{1}{2\sigma_\nu} \sum_i (\vec{x}_i - \vec{X}_\nu - \vec{v}_\nu(t_i - T_\nu))^2} \\
&\times e^{-i(E(\vec{p}_\pi)(t_1 - t_2) - \vec{p}_\pi \cdot (\vec{x}_1 - \vec{x}_2))} \times e^{i(E(\vec{p}_\mu)(t_1 - t_2) - \vec{p}_\mu \cdot (\vec{x}_1 - \vec{x}_2))} \\
&\times e^{-\frac{1}{2\sigma_\pi} \sum_j (\vec{x}_j - \vec{X}_\pi - \vec{v}_\pi(t_j - T_\pi))^2}, \tag{211}
\end{aligned}$$

where $S_5(s_1, s_2)$ stands for products of Dirac spinors and their complex conjugates,

$$S_5(s_1, s_2) = (\bar{u}(\vec{p}_\mu)(1 - \gamma_5)\nu(\vec{p}_\nu)) (\bar{u}(\vec{p}_\mu)(1 - \gamma_5)\nu(\vec{p}_\nu))^*, \tag{212}$$

and its spin summation is given by

$$S^5 = \sum_{s_1, s_2} S^5(s_1, s_2) = \frac{2p_\mu \cdot p_\nu}{m_\nu m_\mu}. \tag{213}$$

Now the probability is finite and an order of integrations are interchangeable. Integrating momenta of the final state and taking average over the initial momentum, we have the total

probability in the form

$$\begin{aligned}
& \int d\vec{p}_\pi \rho_{exp}(\vec{p}_\pi) \frac{d\vec{X}_\nu}{(2\pi)^3} d\vec{p}_\mu d\vec{p}_\nu \sum_{s_1, s_2} |\mathcal{M}|^2 \\
& = g^2 m_\mu^2 |N_{\pi\nu}|^2 \frac{2}{(2\pi)^3} \int \frac{d\vec{X}_\nu}{(2\pi)^3} d\vec{p}_\nu \rho_\nu^2 d^4 x_1 d^4 x_2 e^{-\frac{1}{2\sigma_\nu} \sum_i (\vec{x}_i - \vec{X}_\nu - \vec{v}_\nu (t_i - T_\nu))^2} \\
& \times \Delta_{\pi, \mu}(\delta t, \delta \vec{x}) e^{i\phi(\delta x_\mu)} e^{-\frac{1}{2\sigma_\pi} \sum_j (\vec{x}_j - \vec{X}_\pi - \vec{v}_\pi (t_j - T_\pi))^2}, \tag{214}
\end{aligned}$$

$$N_{\pi\nu} = \left(\frac{4\pi}{\sigma_\pi}\right)^{\frac{3}{4}} \left(\frac{4\pi}{\sigma_\nu}\right)^{\frac{3}{4}}, \quad \rho_\nu = \left(\frac{1}{2E_\nu(2\pi)^3}\right)^{\frac{1}{2}}, \quad \delta x = x_1 - x_2, \tag{215}$$

with a correlation function $\Delta_{\pi, \mu}(\delta t, \delta \vec{x})$. The correlation function is defined with a pion's momentum distribution $\rho_{exp}(\vec{p}_\pi)$, by

$$\Delta_{\pi, \mu}(\delta t, \delta \vec{x}) = \frac{1}{(2\pi)^3} \int \frac{d\vec{p}_\pi}{E(\vec{p}_\pi)} \rho_{exp}(\vec{p}_\pi) \frac{d\vec{p}_\mu}{E(\vec{p}_\mu)} (p_\mu \cdot p_\nu) e^{-i(\{E(\vec{p}_\pi) - E(\vec{p}_\mu)\}\delta t - (\vec{p}_\pi - \vec{p}_\mu) \cdot \delta \vec{x})}. \tag{216}$$

In the above equation, the final states are integrated over a complete set [5]. The muon and neutrino momenta are integrated over entire positive energy regions, and the neutrino position is integrated over the region of the detector. The pion in the initial state is assumed to be the statistical ensemble of the distribution $\rho_{exp}(\vec{p}_\pi)$. If the momentum distribution is narrow around the central value, the velocity \vec{v}_π in the pion Gaussian factor was replaced with its average \vec{v}_π . This is verified from the large spatial size of the pion wave packet discussed in the previous section. For the probability of a fixed pion momentum, the correlation function

$$\tilde{\Delta}_{\pi, \mu}(\delta t, \delta \vec{x}) = \frac{1}{(2\pi)^3} \frac{1}{E(\vec{p}_\pi)} \int \frac{d\vec{p}_\mu}{E(\vec{p}_\mu)} (p_\mu \cdot p_\nu) e^{-i(\{E(\vec{p}_\pi) - E(\vec{p}_\mu)\}\delta t - (\vec{p}_\pi - \vec{p}_\mu) \cdot \delta \vec{x})} \tag{217}$$

is used instead of Eq. (216).

B. Light-cone singularity

The correlation function $\tilde{\Delta}_{\pi, \mu}(\delta t, \delta \vec{x})$ is a standard form of Green's function and has the light-cone singularity that is real and decreases very slowly along the light cone. The singularity is generated by the states at the ultraviolet energy region near the light-cone region

$$\lambda = \delta t^2 - |\delta \vec{x}|^2 = 0, \tag{218}$$

and is extended in a large $|\delta \vec{x}|$ independently of \vec{p}_π . Thus the probability Eq. (214) gets a finite $\Gamma (= T_\nu - T_\pi)$ correction from the integration over t_1 and t_2 at $|t_1 - t_2| \rightarrow T$. We find

that the light-cone singularity of $\tilde{\Delta}_{\pi,\mu}(\delta t, \delta \vec{x})$ [35] gives a large finite-size correction to the probability in the following.

1. Separation of singularity

For the particles expressed by plane waves, the integration over the space time is made over the infinite-time interval, and the kinetic-energy is strictly conserved and 4-dimensional momenta satisfy

$$p_\pi = p_\mu + p_\nu, \quad (p_\pi - p_\mu)^2 = m_\nu^2 \approx 0. \quad (219)$$

Conversely, $\tilde{\Delta}_{\pi,\mu}(\delta t, \delta \vec{x})$ becomes, from an integral over the momentum in the region where the momentum difference $p_\pi - p_\mu$ is almost light-like, to have a singularity around the light cone, $\lambda = 0$. In order to extract the singular term from $\tilde{\Delta}_{\pi,\mu}(\delta t, \delta \vec{x})$, we write the integral in a four-dimensional form

$$\tilde{\Delta}_{\pi,\mu}(\delta t, \delta \vec{x}) = \frac{1}{(2\pi)^3} \frac{1}{E(\vec{p}_\pi)} I(p_\pi, \delta x), \quad (220)$$

$$I(p_\pi, \delta x) = \frac{2}{\pi} \int d^4 p_\mu \theta(p_\mu^0) (p_\mu \cdot p_\nu) \text{Im} \left[\frac{1}{p_\mu^2 - m_\mu^2 - i\epsilon} \right] e^{-i(\{E(\vec{p}_\pi) - E(\vec{p}_\mu)\}\delta t - (\vec{p}_\pi - \vec{p}_\mu) \cdot \delta \vec{x})}, \quad (221)$$

first, and change the integration variable from p_μ to $q = p_\mu - p_\pi$ that is conjugate to δx . Next, we separate the integration region into two parts, $0 \leq q^0$ and $-p_\pi^0 \leq q^0 \leq 0$, and have the expressions,

$$I(p_\pi, \delta x) = I_1(p_\pi, \delta x) + I_2(p_\pi, \delta x), \quad (222)$$

$$I_1(p_\pi, \delta x) = \left\{ p_\pi \cdot p_\nu + p_\nu \cdot \left(-i \frac{\partial}{\partial \delta x} \right) \right\} \tilde{I}_1, \quad (223)$$

$$\tilde{I}_1 = \frac{2}{\pi} \int d^4 q \theta(q^0) \text{Im} \left[\frac{1}{(q + p_\pi)^2 - m_\mu^2 - i\epsilon} \right] e^{iq \cdot \delta x}, \quad (224)$$

$$I_2(p_\pi, \delta x) = \frac{2}{\pi} \int_{-p_\pi^0}^0 d^4 q p_\nu \cdot (p_\pi + q) \text{Im} \left[\frac{1}{(q + p_\pi)^2 - m_\mu^2 - i\epsilon} \right] e^{iq \cdot \delta x}. \quad (225)$$

$I_1(p_\pi, \delta x)$ is the integral over the infinite region and has the light-cone singularity and $I_2(p_\pi, \delta x)$ is the integral over the finite region and is regular.

$I_1(p_\pi, \delta x)$ comes from the states of non-conserving kinetic energy and does not contribute to the total probability at an infinite-time interval. $I_2(p_\pi, \delta x)$, on the other hand, contributes to that at the infinite-time and finite-time intervals. So the leading finite-size correction to a physical quantity is computed using the most singular term of I_1 .

Next we compute \tilde{I}_1 . Expanding the integrand with $p_\pi \cdot q$, we have \tilde{I}_1 in the form

$$\begin{aligned}
& \tilde{I}_1(p_\pi, \delta x) \\
&= \frac{2}{\pi} \int d^4 q \theta(q^0) \operatorname{Im} \left[\frac{1}{q^2 + m_\pi^2 - m_\mu^2 + 2q \cdot p_\pi - i\epsilon} \right] e^{iq \cdot \delta x} \\
&= \frac{2}{\pi} \int d^4 q \theta(q^0) \left\{ 1 + 2p_\pi \cdot \left(i \frac{\partial}{\partial \delta x} \right) \frac{\partial}{\partial \tilde{m}^2} + \dots \right\} \operatorname{Im} \left[\frac{1}{q^2 + \tilde{m}^2 - i\epsilon} \right] e^{iq \cdot \delta x} \\
&= 2 \left\{ 1 + 2p_\pi \cdot \left(i \frac{\partial}{\partial \delta x} \right) \frac{\partial}{\partial \tilde{m}^2} + \dots \right\} \int d^4 q \theta(q^0) \delta(q^2 + \tilde{m}^2) e^{iq \cdot \delta x}, \tag{226}
\end{aligned}$$

where

$$\tilde{m}^2 = m_\pi^2 - m_\mu^2. \tag{227}$$

The expansion in $2p_\pi \cdot q$ of Eq. (226) converges in the region

$$\frac{2p_\pi \cdot q}{q^2 + \tilde{m}^2} < 1. \tag{228}$$

Here q is the integration variable and varies. So we evaluate the series after the integration over q , and find a condition for its convergence. We find later that the series after the momentum integration converges in the region $\frac{2p_\pi \cdot p_\nu}{\tilde{m}^2} \leq 1$.

$\tilde{I}_1(p_\pi, \delta x)$ is written in the form

$$\tilde{I}_1(p_\pi, \delta x) = 2(2\pi)^3 i \left\{ 1 + 2p_\pi \cdot \left(i \frac{\partial}{\partial \delta x} \right) \frac{\partial}{\partial \tilde{m}^2} + \dots \right\} \left(\frac{1}{4\pi} \delta(\lambda) \epsilon(\delta t) + f_{short} \right), \tag{229}$$

where f_{short} is written by Bessel functions and a formula for a relativistic field Eq. (120) is used.

Next I_2 is evaluated. For I_2 , we use a momentum $\tilde{q} = q + p_\pi$ and write in the form

$$\begin{aligned}
I_2(p_\pi, \delta x) &= \frac{2}{\pi} \int_{0 < \tilde{q}^0 < p_\pi^0} d^4 \tilde{q} (p_\nu \cdot \tilde{q}) \operatorname{Im} \left[\frac{1}{\tilde{q}^2 - m_\mu^2 - i\epsilon} \right] e^{i(\tilde{q} - p_\pi) \cdot \delta x} \\
&= e^{-ip_\pi \cdot \delta x} \left\{ p_\nu \cdot \left(-i \frac{\partial}{\partial \delta x} \right) \right\} \frac{2}{\pi} \int_{0 < \tilde{q}^0 < p_\pi^0} d^4 \tilde{q} \pi \delta(q^2 - m_\mu^2) e^{i\tilde{q} \cdot \delta x} \\
&= e^{-ip_\pi \cdot \delta x} \left\{ p_\nu \cdot \left(-i \frac{\partial}{\partial \delta x} \right) \right\} \int \frac{d\tilde{q}}{\sqrt{\tilde{q}^2 + m_\mu^2}} \theta \left(p_\pi^0 - \sqrt{\tilde{q}^2 + m_\mu^2} \right) e^{i\tilde{q} \cdot \delta x}. \tag{230}
\end{aligned}$$

The regular part I_2 has no singularity because the integration domain is finite and becomes short-range.

Thus the first term in \tilde{I}_1 gives the most singular term and the rests, the second term in I_1 and I_2 , give regular terms. The correlation function, $\tilde{\Delta}_{\pi,\mu}(\delta t, \delta \vec{x})$ is written in the form

$$\begin{aligned} \tilde{\Delta}_{\pi,\mu}(\delta t, \delta \vec{x}) &= \frac{1}{(2\pi)^3} \frac{1}{E(p_\pi)} \left[\left\{ p_\pi \cdot p_\nu - p_\nu \cdot \left(i \frac{\partial}{\partial \delta x} \right) \right\} 2(2\pi)^3 i \right. \\ &\times \left. \left\{ 1 + 2p_\pi \cdot \left(i \frac{\partial}{\partial \delta x} \right) \frac{\partial}{\partial \tilde{m}^2} + \dots \right\} \left(\frac{1}{4\pi} \delta(\lambda) \epsilon(\delta t) + f_{short} \right) + I_2 \right], \end{aligned} \quad (231)$$

where the dots stand for the higher order terms.

C. Integration over spatial coordinates

Next, we integrate over the coordinates \vec{x}_1 and \vec{x}_2 in

$$\int d\vec{x}_1 d\vec{x}_2 e^{i\phi(\delta x)} e^{-\frac{1}{2\sigma_\nu} \sum_i (\vec{x}_i - \vec{X}_\nu - \vec{v}_\nu(t_i - T_\nu))^2} \tilde{\Delta}_{\pi,\mu}(\delta t, \delta \vec{x}). \quad (232)$$

1. Singular terms: long-range correlation

The most singular term of $\tilde{\Delta}_{\pi,\mu}(\delta t, \delta \vec{x})$ is substituted, then Eq. (232) becomes

$$J_{\delta(\lambda)} = \int d\vec{x}_1 d\vec{x}_2 e^{i\phi(\delta x)} e^{-\frac{1}{2\sigma_\nu} \sum_i (\vec{x}_i - \vec{X}_\nu - \vec{v}_\nu(t_i - T_\nu))^2} \frac{\epsilon(\delta t)}{4\pi} \delta(\lambda), \quad (233)$$

and is computed easily using a center coordinate $R^\mu = \frac{x_1^\mu + x_2^\mu}{2}$ and a relative coordinate $\vec{r} = \vec{x}_1 - \vec{x}_2$. After the center coordinate \vec{R} is integrated, $J_{\delta(\lambda)}$ becomes the integral of the transverse and longitudinal component (\vec{r}_T, r_l) of the relative coordinates,

$$\epsilon(\delta t) (\sigma_\nu \pi)^{\frac{3}{2}} \int d\vec{r}_T dr_l e^{i\phi(\delta t, \vec{r}) - \frac{1}{4\sigma_\nu} (\vec{r}_T^2 + (r_l - v_\nu \delta t)^2)} \frac{1}{4\pi} \delta(\delta t^2 - \vec{r}_T^2 - r_l^2). \quad (234)$$

The transverse coordinate \vec{r}_T is integrated using the Dirac delta function and r_l is integrated next. Finally we have

$$\begin{aligned} J_{\delta(\lambda)} &= (\sigma_\nu \pi)^{\frac{3}{2}} \frac{\sigma_\nu}{2} \frac{\epsilon(\delta t)}{|\delta t|} e^{i\bar{\phi}_c(\delta t) - \frac{m_\nu^4}{16\sigma_\nu E_\pi^3} \delta t^2} \\ &\approx (\sigma_\nu \pi)^{\frac{3}{2}} \frac{\sigma_\nu}{2} \frac{\epsilon(\delta t)}{|\delta t|} e^{i\bar{\phi}_c(\delta t)}. \end{aligned} \quad (235)$$

The next term of $\tilde{\Delta}_{\pi,\mu}(\delta t, \delta \vec{x})$, of the form $1/\lambda$, in Eq. (232) leads

$$J_{1/\lambda} = \int d\vec{x}_1 d\vec{x}_2 e^{i\phi(\delta x)} e^{-\frac{1}{2\sigma_\nu} \sum_i (\vec{x}_i - \vec{X}_\nu - \vec{v}_\nu(t_i - T_\nu))^2} \frac{i}{4\pi^2 \lambda}, \quad (236)$$

which becomes

$$J_{1/\lambda} \approx (\sigma_\nu \pi)^{\frac{3}{2}} \frac{\sigma_\nu}{2} \left(\frac{1}{\pi \sigma_\nu |\vec{p}_\nu|^2} \right)^{\frac{1}{2}} e^{-\sigma_\nu |\vec{p}_\nu|^2} \frac{1}{|\delta t|} e^{i\bar{\phi}_c(\delta t)}. \quad (237)$$

This term also has the universal $|\delta t|$ dependence but its magnitude is much smaller than that of $J_{\delta(\lambda)}$ and is negligible in the present decay mode.

From Eqs. (235) and (237), the singular terms $J_{\delta(\lambda)}$ and $J_{1/\lambda}$ have the slow phase $\bar{\phi}_c(\delta t)$ and the magnitudes that are inversely proportional to δt . Thus these terms are long-range with the small angular velocity and are insensitive to the \tilde{m}^2 . These properties of the time-dependent correlation functions $J_{\delta(\lambda)}$ hold for the general wave packets, and the following theorem is proved.

Theorem

The singular part $J_{\delta(\lambda)}$ of the correlation function has the slow phase that is determined with the absolute value of the neutrino mass and the magnitude inversely proportional to δt , of the form Eq. (235), at the large distance. The phase is given in the form of a sum of $\bar{\phi}_c(\delta t)$ and small corrections, which are inversely proportional to the neutrino energy in general systems and become $1/E^2$ if the neutrino wave packet is invariant under the time inversion.

(Proof: General cases including spreading of wave packet)

We prove the theorem for general wave packets. $J_{\delta(\lambda)}$ is written in the form,

$$J_{\delta(\lambda)} = \int d\vec{r} e^{i\phi(\delta x)} \tilde{w}(\vec{r} - \vec{v}_\nu \delta t) \frac{\epsilon(\delta t)}{4\pi} \delta(\lambda), \quad (238)$$

where $\tilde{w}(\vec{x} - \vec{v}t)$ is expressed with a wave packet in the coordinate representation $w(\vec{x} - \vec{v}t)$ and its complex conjugate as,

$$\begin{aligned} \tilde{w}(r_l - v_\nu \delta t, \vec{r}_T) &= \int d\vec{R} w\left(\vec{R} + \frac{\vec{r}}{2}\right) w^*\left(\vec{R} - \frac{\vec{r}}{2}\right) \\ &= \int dk_l d\vec{k}_T e^{ik_l(r_l - v_\nu \delta t) + i\vec{k}_T \cdot \vec{r}_T + iC_0(\vec{k}_T^2)\delta t} |w(k_l, \vec{k}_T)|^2. \end{aligned} \quad (239)$$

The wave function $w(\vec{x} - \vec{v}t)$ that includes the spreading effect is expressed in the following form

$$w(\vec{x} - \vec{v}t) = \int dk_l d\vec{k}_T e^{ik_l(x_l - v_\nu t) + i\vec{k}_T \cdot \vec{x}_T + iC_{ij}k_T^i k_T^j t} w(k_l, \vec{k}_T), \quad (240)$$

$$C_{ij} = C_0 \delta_{ij}, \quad C_0 = \frac{1}{2E}, \quad (241)$$

instead of the Gaussian function of Eq. (233). A quadratic form in \vec{k} in an expansion of $E(\vec{p} + \vec{k})$ is included and this makes the wave packet spread with time. The coefficient C_{ij} in the longitudinal direction is negligible for the neutrino and is neglected. Expanding the delta function in the form,

$$\delta(\delta t^2 - r_l^2 - \vec{r}_T^2) = \sum_l \frac{1}{l!} (-\vec{r}_T^2)^l \left(\frac{\partial}{\partial \delta t^2} \right)^l \delta(t^2 - r_l^2), \quad (242)$$

we have the correlation function

$$\begin{aligned} J_{\delta(\lambda)} &= \int dr_l d\vec{r}_T e^{i\phi(\delta t, r_l)} \tilde{w}(r_l - v_\nu \delta t, \vec{r}_T) \frac{1}{4\pi} \left\{ 1 + \sum_{n=1} \frac{1}{n!} (-\vec{r}_T^2)^n \left(\frac{\partial}{\partial (\delta t)^2} \right)^n \right\} \\ &\times \delta(\delta t^2 - r_l^2) \epsilon(\delta t) \\ &= \int dr_l d\vec{r}_T dk_l d\vec{k}_T e^{i\phi(\delta t, r_l) + ik_l(r_l - v_\nu \delta t) + i\vec{k}_T \cdot \vec{r}_T + iC_0 \vec{k}_T^2 \delta t} |w(k_l, \vec{k}_T)|^2 \\ &\times \frac{1}{4\pi} \left\{ 1 + \sum_{n=1} \frac{1}{n!} (-\vec{r}_T^2)^n \left(\frac{\partial}{\partial (\delta t)^2} \right)^n \right\} \delta(\delta t^2 - r_l^2) \epsilon(\delta t) \\ &= \int dr_l dk_l e^{i\phi(\delta t, r_l) + ik_l(r_l - v_\nu \delta t)} d\vec{r}_T d\vec{k}_T e^{+iC_0 \vec{k}_T^2 \delta t} |w(k_l, \vec{k}_T)|^2 \\ &\times \frac{1}{4\pi} \left\{ 1 + \sum_{n=1} \frac{1}{n!} \left(\frac{\partial^2}{(\partial \vec{k}_T)^2} \right)^n \left(\frac{\partial}{\partial (\delta t)^2} \right)^n \right\} e^{i\vec{k}_T \cdot \vec{r}_T} \delta(\delta t^2 - r_l^2) \epsilon(\delta t). \end{aligned} \quad (243)$$

The variable \vec{r}_T is integrated first and \vec{k}_T is integrated next. Then we have the expression

$$\begin{aligned} J_{\delta(\lambda)} &= \int dr_l dk_l e^{i\phi(\delta t, r_l) + ik_l(r_l - v_\nu \delta t)} |w(k_l, 0)|^2 \\ &\times \frac{1}{4\pi} \left\{ 1 + \sum_{n=1} \frac{1}{n!} (-2iC_0 \delta t)^n \left(\frac{\partial}{2\delta t \partial \delta t} \right)^n \right\} (2\pi)^2 \delta(\delta t^2 - r_l^2) \epsilon(\delta t). \end{aligned} \quad (244)$$

Using the following identity

$$(2\delta t)^n \left(\frac{\partial}{2\delta t \partial \delta t} \right)^n = \left(\frac{\partial}{\partial \delta t} \right)^n + O\left(\frac{1}{\delta t} \right) \left(\frac{\partial}{\partial \delta t} \right)^{n-1}, \quad (245)$$

and taking a leading term in $1/\delta t$, we have the final expression of the correlation function at the long-distance region

$$J_{\delta(\lambda)} = \pi e^{-C_0 p} \epsilon(\delta t) \frac{e^{i\bar{\phi}_c(\delta t)}}{2\delta t} \int dk_l e^{k_l(i(1-v_\nu)\delta t + C_0)} |w(k_l, 0)|^2. \quad (246)$$

Hence $J_{\delta(\lambda)}$ in Eq. (246) becomes almost the same form as Eq. (235) and the slow phase $\bar{\phi}_c(\delta t)$ is modified slightly and the magnitude that is inversely proportional to the time difference. $J_{\delta(\lambda)}$ has the universal form for the general wave packets. By expanding

the exponential factor and taking the quadratic term of the exponent, the above integral is written in the form

$$\begin{aligned} & \int dk_l (1 + k_l(i(1 - v_\nu)\delta t + C_0) + \frac{1}{2!}(k_l(i(1 - v_\nu)\delta t + C_0))^2) |w(k_l, 0)|^2 \\ & = w_0 \left(1 + C_0 d_1 + \frac{d_2}{2!} C_0^2 - (1 - v_\nu)^2 \delta t^2 \right) + i(d_1(1 - v_\nu)\delta t + d_2 C_0(1 - v_\nu)\delta t), \end{aligned} \quad (247)$$

where

$$\delta = \frac{d_1}{E} + \frac{d_2}{2} \frac{1}{E^2}, \quad \gamma = \frac{d_1}{2E} + \frac{d_2}{2!} \left(\frac{1}{2E} \right)^2 - (1 - v_\nu)^2 \delta t^2, \quad (248)$$

$$d_1 = \frac{1}{w_0} \int dk_l k_l |w(k_l, 0)|^2, \quad d_2 = \frac{1}{w_0} \int dk_l k_l^2 |w(k_l, 0)|^2. \quad (249)$$

We substitute this expression into the correlation function and have

$$J_{\delta(\lambda)} = \pi e^{-C_0 |\vec{p}|} \omega_0 (1 + \gamma) \epsilon(\delta t) \frac{e^{i\vec{\phi}_c(\delta t)(1+\delta)}}{2\delta t}, \quad w_0 = \int dk_l |w(k_l, 0)|^2. \quad (250)$$

In wave packets of time reversal invariance, $|w(k_l, 0)|^2$ is the even function of k_l . Hence d_1 vanishes

$$d_1 = 0, \quad (251)$$

and the correction are

$$\delta = \frac{d_2}{2} \frac{1}{E^2}, \quad \gamma = \frac{d_2}{2!} \left(\frac{1}{2E} \right)^2 - (1 - v_\nu)^2 \delta t^2. \quad \square \quad (252)$$

The light-cone region $\delta t^2 - |\delta \vec{x}|^2 = 0$ is so close to neutrino orbits that it gives a finite contribution to the integral Eq. (232). Since the light-cone singularity is real, the integral is sensitive only to the slow neutrino phase and shows interference of the neutrino. This theorem is applied to quite general systems, where the neutrino interacts with a nucleus in a target.

2. Regular terms: short-range correlation

Next, we study regular terms of $\tilde{\Delta}_{\pi,\mu}(\delta t, \delta \vec{x})$ in Eq. (232). Regular terms are short-range and the spreading effect is ignored and the Gaussian wave packet is studied. First term is f_{short} in I_1 and is composed of Bessel functions. We have

$$L_1 = \int d\vec{x}_1 d\vec{x}_2 e^{i\phi(\delta x)} e^{-\frac{1}{2\sigma_\nu} \sum_i (\vec{x}_i - \vec{X}_\nu - \vec{v}_\nu(t_i - T_\nu))^2} f_{short}. \quad (253)$$

L_1 is evaluated at a large $|\delta t|$ in the form

$$L_1 = (\pi\sigma_\nu)^{\frac{3}{2}} e^{iE_\nu\delta t} \int d\vec{r} e^{-i\vec{p}_\nu\cdot\vec{r} - \frac{1}{4\sigma_\nu}(\vec{r}-\vec{v}_\nu\delta t)^2} f_{short}, \quad \vec{r} = \vec{x}_1 - \vec{x}_2. \quad (254)$$

Here the integration is made in the space-like region $\lambda < 0$. We write

$$r_l = v_\nu\delta t + \tilde{r}_l, \quad (255)$$

and rewrite λ in the form

$$\lambda = \delta t^2 - r_l^2 - \vec{r}_T^2 = \delta t^2 - (v_\nu\delta t + \tilde{r}_l)^2 - \vec{r}_T^2 \approx -2v_\nu\tilde{r}_l\delta t - \tilde{r}_l^2 - \vec{r}_T^2. \quad (256)$$

The L_1 for the large $|\delta t|$ is written with these variables. Using the asymptotic expression of the Bessel functions, we have

$$L_1 = (\pi\sigma_\nu)^{\frac{3}{2}} e^{i(E_\nu - |\vec{p}_\nu|v_\nu)\delta t} \int d\vec{r}_T d\tilde{r}_l e^{-i(|\vec{p}_\nu|\tilde{r}_l) - \frac{1}{4\sigma_\nu}(\tilde{r}_l^2 + \vec{r}_T^2)} \frac{i\tilde{m}}{4\pi^2} \left(\frac{\pi}{2\tilde{m}}\right)^{\frac{1}{2}} \\ \times \left(\frac{1}{2v_\nu\tilde{r}_l|\delta t| + \tilde{r}_l^2 + \vec{r}_T^2}\right)^{\frac{3}{4}} e^{i\tilde{m}\sqrt{2v_\nu\tilde{r}_l|\delta t| + \tilde{r}_l^2 + \vec{r}_T^2}}. \quad (257)$$

The Gaussian integration around $\vec{r}_T = \vec{0}$, $\tilde{r}_l = -2i\sigma_\nu|\vec{p}_\nu|$ give the asymptotic expression of L_1 at a large $|\delta t|$

$$L_1 = (\pi\sigma_\nu)^{\frac{3}{2}} \tilde{L}_1, \quad (258) \\ \tilde{L}_1 = e^{i(E_\nu - |\vec{p}_\nu|v_\nu)\delta t} e^{-\sigma_\nu|\vec{p}_\nu|^2} \frac{i\tilde{m}}{4\pi^2} \left(\frac{\pi}{2\tilde{m}}\right)^{\frac{1}{2}} \left(\frac{1}{4v_\nu\sigma_\nu|\vec{p}_\nu||\delta t|}\right)^{\frac{3}{4}} e^{i\tilde{m}\sqrt{2v_\nu\sigma_\nu|\vec{p}_\nu||\delta t|}}.$$

Obviously L_1 oscillates fast as $e^{i\tilde{m}c_1|\delta t|^{\frac{1}{2}}}$ where c_1 is determined by $|\vec{p}_\nu|$ and σ_ν and is short-range. The integration carried out with a different stationary value of r_l which takes into account the last term in the right-hand side gives almost equivalent result. The integration in the time-like region, $\lambda > 0$, is carried in a similar manner and L_1 decreases with time as $e^{-\tilde{m}c_1|\delta t|^{\frac{1}{2}}}$ and final result is almost the same as that of the space-like region. It is noted that the long-range term which appeared from the isolated $1/\lambda$ singularity in Eq. (237) does not exist in L_1 in fact. The reason for its absence is that the Bessel function decreases much faster in the space-like region than $1/\lambda$ and oscillates much faster than $1/\lambda$ in the time-like region. Hence the long-range correlation is not generated from the L_1 and the light-cone singularity $\delta(\lambda)\epsilon(\delta t)$ and $1/\lambda$ are the only source of the long-range correlation.

Second term of Eq. (232) is from I_2 , of Eq. (230). We have,

$$L_2 = 2p_\nu \cdot (p_\pi - p_\nu) (\pi\sigma_\nu)^{\frac{3}{2}} (4\pi\sigma_\nu)^{\frac{3}{2}} \frac{1}{(2\pi)^3} \tilde{L}_2, \quad (259)$$

$$\begin{aligned} \tilde{L}_2 &= \int \frac{d\vec{q}}{2\sqrt{\vec{q}^2 + m_\mu^2}} e^{-i(E_\pi - E_\nu - \sqrt{\vec{q}^2 + m_\mu^2} - \vec{v}_\nu \cdot (\vec{p}_\pi - \vec{q} - \vec{p}_\nu))\delta t} \\ &\quad \times e^{-\sigma_\nu (\vec{p}_\pi - \vec{q} - \vec{p}_\nu)^2} \theta \left(E_\pi - \sqrt{\vec{q}^2 + m_\mu^2} \right). \end{aligned} \quad (260)$$

The angular velocity of the integrand in L_2 varies with \vec{q} and the integral L_2 has a short-range correlation of the length, $2\sqrt{\sigma_\nu}$, in the time direction. So the L_2 's contribution to the total probability comes from the small $|\delta t|$ region and corresponds to the short-range component.

Thus the integral over the coordinates is written in the form

$$\begin{aligned} &\int d\vec{x}_1 d\vec{x}_2 e^{i\phi(\delta x)} e^{-\frac{1}{2\sigma_\nu} \sum_i (\vec{x}_i - \vec{X}_\nu - \vec{v}_\nu (t_i - T_\nu))^2} \tilde{\Delta}_{\pi,\mu}(\delta t, \delta \vec{x}) \\ &= 2i \frac{p_\pi \cdot p_\nu}{E_\pi} \left[\left(1 + 2p_\pi \cdot p_\nu \frac{\partial}{\partial \tilde{m}^2} + \dots \right) e^{i\bar{\phi}(\delta t)} (J_{\delta(\lambda)} + L_1) + L_2 \right] \\ &\approx 2i (\pi\sigma_\nu)^{\frac{3}{2}} \frac{p_\pi \cdot p_\nu}{E_\pi} \left[\left(1 + 2p_\pi \cdot p_\nu \frac{\partial}{\partial \tilde{m}^2} + \dots \right) \right. \\ &\quad \left. \times \left(\frac{\sigma_\nu}{2} e^{i\bar{\phi}_c(\delta t)} \frac{\epsilon(\delta t)}{|\delta t|} + \tilde{L}_1 \right) - i \left(\frac{\sigma_\nu}{\pi} \right)^{\frac{3}{2}} \tilde{L}_2 \right]. \end{aligned} \quad (261)$$

In the above equation, $p_\nu^2 = m_\nu^2$ is negligibly small compared to \tilde{m}^2 , $p_\pi \cdot p_\nu$ and σ_ν^{-1} , and is neglected in most places except the slow phase $\bar{\phi}(\delta t)$. The first term in the right-hand side of Eq. (261) is long-range and the second term is short-range. The long-range term is separated from others in a clear manner.

3. Convergence condition

Now we find a condition for our method to be valid. In Eq. (222), the integration region was split into the one of finite region $-p_\pi^0 \leq q^0 \leq 0$ and the region $0 \leq q^0$. Accordingly, the correlation function is written into a sum of the singular term and the regular term. The singular term is written with the light-cone singularity and the power series in Eq. (226). Hence this series must converge for the present method of extracting the light-cone singularity to be applicable.

We study the power series

$$\sum_n (-2p_\pi \cdot p_\nu)^n \frac{1}{n!} \left(\frac{\partial}{\partial \tilde{m}^2} \right)^n \tilde{L}_1, \quad (262)$$

using the asymptotic expression of \tilde{L}_1 , Eq. (258), first. The most weakly converging term in \tilde{L}_1 , is from $\tilde{m}^{\frac{1}{2}}$ and other terms converge when this converges. The series

$$S_1 = \sum_n (-2p_\pi \cdot p_\nu)^n \frac{1}{n!} \left(\frac{\partial}{\partial \tilde{m}^2} \right)^n (\tilde{m}^2)^{\frac{1}{4}} \quad (263)$$

becomes the form,

$$\begin{aligned} S_1 &= \sum_n \left(\frac{-2p_\pi \cdot p_\nu}{\tilde{m}^2} \right)^n \frac{1}{n!} \left(n - \frac{1}{4} \right)! (-1)^n (\tilde{m})^{\frac{1}{2}} \\ &\approx \sum_n \left(-\frac{2p_\pi \cdot p_\nu}{\tilde{m}^2} \right)^n (-1)^n n^{-\frac{5}{4}} (\tilde{m})^{\frac{1}{2}} = \sum_n \left(\frac{2p_\pi \cdot p_\nu}{\tilde{m}^2} \right)^n n^{-\frac{5}{4}} (\tilde{m})^{\frac{1}{2}}. \end{aligned} \quad (264)$$

Hence the series converges if the geometric ration is less than 1. At $2p_\pi \cdot p_\nu = \tilde{m}^2$ S_1 becomes finite, and the value is expressed by the zeta function,

$$S_1 = \sum_n n^{-\frac{5}{4}} (\tilde{m})^{\frac{1}{2}} = \zeta \left(\frac{5}{4} \right) (\tilde{m})^{\frac{1}{2}}. \quad (265)$$

Thus in the region,

$$\frac{2p_\pi \cdot p_\nu}{\tilde{m}^2} \leq 1, \quad (266)$$

the series converges and the correlation function $\tilde{I}_1(p_\pi, \delta x)$ has the singular terms. Outside this region, the power series diverges and the present method of extracting the light-cone singularity does not work. I is evaluated directly and agree with the I_2 .

The power series Eq. (262) is estimated with $\tilde{L}_1 \approx e^{i\tilde{m}\sqrt{2v_\nu\sigma_\nu|\vec{p}_\nu||\delta t|}}$ as

$$S_2 = \sum_n (-2p_\pi \cdot p_\nu)^n \frac{1}{n!} \left(\frac{\partial}{\partial \tilde{m}^2} \right)^n e^{i\tilde{m}\sqrt{2v_\nu\sigma_\nu|\vec{p}_\nu||\delta t|}}, \quad (267)$$

and becomes oscillating with $\sqrt{|\delta t|}$ of the form,

$$S_2 = e^{i\tilde{m}\sqrt{2v_\nu\sigma_\nu|\vec{p}_\nu||\delta t|}} \left(1 - \frac{p_\pi \cdot p_\nu}{\tilde{m}^2} \right). \quad (268)$$

The present method of separating the light-cone singularity from the correlation function and of evaluating the finite-size correction of the probability is valid in the kinematical region Eq. (266).

D. Time-dependent probability

Substituting Eq. (261) into Eq. (214), we have the probability of the event that the neutrino is detected at a space-time position (T_ν, \vec{X}_ν) , when the pion momentum distribution $\rho_{exp}(\vec{p}_\pi)$ is known, in the following form

$$\begin{aligned} & \int d\vec{p}_\pi \rho_{exp}(\vec{p}_\pi) d\vec{p}_\mu \frac{d\vec{X}_\nu}{(2\pi)^3} d\vec{p}_\nu \sum_{s_1, s_2} |\mathcal{M}|^2 = g^2 m_\mu^2 |N_{\pi\nu}|^2 (\sigma_\nu \pi)^{\frac{3}{2}} \frac{\sigma_\nu}{(2\pi)^6} \int \frac{d\vec{p}_\pi}{E_\pi} \rho_{exp}(\vec{p}_\pi) \\ & \times \int d\vec{X}_\nu \frac{d\vec{p}_\nu}{E_\nu} p_\pi \cdot p_\nu \int dt_1 dt_2 \left[e^{i \frac{m_\nu^2}{2E_\nu} \delta t} \frac{\epsilon(\delta t)}{|\delta t|} + \frac{2\tilde{L}_1}{\sigma_\nu} - i \frac{2}{\pi} \left(\frac{\sigma_\nu}{\pi} \right)^{\frac{1}{2}} \tilde{L}_2 \right] \\ & \times e^{-\frac{1}{2\sigma_\pi} (\vec{X}_\nu - \vec{X}_\pi + (\vec{v}_\nu - \vec{v}_\pi)(t_1 - T_\nu) + \vec{v}_\pi(T_\pi - T_\nu))^2 - \frac{1}{2\sigma_\pi} (\vec{X}_\nu - \vec{X}_\pi + (\vec{v}_\nu - \vec{v}_\pi)(t_2 - T_\nu) + \vec{v}_\pi(T_\pi - T_\nu))^2}. \end{aligned} \quad (269)$$

From a pion mean free path obtained in the Appendix, the coherence condition, Eq. (173), is satisfied and the pion Gaussian parts are regarded as constant in t_1 and t_2 ,

$$e^{-\frac{1}{2\sigma_\pi} (\vec{X}_\nu - \vec{X}_\pi + (\vec{v}_\nu - \vec{v}_\pi)(t_1 - T_\nu) + \vec{v}_\pi(T_\pi - T_\nu))^2} \approx \text{constant in } t_1, \quad (270)$$

$$e^{-\frac{1}{2\sigma_\pi} (\vec{X}_\nu - \vec{X}_\pi + (\vec{v}_\nu - \vec{v}_\pi)(t_2 - T_\nu) + \vec{v}_\pi(T_\pi - T_\nu))^2} \approx \text{constant in } t_2, \quad (271)$$

when an integration over t_1 and t_2 are made in a distance of our interest which is of the order of a few 100 [m]. The integration over t_1 and t_2 will be made in the next section.

When the above conditions Eq. (271) are fulfilled, an area where the neutrino is produced is inside of a same pion and neutrino waves are treated coherently and are capable of showing interference. In a much larger distance where this condition is not satisfied, two positions can not be in the same pion and the interference disappears.

1. Integrations over times

Integrations over the times t_1 and t_2 are carried and a probability at a finite T is obtained here. The following integral of the slowly decreasing term is

$$i \int_0^T dt_1 dt_2 \frac{e^{i\omega_\nu \delta t}}{|\delta t|} \epsilon(\delta t) = T \{ \tilde{g}(T, \omega_\nu) + g(\infty, \omega_\nu) \}, \quad \omega_\nu = \frac{m_\nu^2}{2E_\nu}, \quad (272)$$

where $\tilde{g}(T, \omega_\nu)$ vanishes at $T \rightarrow \infty$. We understand that the short-range part L_1 cancels with $g(\infty, \omega_\nu)$ and write the total probability with $\tilde{g}(T, \omega_\nu)$ and the short-range term from I_2 .

The integral of the short-range term, \tilde{L}_2 , is

$$\begin{aligned}
& \frac{2}{\pi} \sqrt{\frac{\sigma_\nu}{\pi}} \int dt_1 dt_2 \tilde{L}_2(\delta t) \\
&= \frac{2}{\pi} \sqrt{\frac{\sigma_\nu}{\pi}} \int_0^T dt_1 dt_2 \int \frac{d\vec{q}}{2\sqrt{\vec{q}^2 + m_\mu^2}} e^{-i(E_\pi - E_\nu - \sqrt{\vec{q}^2 + m_\mu^2} - \vec{v}_\nu \cdot (\vec{p}_\pi - \vec{q} - \vec{p}_\nu))\delta t} \\
&\quad \times e^{-\sigma_\nu(\vec{p}_\pi - \vec{q} - \vec{p}_\nu)^2} \theta\left(E_\pi - \sqrt{\vec{q}^2 + m_\mu^2}\right) \\
&= \text{T}G_0,
\end{aligned} \tag{273}$$

where the constant G_0 is given in the integral

$$\begin{aligned}
G_0 &= 2\sqrt{\frac{\sigma_\nu}{\pi}} \int \frac{d\vec{q}}{\sqrt{\vec{q}^2 + m_\mu^2}} \delta\left(E_\pi - E_\nu - \sqrt{\vec{q}^2 + m_\mu^2} - \vec{v}_\nu \cdot (\vec{p}_\pi - \vec{q} - \vec{p}_\nu)\right) \\
&\quad \times e^{-\sigma_\nu(\vec{p}_\pi - \vec{q} - \vec{p}_\nu)^2} \theta\left(E_\pi - \sqrt{\vec{q}^2 + m_\mu^2}\right),
\end{aligned} \tag{274}$$

and is estimated numerically. Due to the rapid oscillation in δt , \tilde{L}_2 's contribution to the probability comes from the small $|\delta t|$ region and the integrations over the time becomes constant in T. Hence this has no finite-size correction. The regular term \tilde{L}_1 is also the same.

2. Total transition probability

Adding the slowly decreasing part and the short-range part, we have the final expression of the total probability. The neutrino coordinate \vec{X}_ν is integrated in Eq. (269) and a factor $(\sigma_\pi \pi)^{\frac{3}{2}}$ emerges. This factor is cancelled with $(4\pi/\sigma_\pi)^{\frac{3}{2}}$ of the normalization in Eq. (211) and a final result is independent of σ_π . The total transition probability is expressed in the form,

$$P = \text{T}g^2 m_\mu^2 D_0 \sigma_\nu \int \frac{d\vec{p}_\pi}{E_\pi} \rho_{exp}(\vec{p}_\pi) \int \frac{d\vec{p}_\nu}{E_\nu} (p_\pi \cdot p_\nu) [\tilde{g}(\text{T}, \omega_\nu) + G_0], \tag{275}$$

$$D_0 = |N_{\pi\nu}|^2 (\sigma_\nu \pi)^{\frac{3}{2}} (\sigma_\pi \pi)^{\frac{3}{2}} \frac{1}{(2\pi)^6} = \frac{1}{(2\pi)^3}, \tag{276}$$

where $L = c\text{T}$ is the length of decay region. The first term in the right-hand side of Eq. (275) depends on the time interval T, and the neutrino wave packet size σ_ν , but the second term does not.

At a finite T, the first term does not vanish and the probability Eq. (275) has the finite-size correction. Its relative ratio over G_0 is independent of detection process. So we compute

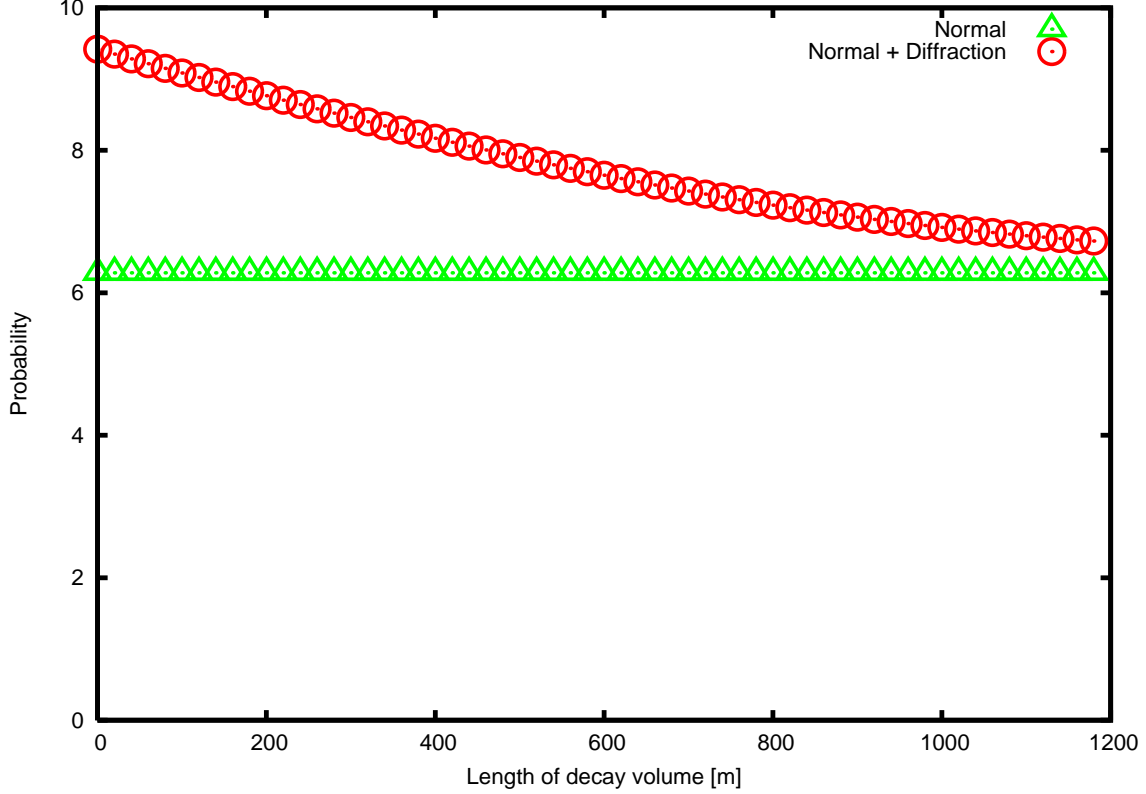


FIG. 5. The probability per unit time of the event that the neutrino is detected in the forward direction at a distance L is given. The constant shows the short-range normal term and the long-range diffraction term is written on top of the normal term. The horizontal axis shows the distance in [m] and the probability of the normal term is normalized to 2π . Clear excess of more than $2/5$ of the normal term is seen in the distance below 1200 [m]. The neutrino mass, pion energy, neutrino energy are 1 [eV/ c^2], 4 [GeV], and 800 [MeV]. A target nucleus with which the neutrino interacts in a detector is ^{16}O .

$\tilde{g}(T, \omega_\nu)$ and G_0 of Eq. (276) at the forward direction $\theta = 0$ and the energy dependent total probability that is integrated over the neutrino angle in the following.

The probabilities per unit time in the forward direction are plotted in Fig. 5 for $m_\nu = 1$ [eV/ c^2], $E_\pi = 4$ [GeV], and the neutrino energy $E_\nu = 800$ [MeV]. For the wave packet size of the neutrino, the size of the nucleus of the mass number A , $\sigma_\nu = A^{2/3}/m_\pi^2$ is used. The value becomes $\sigma_\nu = 6.4/m_\pi^2$ for the ^{16}O nucleus and this is used for the following evaluations. From this figure it is seen that there is an excess of the flux at short distance region $L < 600$ [m] and the maximal excess is about 0.4 at $L = 0$. The slope at $L = 0$ is determined by ω_ν .

The slowly decreasing term has the finite magnitude and the finite-size correction is large.

VI. NEUTRINO SPECTRUM

A. Integration over neutrino angle

In Eq. (276), $\tilde{g}(T, \omega_\nu)$ has an angle dependence different from that of G_0 . In G_0 , the cosine of neutrino angle θ is determined approximately from a mass-shell condition,

$$(p_\pi - p_\nu)^2 = p_\mu^2 = m_\mu^2, \quad (277)$$

because the energy and momentum conservation is approximately well satisfied. Hence the product of the momenta is expressed with the masses

$$p_\pi \cdot p_\nu = \frac{m_\pi^2 - m_\mu^2}{2}, \quad (278)$$

and the cosine of the angle satisfies

$$1 - \cos \theta = \frac{m_\pi^2 - m_\mu^2}{2|\vec{p}_\pi||\vec{p}_\nu|} - \frac{m_\pi^2}{2|\vec{p}_\pi|^2}. \quad (279)$$

The $\cos \theta$ is very close to 1 in a high-energy region. On the other hand, $\tilde{g}(T, \omega_\nu)$ of Eq. (276), is present in the domain of the momenta Eq. (266) i.e., in the kinematical region,

$$|\vec{p}_\nu|(E_\pi - |\vec{p}_\pi|) \leq p_\pi \cdot p_\nu \leq \frac{m_\pi^2 - m_\mu^2}{2}. \quad (280)$$

Since the angular region of Eq. (280) is slightly different from Eq. (278) and it is impossible to distinguish the latter from the former region experimentally, the neutrino angle is integrated. We integrate over the neutrino angle of both terms separately. We have the normal term, G_0 , in the form

$$\begin{aligned} & \int \frac{d\vec{p}_\nu}{E_\nu} (p_\pi \cdot p_\nu) G_0 \\ & \simeq \int \frac{d\vec{p}_\nu}{E_\nu} (p_\pi \cdot p_\nu) 2\sqrt{\frac{\sigma_\nu}{\pi}} \left(\frac{\pi}{\sigma_\nu}\right)^{\frac{3}{2}} \int \frac{d\vec{q}}{\sqrt{\vec{q}^2 + m_\mu^2}} \\ & \times \delta\left(E_\pi - E_\nu - \sqrt{\vec{q}^2 + m_\mu^2}\right) \delta^{(3)}(\vec{p}_\pi - \vec{p}_\nu - \vec{q}) \theta\left(E_\pi - \sqrt{\vec{q}^2 + m_\mu^2}\right) \\ & = \frac{(2\pi)^2}{\sigma_\nu} \left(\frac{m_\pi^2 - m_\mu^2}{2}\right) \frac{1}{|\vec{p}_\pi|} \int_{E_\nu, min}^{E_\nu, max} dE_\nu, \end{aligned} \quad (281)$$

where

$$E_{\nu,min} = \frac{m_\pi^2 - m_\mu^2}{2(E_\pi + |\vec{p}_\pi|)}, \quad E_{\nu,max} = \frac{m_\pi^2 - m_\mu^2}{2(E_\pi - |\vec{p}_\pi|)}, \quad (282)$$

and the Gaussian function is approximated by the delta function for the computational convenience. The angle is determined uniquely.

We compute the correction term next. There are two cases depending on the minimum angle of satisfying the convergence condition Eq. (266),

$$\cos \theta_c = \frac{E_\pi E_\nu - \frac{1}{2}(m_\pi^2 - m_\mu^2)}{|\vec{p}_\pi| |\vec{p}_\nu|}. \quad (283)$$

In the first energy region,

$$-1 \leq \cos \theta_c, \quad (284)$$

the convergence condition is satisfied in $\cos \theta_c \leq \cos \theta$, and we have the integral

$$\begin{aligned} & \int \frac{d\vec{p}_\nu}{E_\nu} (p_\pi \cdot p_\nu) \tilde{g}(T, \omega_\nu) \\ &= 2\pi \int \frac{|\vec{p}_\nu|^2 d|\vec{p}_\nu|}{E_\nu} \int_{\cos \theta_c}^1 d \cos \theta (E_\pi E_\nu - |\vec{p}_\pi| |\vec{p}_\nu| \cos \theta) \tilde{g}(T, \omega_\nu) \\ &= 2\pi \int_{E_{\nu,min}}^{E_{\nu,max}} \frac{dE_\nu}{2|\vec{p}_\pi|} \left\{ \frac{1}{4} (m_\pi^2 - m_\mu^2)^2 - (E_\pi E_\nu - |\vec{p}_\pi| |\vec{p}_\nu|)^2 \right\} \tilde{g}(T, \omega_\nu). \end{aligned} \quad (285)$$

Here the angle is very close to the former value but is not unique.

In the second region,

$$\cos \theta_c \leq -1, \quad (286)$$

the convergence condition is satisfied in arbitrary angle, and we have the integral

$$\begin{aligned} & \int \frac{d\vec{p}_\nu}{E_\nu} (p_\pi \cdot p_\nu) \tilde{g}(T, \omega_\nu) \\ &= 2\pi \int \frac{|\vec{p}_\nu|^2 d|\vec{p}_\nu|}{E_\nu} \int_{-1}^1 d \cos \theta (E_\pi E_\nu - |\vec{p}_\pi| |\vec{p}_\nu| \cos \theta) \tilde{g}(T, \omega_\nu) \\ &= 4\pi \int_0^{E_{\nu,min}} dE_\nu E_\pi E_\nu^2 \tilde{g}(T, \omega_\nu). \end{aligned} \quad (287)$$

The angle is fixed to one value, Eq. (279), in the normal asymptotic term and is in a continuous range in the correction term. The angle dependences of the energies are given in Fig. 3. Finally we have

$$\frac{dP}{dE_\nu} = \frac{dP^{(0)}}{dE_\nu} + \frac{dP^{(d)}}{dE_\nu}, \quad (288)$$

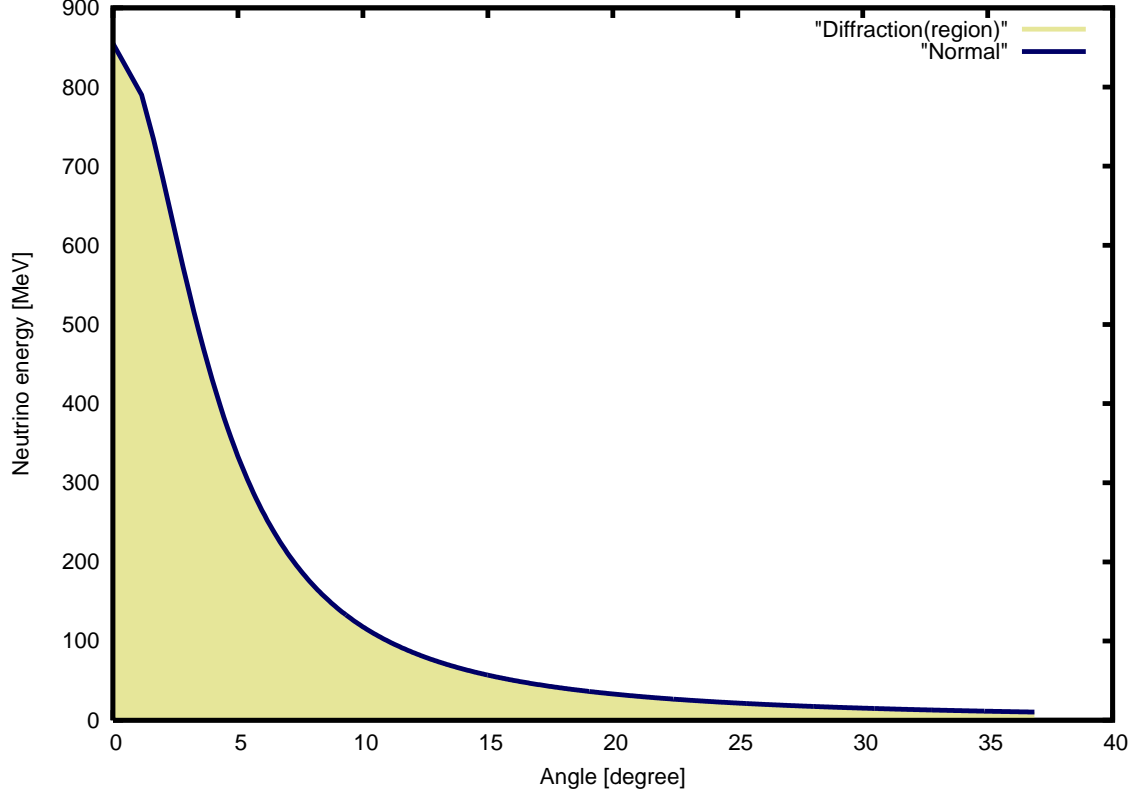


FIG. 6. The relation between the neutrino angle and energy is shown. The kinetic-energy is determined uniquely as Eq. (279) in the normal term and is not in the diffraction term. The value in the normal component is on the line and that in the diffraction component is under the line. The horizontal axis shows the angle and the vertical axis shows the energy. The energy of the pion is $E_\pi = 2$ [GeV].

where

$$\frac{dP^{(0)}}{dE_\nu} = Tg^2m_\mu^2D_0 \int \frac{d\vec{p}_\pi}{E_\pi} \rho_{exp}(\vec{p}_\pi) \frac{2\pi}{|\vec{p}_\pi|} \times \pi(m_\pi^2 - m_\mu^2), \quad (289)$$

$$\begin{aligned} \frac{dP^{(d)}}{dE_\nu} = Tg^2m_\mu^2D_0 \int \frac{d\vec{p}_\pi}{E_\pi} \rho_{exp}(\vec{p}_\pi) \frac{2\pi}{|\vec{p}_\pi|} & \left(\theta(E_\nu - E_{\nu,min}) \left\{ \frac{1}{4} (m_\pi^2 - m_\mu^2)^2 \right. \right. \\ & \left. \left. - (E_\pi E_\nu - |\vec{p}_\pi||\vec{p}_\nu|)^2 \right\} + \theta(E_{\nu,min} - E_\nu) 2p_\pi E_\pi E_\nu^2 \right) \frac{\sigma_\nu}{2} \tilde{g}(T, \omega_\nu). \end{aligned} \quad (290)$$

$\frac{dP^{(0)}}{dE_\nu}$ is proportional to T and $\frac{dP^{(d)}}{dE_\nu}$ is constant.

B. Neutrino spectrum

1. Sharp pion momentum

For the initial pion of a discrete momentum \vec{P}_π ,

$$\rho_{exp}(\vec{p}_\pi) = \delta(\vec{p}_\pi - \vec{P}_\pi), \quad (291)$$

the rates are expressed in the form,

$$\frac{1}{\Gamma} \frac{dP^{(0)}}{dE_\nu} = g^2 m_\mu^2 D_0 \frac{1}{E_\pi} \frac{2\pi}{|\vec{P}_\pi|} \pi(m_\pi^2 - m_\mu^2), \quad (292)$$

$$\begin{aligned} \frac{1}{\Gamma} \frac{dP^{(d)}}{dE_\nu} &= g^2 m_\mu^2 D_0 \frac{1}{E_\pi} \frac{2\pi}{|\vec{P}_\pi|} \left(\theta(E_\nu - E_{\nu,min}) \left\{ \frac{1}{4} (m_\mu^2 - m_\pi^2)^2 - (E_\pi E_\nu - |\vec{P}_\pi| |\vec{p}_\nu|)^2 \right\} \right. \\ &\left. + \theta(E_{\nu,min} - E_\nu) 2p_\pi E_\pi E_\nu^2 \right) \frac{\sigma_\nu}{2} \tilde{g}(\Gamma, \omega_\nu). \end{aligned} \quad (293)$$

Equations (292) and (293) are independent of the position \vec{X}_π and an average over \vec{X}_π is easily made and the results are obviously the same.

The rate $P^{(0)}$ is independent of σ_ν [42], and agrees with the standard value,

$$\begin{aligned} \Gamma &= g^2 m_\mu^2 D_0 \frac{1}{E_\pi} \frac{2\pi}{|\vec{P}_\pi|} \pi(m_\pi^2 - m_\mu^2) \int_{E_{\nu,min}}^{E_{\nu,max}} dE_\nu \\ &= g^2 m_\mu^2 \frac{1}{4\pi} \frac{m_\pi^2}{E_\pi} \left(1 - \frac{m_\mu^2}{m_\pi^2} \right)^2. \end{aligned} \quad (294)$$

$\tilde{g}(\Gamma, \omega_\nu)$ behaves as $2/(\omega_\nu \Gamma)$ at a large Γ , where $\Gamma = \Gamma_\nu - \Gamma_\pi$, and the correction term at high energy pion becomes,

$$\Gamma^{(d)} = \frac{m_\pi^2 \sigma_\nu}{8\pi} \left(1 - \frac{m_\mu^2}{m_\pi^2} \right)^2 \frac{E_\pi}{m_\nu^2 \Gamma} \Gamma. \quad (295)$$

2. Position dependence

In P/Γ , $\tilde{g}(\Gamma, \omega_\nu)$ varies with the distance L defined by $L = c\Gamma$. P/Γ for $m_\nu = 1.0$ [eV/c²] and $E_\pi = 4$ [GeV] and 4.5 [GeV] are given in Fig. 7, and for $m_\nu = 0.6$ [eV/c²] are given in Fig. 8. The rate decreases extremely slowly for a light neutrino and a longer distance is necessary to observe the non-uniform behavior for smaller neutrino mass. For the detection of the muon neutrino, the neutrino energy should be larger than the muon mass. For smaller energy, the electron neutrino is observed. The probability for $m_\nu = 1.0$ [eV/c²] with

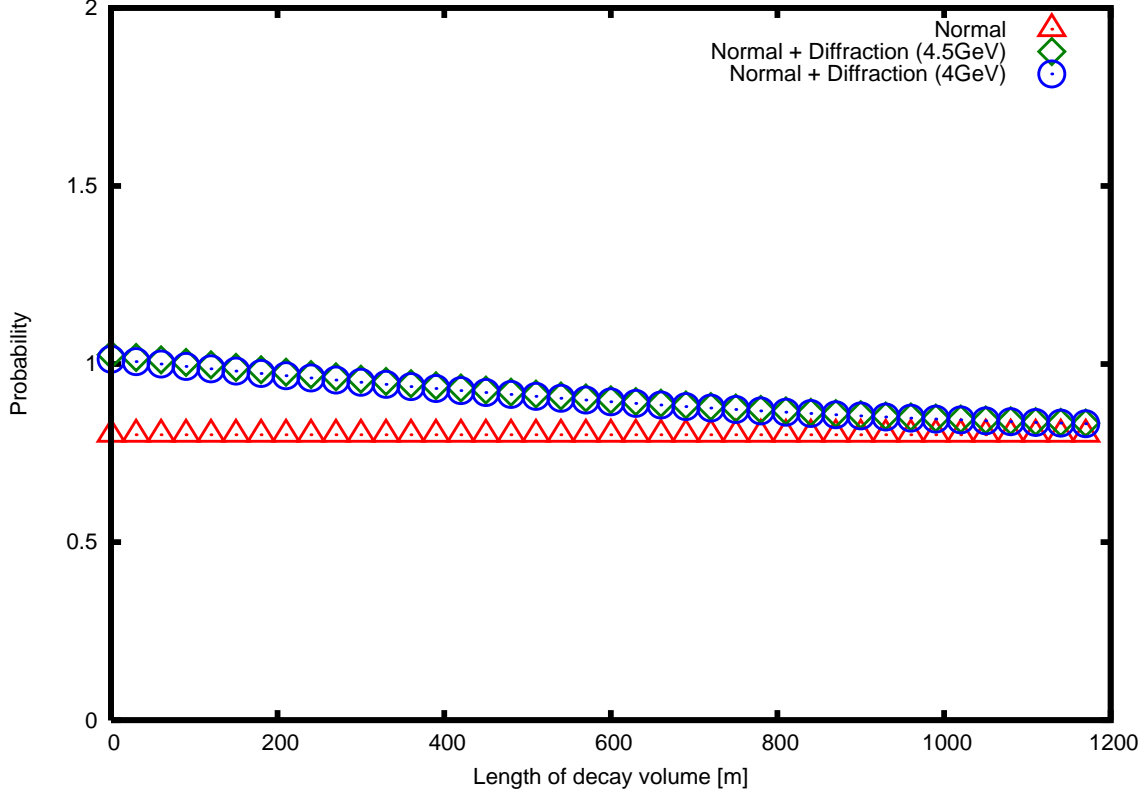


FIG. 7. The total probability per unit time of the event that the neutrino is detected in any angle at L is given. The constant shows the normal term and the diffraction term is written on top of the normal term. The horizontal axis shows the distance in [m] and the total probability is normalized to a unity at $L = 0$. The excess becomes less clear than the forward direction, but is seen in the distance below 1200 [m]. The neutrino mass, pion energy, neutrino energy are 1.0 [eV/c²], 4 [GeV] and 4.5 [GeV], and 800 [MeV]. A target nucleus with which the neutrino interacts in a detector is ¹⁶O.

the energy 100 [MeV] is given in Fig. 9. The slowly decreasing component of the probability becomes more prominent with lower values. Hence to observe this component, the experiment of the lower neutrino energy is more convenient. We plot P/T for $m_\nu = 0.1$ [eV/c²], $E_\nu = 10$ [MeV] in Fig. 10. P/T decreases more slowly than before. So in order to observe the T-dependent behavior for the small neutrino mass less than or about the same as 0.1 [eV/c²], the electron neutrino should be used. The decay of the muon and others will be studied in a forthcoming paper.

From Eq. (276), and $\tilde{g}(T, \omega_\nu) = \frac{c\omega_\nu}{2T}$ at a large T , the typical length l_0 for the decreasing

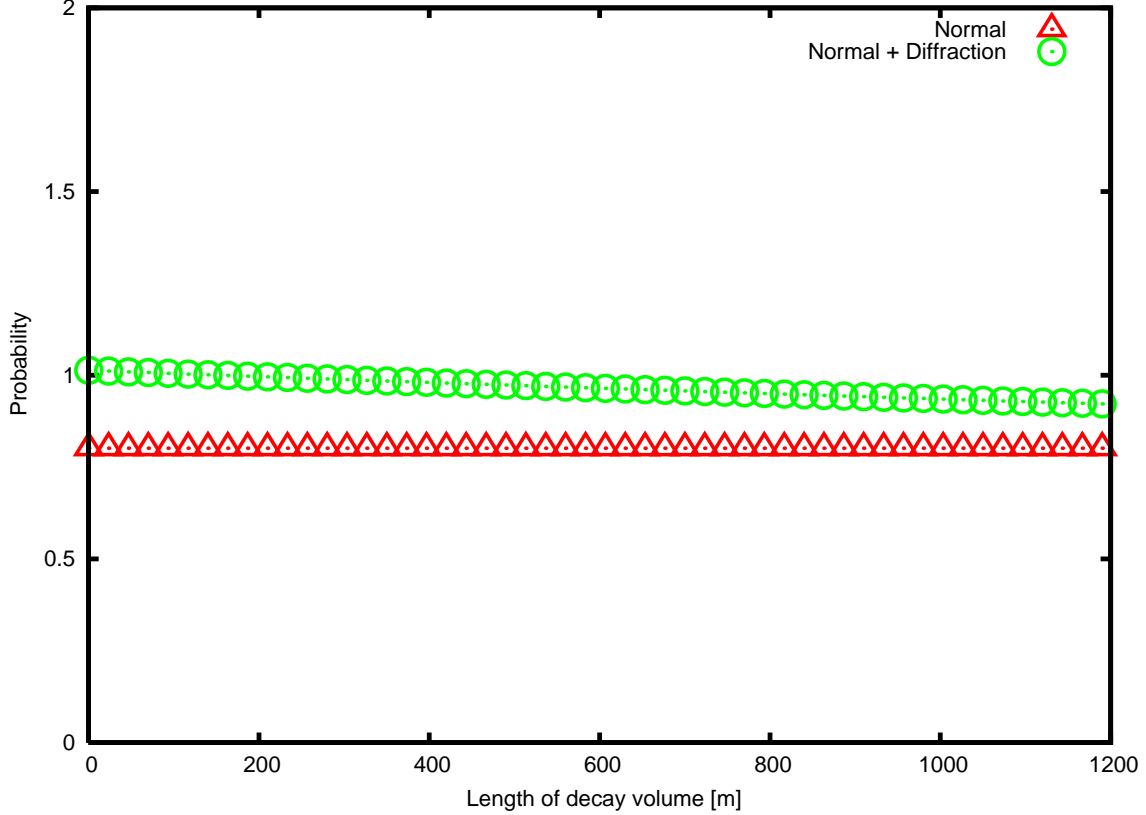


FIG. 8. The total probability per unit time of the event that the neutrino is detected in any angle at L is given. The constant shows the normal term and the diffraction term is written on top of the normal term. The horizontal axis shows the distance in [m] and the probability of the normal term is normalized to 0.8. Clear uniform excess is seen in the distance below 1200 [m]. The neutrino mass, pion energy, neutrino energy are 0.6 [eV/ c^2], 4 [GeV], and 800 [MeV]. A target nucleus with which the neutrino interacts in a detector is ^{16}O .

behavior is

$$l_0 \text{ [m]} = \frac{2E_\nu \hbar c}{m_\nu^2} = 400 \frac{E_\nu \text{ [GeV]}}{m_\nu^2 \text{ [eV}^2/c^4]}. \quad (296)$$

By observing this behavior, the neutrino absolute mass would be determined. The neutrino's energy is measured with uncertainty ΔE_ν , which is of the order of $0.1 \times E_\nu$. This uncertainty is 100 [MeV] for the energy 1 [GeV] and is accidentally same order as that of the minimum uncertainty $\hbar/|\delta\vec{x}|$ derived from the nuclear size $|\delta\vec{x}|$. The total probability for a larger value of energy uncertainty is easily computed using Eq. (288). Figures 4-7 show the distance dependence of the probability. If the mass is around 1 [eV/ c^2] the excess of the neutrino flux of about 20 percent at the distance less than a few hundred meters is found. We use mainly

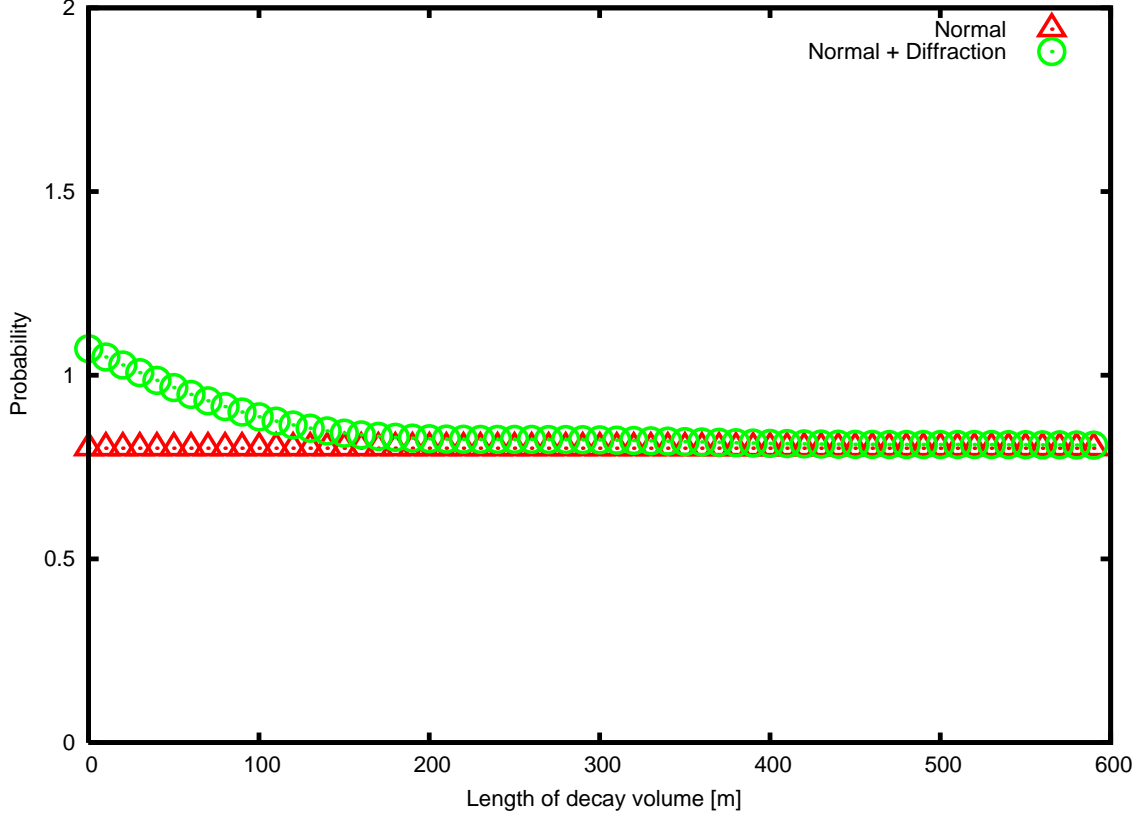


FIG. 9. The total probability per unit time of the event that the neutrino is detected in any angle at L is given. The constant shows the normal term and the diffraction term is written on top of the normal term. The horizontal axis shows the distance in [m] and the probability of the normal term is normalized to 0.8. Clear excess and decreasing behavior are seen in the distance below 600 [m]. The neutrino mass, pion energy, neutrino energy are 1 [eV/c²], 4 [GeV], and 100 [MeV]. A target nucleus with which the neutrino interacts in a detector is ¹⁶O.

$m_\nu = 1$ [eV/c²] throughout this section. Because the rate has a constant term and the T-dependent term, the T-dependent term is extracted easily by subtracting the constant term from the total rate. The slowly decreasing component decreases with the scale l_0 determined by the neutrino's mass and the energy.

3. Energy dependence

The energy spectrum of the neutrino is studied next. Since the correction term has the origin in the final states that do not conserve the kinetic energy, that shows unusual behavior. In Fig. 11, the spectrum for the neutrino mass and pion energy, 1.0 [eV/c²] and

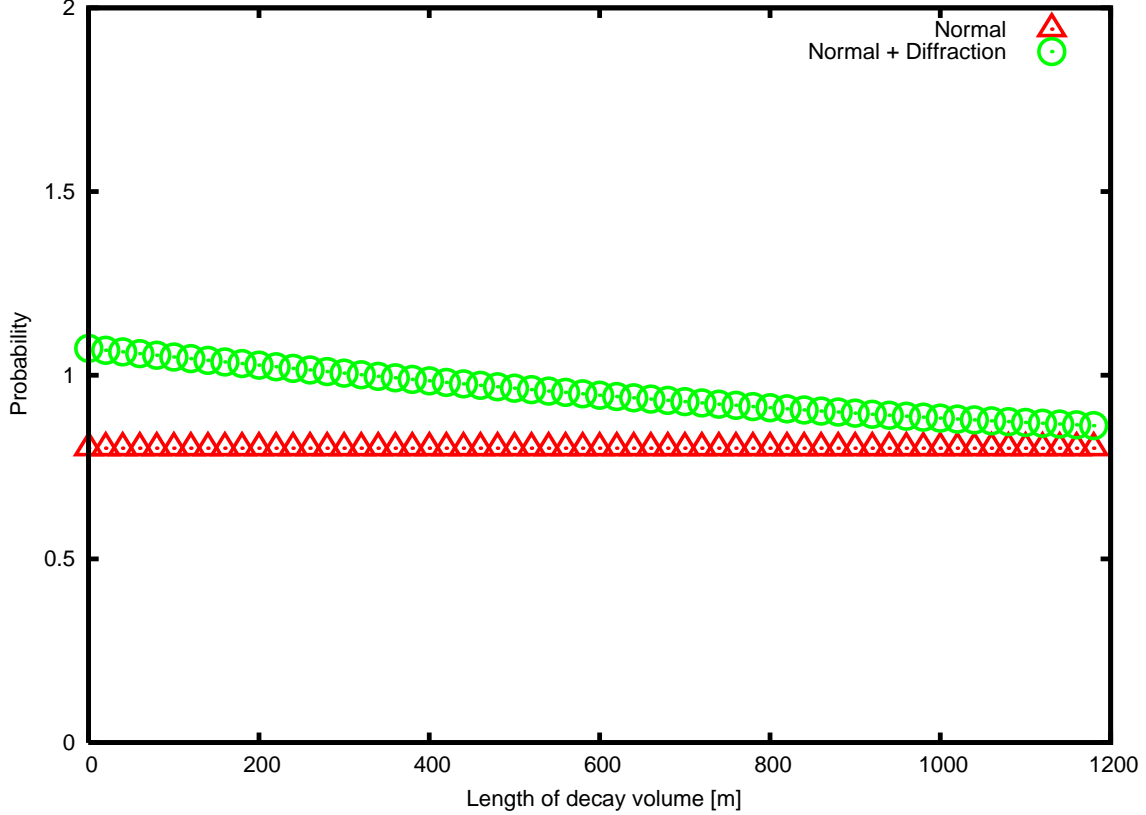


FIG. 10. The probability per unit time of the event that the neutrino is detected in any angle at L is given. The constant shows the normal term and the diffraction term is written on top of the normal term. The horizontal axis shows the distance in [m] and the probability is normalized to 0.8. Clear excess is seen in the distance below 1200 [m]. The neutrino mass, pion energy, neutrino energy are 0.1 [eV/ c^2], 4 [GeV], and 10 [MeV]. A target nucleus with which the neutrino interacts in a detector is ^{16}O .

4 [GeV], are given. The spectrum of the normal term is flat, whereas that of the diffraction is not flat and has a maximum at the energy $E_\nu \approx E_{\nu,max}/3$. The former is caused by the fact that the neutrino energy in the rest system is fixed to one value from the energy-momentum conservation, whereas that of the diffraction is not fixed to one value from the non-conservation of the kinetic energy. A unique property of the correction term for neutrino is identified by its energy spectrum.

The energy spectrum of the normal and correction terms from a pion at rest for the wave packet size of the momentum width 5 [MeV] is given in Fig. 12. The spectrum has a peak

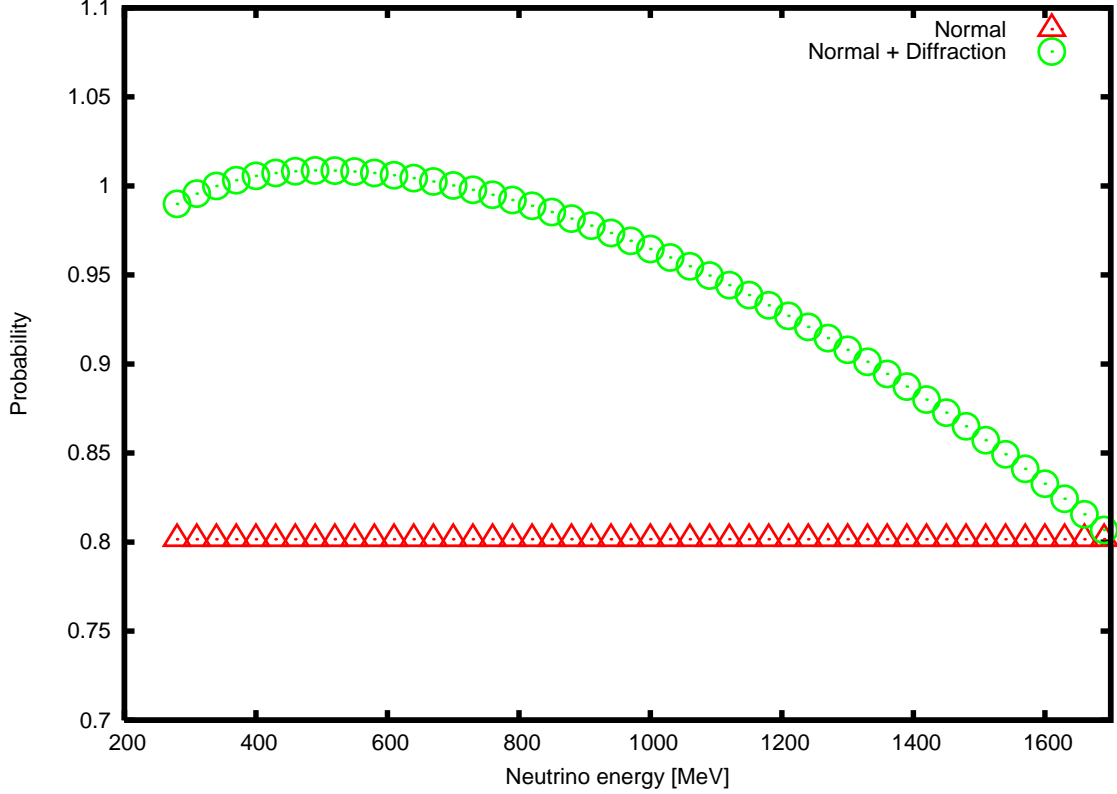


FIG. 11. The energy dependence of probability of the event that the neutrino is detected in any angle at distance $L = 100$ [m] is given. The lower curve shows the normal term and the correction term is added on top of the normal term. The horizontal axis shows the neutrino energy in [MeV] and the probability of the normal term is normalized to 0.8. The neutrino mass and pion energy are 1.0 [eV/ c^2] and 4 [GeV]. A target nucleus with which the neutrino interacts in a detector is ^{16}O .

at the value derived from the energy-momentum conservation,

$$m_\pi = E_\nu + E_\mu, \quad \vec{p}_\nu + \vec{p}_\mu = 0 \quad (297)$$

of the two-body decay. The neutrino energy is uniquely determined to the value

$$E_\nu = \frac{m_\pi^2 - m_\mu^2}{2m_\pi}, \quad (298)$$

for plane waves, but the spectrum becomes broad due to the finite wave packet effect. The correction term derived from the leading singularity is shown in the low energy region at the length is $L = 10$ [m].

Figure 13 shows the energy spectrum of the fraction of the correction term over the normal term for various parameters of the pion energy and distance, which are computed

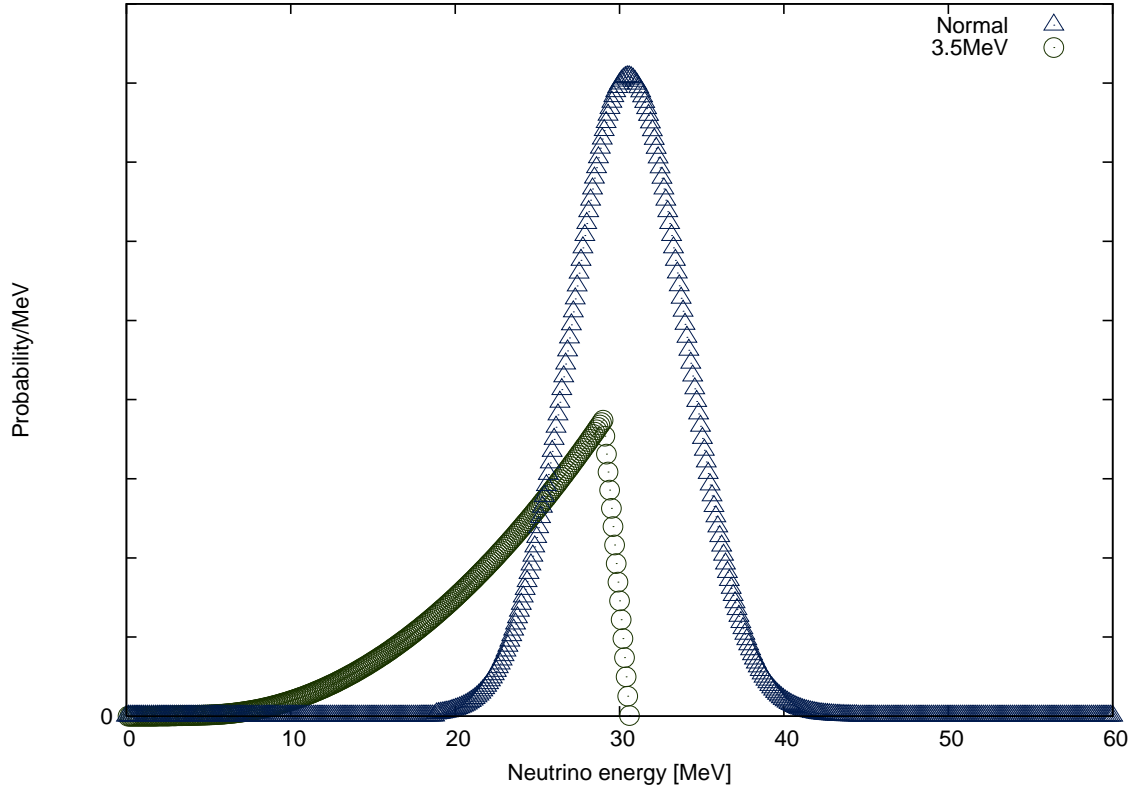


FIG. 12. The energy dependence of probability of the event that the neutrino is detected in the rest system of the pion are given for the wave packet size of 5 [MeV]. The normal component becomes wide due to the wave packet effect. The diffraction component has lower energies and is wider than the normal component. The magnitude of the diffraction term is arbitrary. The neutrino mass is 1.0 [eV/c²]. The length is L = 10 [m].

with the $(V - A) \times (V - A)$ interaction and is represented in a latter section (Sec.7.3) for ^{56}Fe . The neutrino spectrum varies depending on the pion energy. Only the leading term was taken into account. Because the neutrino has the energy different from that of the kinetic-energy conserving term, this component would have been misunderstood as a background that is not connected with the system. This component is derived from the Schrödinger equation, and appears at all times. The finite-size correction is not invariant under the Lorentz transformation and its magnitude becomes larger in higher energy. Thus the fraction of the electron mode varies with the pion's energy. **This unusual behavior is a characteristic feature of the correction component.** Our result, in fact, shows that this background becomes larger as the pion's energy becomes larger but has the universal

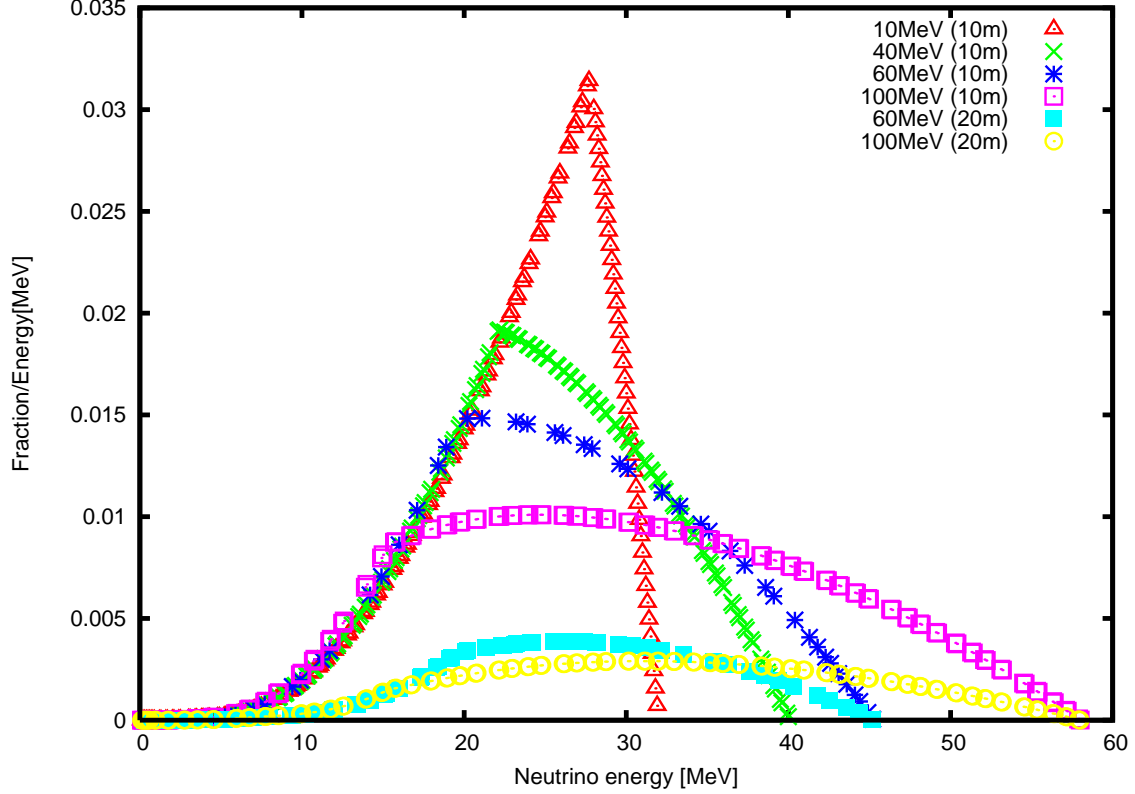


FIG. 13. The fraction of the correction term over the normal term of the event that the neutrino of certain energy is detected. The fractions are given for the energy of the pion 10, 40, 100 [MeV/c] and the length $L = 10$ [m], and for the energy of the pion 60, 100 [MeV/c] and the length $L = 20$ [m]. Target is ^{56}Fe . The fraction is small in lower energy and larger in higher energy. The correction term may be observable in these energy regions too. The neutrino mass is 1.0 [eV/c²].

property.

4. Wide distribution of pion momentum

When a momentum distribution $\rho_{exp}(\vec{p}_\pi)$ of initial pions is known, an energy-dependent probability is computed using the expression Eq. (288). Equation (288) is also independent of the position \vec{X}_π and depends upon a pion momentum and a neutrino momentum and the time interval $T = T_\nu - T_\pi$. In experiments, a position of a pion is not measured and an average over a position is made. An average probability agrees with Eq. (288). This probability varies slowly with the pion's momentum and is regarded constant in the energy range of the order of 100 [MeV]. So the experimental observation of the correction term is

quite easy.

C. On the universality of the finite-size correction

The finite-size correction of the probability of the event that the neutrino is detected has various unique properties.

This component is constant in T , hence the total probability is not proportional to T in this region. In classical particle's decay, the decay process occurs randomly and follows Markov process. Hence an average number of the event is necessary proportional to T . Now due to the finite-size correction, this property does not hold. This is not surprising in $L \leq l_0$, because the quantum mechanical interference modifies the probability.

The finite-size correction is expressed with the universal function $\tilde{g}(T, \omega_\nu)$, where $\omega_\nu = m_\nu^2/(2E_\nu)$. This is determined only with the mass and energy of the neutrino and is independent of details of other parameters of the system such as the size, shape, and position of the wave packets and others. Hence the correction has the genuine property of the wave function $|\text{muon, neutrino}(t)\rangle$, of Eq. (180), and is capable of experimental measurements.

1. Violation of kinetic-energy conservation

The probability computed with $S[T]$ reflects the wave function at a finite time t , and the states of non-conserving kinetic energy lead the finite-size correction. So conservation laws derived from the space-time symmetry get modified and various probabilities become different from those of $T \rightarrow \infty$. The leading finite-size corrections have, nevertheless, universal forms that are proportional to $\tilde{g}(T, \omega)$.

2. Comparisons on the neutrino finite-size correction with diffraction of classical waves through a hole

a. Inelastic channel.

The correction for neutrino emerges as a macroscopic quantum phenomenon. The neutrino of varying kinetic energies is expressed with the many-body wave function composed of the pion, muon, and neutrino. Accordingly, the probability of the event that the neutrino

is detected becomes very different from that of the free isolated neutrino, and its probability receives the large finite-size correction of the universal behavior. Its magnitude is determined by the overlap of wave functions, and depends on the wave packet size. So the finite-size correction is determined by both of initial and final states. We should note that quantum mechanical probability is determined with the overlap of the in-coming waves with the out-going waves and depends on the both states.

In a classical wave phenomenon, on the other hand, an intensity of the wave is determined uniquely with the in-coming wave. Its magnitude is directly observed. Hence the finite-size correction and the interference pattern are determined only by the in-coming wave. Thus interference of the quantum mechanical wave is different from that of the classical wave.

b. Pattern in longitudinal direction

The finite-size correction results from the wave natures at a finite time t , and is generated by the states orthogonal to the states at $t \rightarrow \infty$. Hence its magnitude is positive semi-definite and depends on the time interval T . Consequently the neutrino flux at a finite t has the excess that decreases with the distance in the direction to the neutrino momentum and vanishes at the infinite distance.

The diffraction pattern of light through a hole or the interference pattern of light in a double slit experiment are those of classical waves and different. The intensity has modulations in the perpendicular direction to the wave vector. The interference term is a product of two waves of different phases and so oscillates. Integrating the intensity over the whole screen, the oscillating interference terms cancel and the total intensity is constant.

Thus the pattern of the neutrino is very different from that of light.

c. ω_ν is Einstein minus de Broglie frequencies

The pattern of the finite-size correction for neutrino is determined by the angular velocity $\omega_{\nu,diff} = \omega_{\nu,E} - \omega_{\nu,dB}$. Since $\omega_{\nu,E}$ and $\omega_{\nu,dB}$ are almost the same, they are almost cancelled and $\omega_{\nu,diff}$ becomes extremely small and stable in E_ν .

The interference pattern of the light on the screen of the double slit experiment, on the other hand, is determined with the angular velocity $\omega_{\gamma,dB}$. Since $\omega_{\gamma,dB}$ is large and proportional to the energy, the pattern varies rapidly with the position in the screen and with the energy. The diffraction pattern of the light passing through the hole varies rapidly.

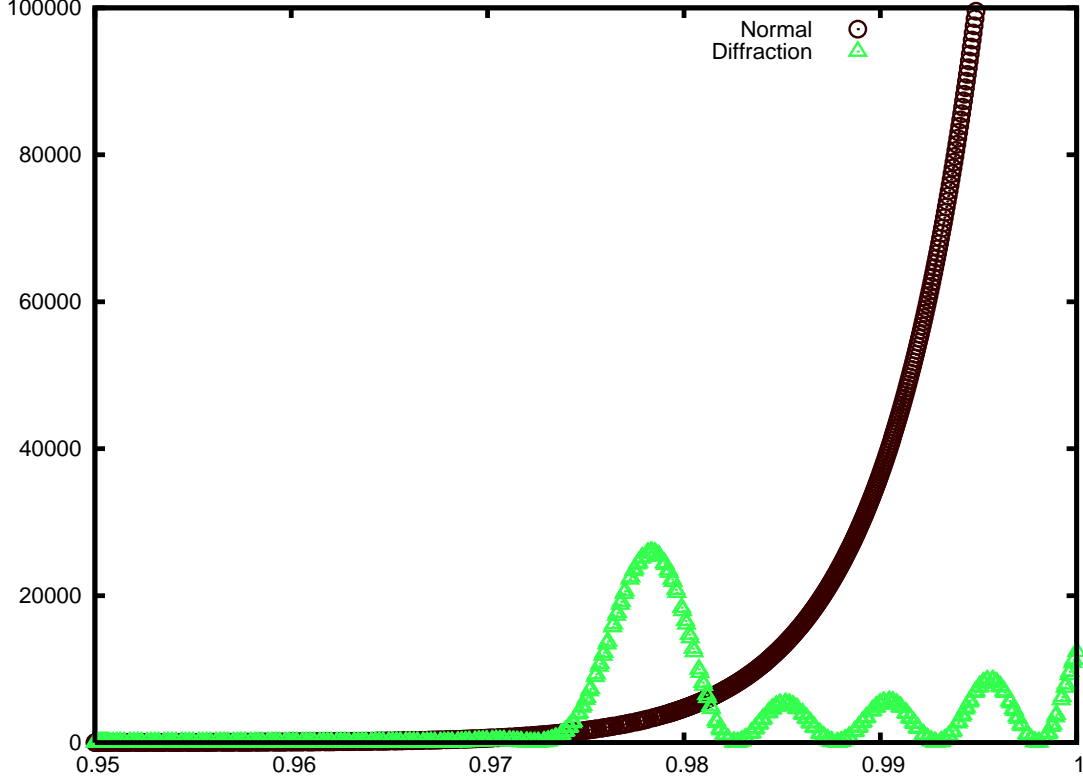


FIG. 14. The probabilities of the events that the neutrino are detected at certain angle in the normal and correction terms are given. The large peak toward $\cos \theta = 1$ shows the normal component and the small peaks at the tail of the previous peak show the correction component. The horizontal axis shows the cosine of the angle between \vec{p}_ν and $\vec{p}_\pi - \vec{p}_\mu$ and the vertical axis shows the probability. The pion energy, muon energy, and time interval are $250 m_\nu$, $210 m_\nu$, and $30 m_\nu^{-1}$.

3. Muon in the pion decay

In experiments of observing the muon in the pion decays, the neutrino is not observed. In this situation, the finite-size correction for the muon has a magnitude that is determined by the ratio of the mass and energy, $m_\mu^2/(2E_\mu)$. Since the muon mass is larger than the neutrino mass by 10^8 , the value $m_\mu^2/(2E_\mu)$ for the muon is much larger than that of the neutrino by 10^{16} . For the muon of energy 1 [GeV], the length is of the order of $l_0 = 10^{-14}$ [m]. This value is a microscopic size and $\tilde{g}(T, \omega_\mu)$ vanishes at a macroscopic T. Hence the probability of the event for the muon at the macroscopic distance becomes constant. The muon from the pion decay has no finite-size correction. This probability agrees with the production probability. The muon and neutrino behave differently at the finite distance.

If the muon is observed under a condition that the neutrino is detected at the finite T , $S[T]$ is applied and the probability of the event that the muon is detected has the contribution from the neutrino diffraction. The diffraction component gives a wide energy spectrum for the muon since that comes from the tail of the distribution function. Fig. 14 shows a probability integrated over the neutrino energy in this condition that both the muon and neutrino are detected, which is obtained from Eq. (210). In this figure, we use units $c = 1, \hbar = 1$ and express the energy and time with the neutrino mass m_ν . Energy of the pion is $250 m_\nu$ and the muon has the energy $210 m_\nu$ and has an angle with the pion of $\cos \theta = 0.95 - 1$. The cosine of the angle between $\vec{p}_\pi - \vec{p}_\mu$ and \vec{p}_ν is in the horizontal axis. T is $30 m_\nu^{-1}$. The neutrino mass of an unphysical magnitude of the order of MeV and the value of T are chosen in such manner that the numerical computation of diffraction component is easily made. Qualitative features of Fig. 14 are that there exist a large peak at $\cos \theta \approx 1$ and small peaks at the tail region. The former is the peak from the root of $\omega = 0$ at $\delta\vec{p} \approx 0$ and $\delta E = 0$ and the latter are the peaks from the roots of $\omega = 0$ of $\delta\vec{p} \neq 0$ and $\delta E \neq 0$. The latter peaks, which do not exist in the probability of detecting only the muon, show the feature of the diffraction component of the probability when the neutrino is detected. Thus the diffraction component is observed in the muon also when the neutrino is detected simultaneously. Experimental verification of the diffraction term of this situation using the muon may be made in future.

As was shown in Section 3, the production rate is common to the muon and neutrino, since they are produced in the same decay process. However because they propagate differently, they are detected independently with the apparatus. The rates are then different. The probability of the event that the neutrino is detected is affected by the large $P^{(d)}$, but that for the muon is negligibly small.

If both particles are measured simultaneously, the rates for both are the same.

Thus the wave-zone for neutrino is quite wide, and the transition amplitude for a neutrino at a finite distance detected by a nucleus becomes different from that of the infinite distance. The neutrino wave is a superposition of those waves that are produced at different space-time positions and the probability is modified by the diffraction term. The overlap between the neutrino wave that is detected with a nucleus in a detector and those that are produced from a pion decay shows the neutrino diffraction of unique properties. So the neutrino flux measured with its collisions with a nucleus in targets is different from that defined from the

norm of wave function.

VII. IMPLICATIONS

In this section, various physical quantities of neutrino processes which are modified by the finite-size correction are studied. Particularly neutrino nucleon total cross sections, quasi-elastic cross sections, electron-neutrino production anomaly, a proton target enhancement, and an anomaly in atmospheric neutrino are such processes that have significant contributions from the neutrino diffraction.

A. Total cross sections of $\nu_\mu N$ scattering

Neutrino collisions with hadrons in high-energy regions are understood well with the quark-parton model. A total cross section of a high-energy neutrino is proportional to the energy and is written in the form

$$\sigma^\nu = \frac{M_N E_\nu G_F^2}{\pi} (Q + \bar{Q}/3), \quad (299)$$

using integrals of quark-parton distribution functions $q(x)$ and $\bar{q}(x)$ and $Q = \int_0^1 dx x q(x)$, $\bar{Q} = \int_0^1 dx x \bar{q}(x)$. The cross section is proportional to the neutrino energy and a current value is $\sigma_\nu/E = 0.67 \times 10^{-38} [\text{cm}^2/\text{GeV}]$.

Now the rate of process of the neutrino produced in a decay of a pion and reacts with a nucleus at a finite distance has a finite-size correction. It modifies the probability of the event that the neutrino collides with the nucleus in target. We estimate its effect hereafter. Including the diffraction term, the effective neutrino flux becomes the sum of the normal and diffraction terms

$$f = f^{(0)}(1 + r^{(d)}), \quad (300)$$

where $f^{(0)}$ is a flux derived from the normal component, and $r^{(d)}$ is the rate of the diffraction component over the normal component and is a function of the combination $(\frac{m_\nu^2}{2cE_\nu}L)$,

$$r^{(d)} = d_0 \tilde{g}(\frac{m_\nu^2}{2cE_\nu}L), \quad (301)$$

where L is a length of the decay volume and the coefficient d_0 is determined from geometries of experiments.

When a detector is located at the end of the decay volume, the correction factor Eq. (301) is used. In actual case, the detector is located in a distant region from the decay volume. There are material or soil between them and pions are stopped in beam dump. The neutrino is produced in the decay region and propagates freely afterward. Since the wave packets of one σ_ν form the complete set [5], the wave packet of the size at the decay volume is the σ_ν determined with the detector. The neutrino flux at the end of the decay volume is computed with the diffraction term of the decay volume 's length L and the wave packet size of the detector. Wave packets of this σ_ν propagate freely from the end of decay volume to the detector. The final value of neutrino flux at the detector is found combining both effects. When neutrino changes its flavor in this period, the final probability for each flavor is written with a usual formula of flavor oscillation.

The true neutrino events in experiment is converted to the cross section $\sigma^{exp}(E_\nu)$ that includes the diffraction component and is connected with the cross section computed with only the normal component $\sigma^{the}(E_\nu)$ by the rate

$$\sigma^{the}(E) = \sigma^{exp}(E_\nu) \frac{1}{1 + r^{(d)}}. \quad (302)$$

Conversely the experimental cross section is written as

$$\sigma^{exp}(E_\nu)/E_\nu = (1 + r^{(d)})(\sigma^{the}(E_\nu)/E_\nu). \quad (303)$$

$\sigma^{the}(E_\nu)/E_\nu$ is constant from Eq. (299) so the E-dependence of $\sigma^{exp}(E_\nu)/E_\nu$ is due to E-dependence of $r^{(d)}$, Eq. (301).

The correction $r^{(d)}$ depends on the geometry of experiments and the material of the detector. We compute $r^{(d)}$ using the experimental conditions of MINOS [46] and NOMAD [47] and the total cross sections. The geometry of MINOS and NOMAD are the following. The lengths between the pion source and the neutrino detector, L_{det-so} , and those of the decay region, $L_{decay-reg}$, are:

$$NOMAD : L_{det-so} = 835 \text{ [m]}, L_{decay-reg} = 290 \text{ [m]}, \quad (304)$$

$$MINOS : L_{det-so} = 1040 \text{ [m]}, L_{decay-reg} = 675 \text{ [m]}. \quad (305)$$

Also pion beam spreading was included from angle of initial pion; 0 to 10 [mrad] for NOMAD and 0 to 15 [mrad] for MINOS.

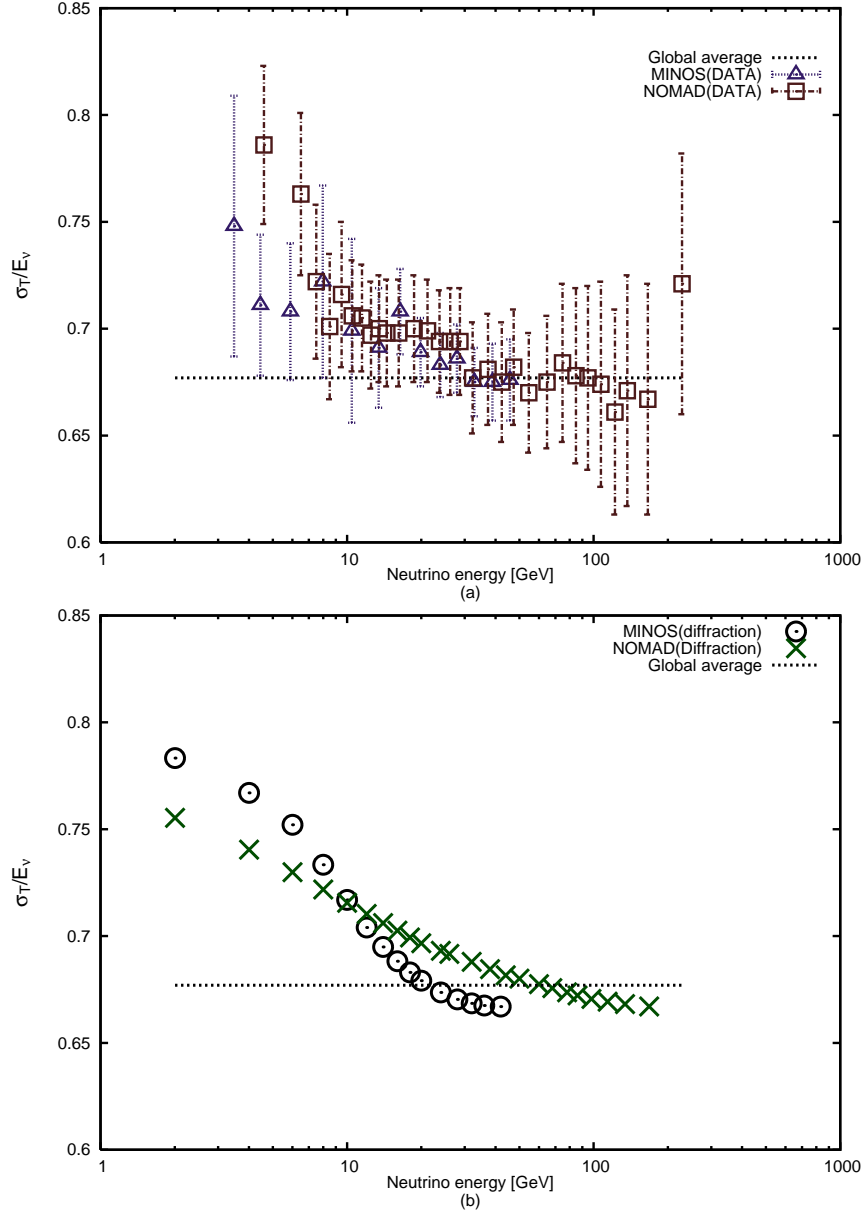


FIG. 15. Neutrino-Nucleon total cross section of MINOS and NOMAD (a) and total cross sections of the sums of normal and correction terms in geometries of MINOS and NOMAD (b) are given. The horizontal axis shows the neutrino energies in [GeV] and the vertical axis shows the ratio of the cross section over the energy.

The wave packet size is estimated with the size of target nucleus. From the size of the nucleus of the mass number A , we have $\sigma_\nu = A^{2/3}/m_\pi^2$. For various material the value are

$$\sigma_\nu = 5.2/m_\pi^2; \text{ } ^{12}\text{C nucleus}, \quad (306)$$

$$\sigma_\nu = 14.6/m_\pi^2; \text{ } ^{56}\text{Fe nucleus}. \quad (307)$$

Including the geometries, beam spreadings, and wave packet sizes, we computed the total cross sections and compared with the experiments in Fig. 15. These cross sections computed theoretically slowly decrease with the energy in the geometry dependent manner and agree with the experiments. Since the experimental parameters such as the neutrino energy and others are different in two experiments, the agreements of the theory with the experiments are highly non-trivial. So the large cross sections at low-energy regions may be attributed to the diffraction component.

We have compared only NOMAD and MINOS here. Many experiments are listed in particle data [22] and most of them have similar energy dependences and agree qualitatively with the presence of the diffraction components. It is important to notice that the magnitude of diffraction component is sensitive to geometry. Furthermore, if a kinematical constraint Eq. (279) on the angle between \vec{p}_π and \vec{p}_ν was required, only the events of the normal term was selected. Then the cross section should agree with that of the normal term.

B. Quasi-elastic cross sections

Quasi-elastic or one pion production processes are understood relatively well theoretically. The diffraction modifies the total events of these processes also.

The cross sections for

$$\nu + n \rightarrow \mu^- + p(+\pi^0), \quad (308)$$

$$\nu + p \rightarrow \mu^- + p + \pi^+, \quad (309)$$

$$\bar{\nu} + p \rightarrow \mu^+ + n(+\pi^0), \quad (310)$$

and the neutral current process

$$\nu + N \rightarrow \nu + N(+\pi^0), \quad (311)$$

are known well using CVC, PCAC, and vector dominance and are studied recently by Mini-BooNE [48]. The parameter is the axial vector meson M_A and higher mass contributions. So these cross section are used to study the diffraction terms.

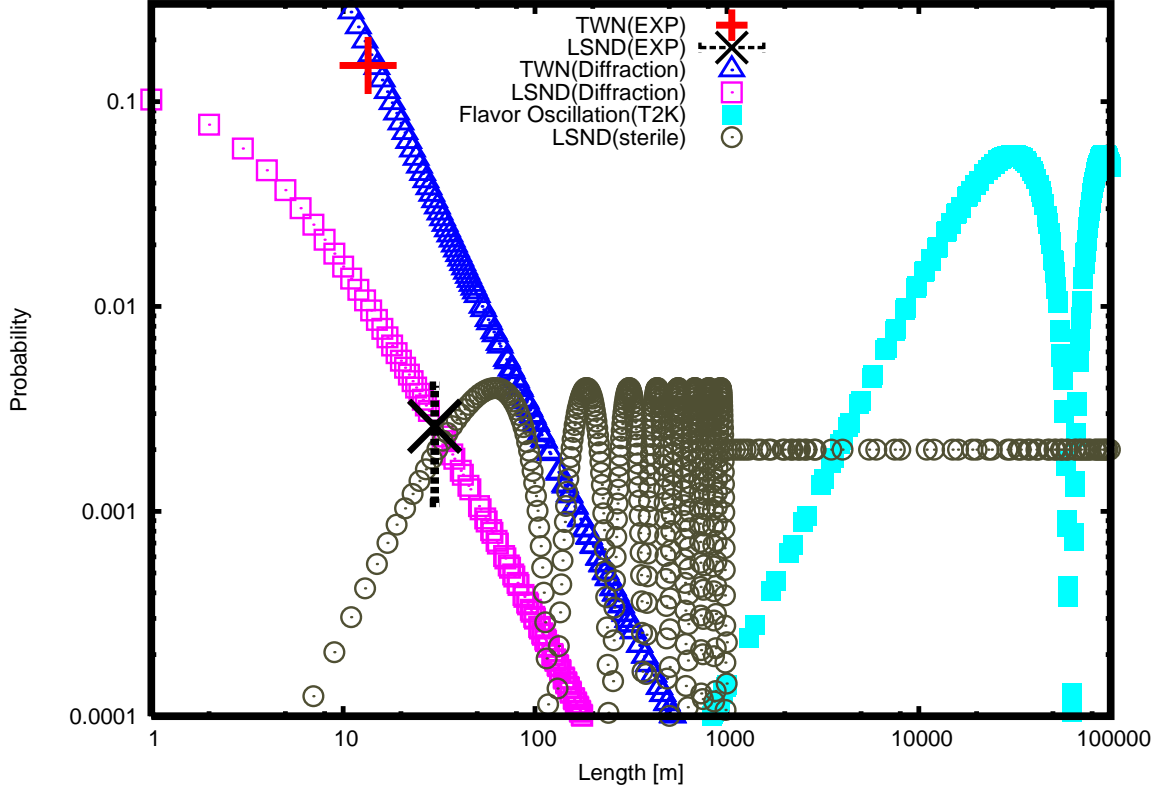


FIG. 16. Experiments of LSND and TWN are compared with the theoretical values of the correction terms. TWN(EXP) and LSND(EXP) show the experimental values and TWN(Diffraction) is computed with the parameters $m_\nu = 0.2$ [eV/c²], $E_\nu = 250$ [MeV], $P_\pi = 2$ [GeV/c], LSND(Diffraction) is computed with $m_\nu = 0.2$ [eV/c²], $E_\nu = 60$ [MeV], $P_\pi = 300$ [MeV/c]. Flavor oscillation oscillation(T2K) [49] shows the values for $\sin^2 \theta_{13} = 0.11$, $\delta m_{23}^2 = 2.4 \times 10^{-3}$ [eV²/c⁴], $E_\nu = 60$ [MeV], and LSND(sterile) shows with $\sin^2 \theta = 0.004$, $\delta m^2 = 1.2$ [eV²/c⁴], $E_\nu = 60$ [MeV].

C. Electron neutrino anomaly

In pion decays, a branching ratio of an electron mode is smaller than that of a muon mode by factor 10^{-4} due to the helicity suppression of the decay of a pseudo-scalar particle caused by the charged current interaction. [12–15]. This behavior of the total rates has been confirmed by the observations of charged leptons.

Now the probability of the event that a neutrino is detected inside the coherence length, where the neutrino retains the wave natures, is affected by the finite-size correction. Because this correction comes from the states that have different kinetic-energy from the initial value, the neutrino in this region does not follow the conservation law satisfied in the asymptotic

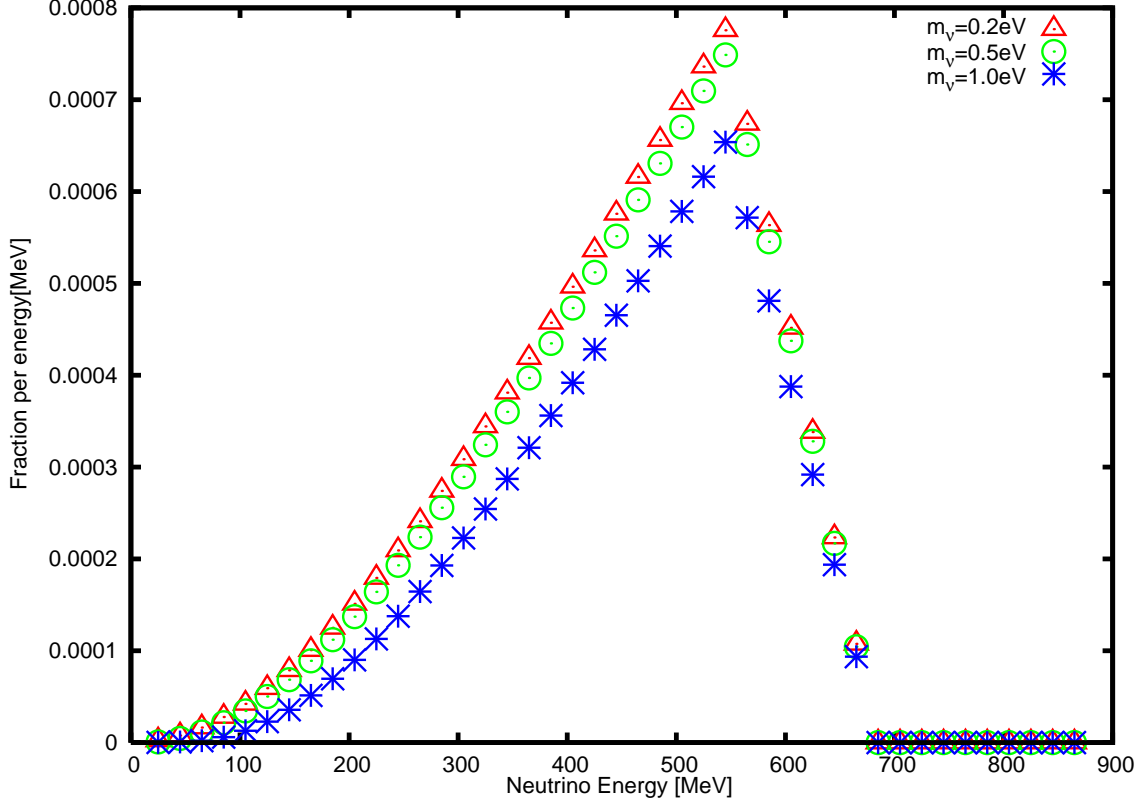


FIG. 17. Fraction of the electron neutrino of the mass 0.2 [eV/c²], 0.5 [eV/c²] and 1[eV/c²] at L=110 [m], distance=170 [m] of T2K geometry and $P_\pi = 2$ [GeV/c].

region $t \rightarrow \infty$. The rate that electron neutrino is detected is not suppressed. The ratio of the probability of the event that the electron neutrino is detected over that of the muon neutrino event becomes substantially larger in near-detector regions.

To compute the transition probability and the spectra of electron and muon neutrinos, we start from the $(V - A) \times (V - A)$ interaction Lagrangian (Hamiltonian). The result of the probability is almost the same as that of Eq. (174) in the muon mode but is different in the electron mode since the diffraction component does not satisfy the rigorous conservation of the kinetic-energy and momentum. In I, it was found that the initial pion is described by a wave packet of a large size. Hence the initial pion of the plane wave is studied here. The amplitude \mathcal{M} is written with the hadronic $V - A$ current and Dirac spinors in the form

$$\mathcal{M} = \int d^4x d\vec{k}_\nu N \langle 0 | J_{V-A}^\mu(x) | \pi \rangle \bar{u}(\vec{p}_l) \gamma_\mu (1 - \gamma_5) \nu(\vec{k}_\nu) \times e^{ip_l \cdot x + ik_\nu \cdot (x - X_\nu) - \frac{\sigma_\nu}{2} (\vec{k}_\nu - \vec{p}_\nu)^2}, \quad (312)$$

where $N = ig (\sigma_\nu / \pi)^{\frac{4}{3}} (m_l m_\nu / E_l E_\nu)^{\frac{1}{2}}$, and the time t is integrated in the region $T_\pi \leq t \leq T_\nu$.

$\delta L_{int} = \frac{\partial}{\partial x_\mu} G^\mu$ in Eq. (177) is included in the amplitude Eq. (312), hence $P^{(d)}$ is neither proportional to $m_{electron}^2$ nor suppressed. The transition probability to this final state is written, after the spin summations are made, with the correlation function and the neutrino wave function in the form

$$\int \frac{d\vec{p}_l}{(2\pi)^3} \sum_{s_1, s_2} |\mathcal{M}|^2 = \frac{N_1}{E_\nu} \int d^4x_1 d^4x_2 e^{-\frac{1}{2\sigma_\nu} \sum_i (\vec{x}_i - \vec{x}_i^0)^2} \Delta_{\pi, l}(\delta x) e^{i\phi(\delta x)}, \quad (313)$$

where $N_1 = g^2 (4\pi/\sigma_\nu)^{\frac{3}{2}} V^{-1}$, V is a normalization volume for the initial pion, $\vec{x}_i^0 = \vec{X}_\nu + \vec{v}_\nu(t_i - T_\nu)$, $\delta x = x_1 - x_2$, $\phi(\delta x) = p_\nu \cdot \delta x$ and

$$\Delta_{\pi, l}(\delta x) = \frac{1}{(2\pi)^3} \int \frac{d\vec{p}_l}{E(\vec{p}_l)} (2(p_\pi \cdot p_\nu)(p_\pi \cdot p_l) - m_\pi^2(p_l \cdot p_\nu)) e^{-i(p_\pi - p_l) \cdot \delta x}. \quad (314)$$

The probability of the event that a neutrino of p_ν is detected at \vec{X}_ν is expressed as the sum of the normal term G_0 and the diffraction term $\tilde{g}(T, \omega_\nu)$,

$$P = N_2 \int \frac{d^3p_\nu}{(2\pi)^3} \frac{p_\pi \cdot p_\nu (m_\pi^2 - 2p_\pi \cdot p_\nu)}{E_\nu} [\tilde{g}(T, \omega_\nu) + G_0], \quad (315)$$

where $N_2 = 8Tg^2\sigma_\nu$ and $L = cT$ is the length of decay region. In G_0 , the energy and momentum are conserved approximately well and

$$p_l \approx p_\pi - p_\nu \quad (316)$$

is satisfied. Hence from a square of the both hand sides, the mass shell condition

$$m_l^2 \approx m_\pi^2 - 2p_\pi \cdot p_\nu \quad (317)$$

is obtained. Thus the normal terms are proportional to the square of lepton masses and the electron mode is suppressed [12–15]. In $\tilde{g}(T, \omega_\nu)$, on the other hand, momenta satisfy

$$p_l \neq p_\pi - p_\nu, \quad (318)$$

and the diffraction terms are not proportional to the square of lepton masses and the electron mode is not suppressed.

The total probability of the events that a neutrino or a charged lepton is detected in the pion decay at macroscopic distance is written in the form,

$$P = P^{(0)} + P_{lepton}^{(d)}. \quad (319)$$

In Eq. (319), $P^{(0)}$ is the normal term that is obtained from the decay probability G_0 in Eq. (315) and $P_{lepton}^{(d)}$ is the diffraction term that is determined from \tilde{g} in Eq. (315). The former

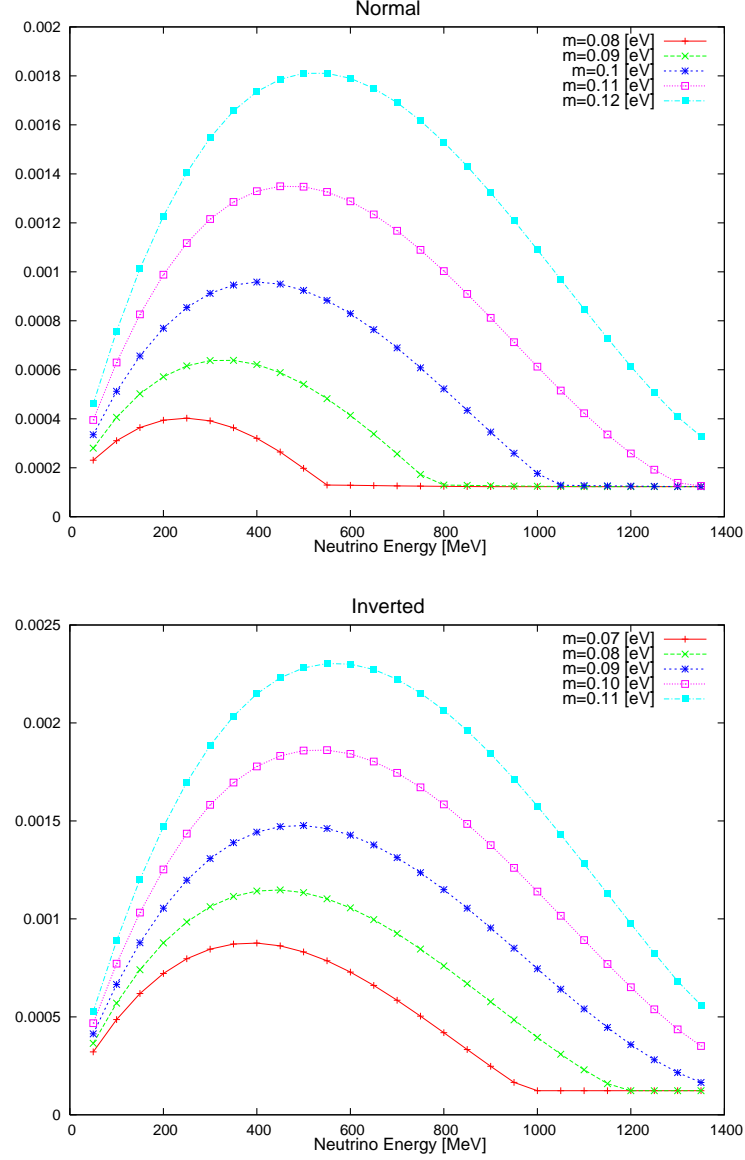


FIG. 18. Fraction of electron neutrino from a pion of 4 [GeV/c] in normal and inverted hierarchies at $L=110$ [m], distance=170 [m]. Pion's life time is included. The neutrino mass is 0.08(red-solid), 0.09(green-cross), 0.10(purple-cross), 0.11(pink-box), 0.12(blue-box) [eV/c²], for normal hierarchy, and 0.07(red-solid), 0.08(green-cross), 0.09(purple-cross), 0.10(pink-box), 0.11(blue-box) [eV/c²], for inverted hierarchy.

probability agrees to that obtained using the plane waves and the latter one has not been included before and its effect is estimated here. The diffraction term at T is described with its mass and energy in the universal form

$$P_{lepton}^{(d)}/\Gamma = \frac{8}{15}g^2m_\pi^4 \left(1 - \frac{m_\mu^2}{m_\pi^2}\right)^4 \left(1 + \frac{3m_\mu^2}{m_\pi^2}\right) \frac{m_\pi^2\sigma_\nu p_\pi}{\Gamma m_\nu^2}, \quad (320)$$

which decreases slowly with a distance L and vanishes at infinite distance. Hence at $L = \infty$, the probability agrees with the normal component,

$$P = P^{(0)} = \Gamma\Gamma. \quad (321)$$

The magnitude of $\tilde{g}(\Gamma, \omega_{lepton})$ at the macroscopic distance is given in Fig. 2. At $L = 100$ [m], $E = 1$ [GeV] for the mass 1 [eV/c²] (ν), 0.5 [MeV/c²] (e), and 100 [MeV/c²] (μ), the values are,

$$\begin{aligned} \tilde{g}(\Gamma, \omega_\nu) &\approx 3, \\ \tilde{g}(\Gamma, \omega_e) &\approx 0, \\ \tilde{g}(\Gamma, \omega_\mu) &\approx 0. \end{aligned} \quad (322)$$

In this region, they satisfy

$$\tilde{g}(\Gamma, \omega_l) \approx \frac{m_\nu^2}{m_l^2} \tilde{g}(\Gamma, \omega_\nu), \quad (323)$$

hence the diffraction component at a macroscopic distance is finite in the neutrino and negligibly small in others. It is striking that the probability of the event that the neutrino is detected has an additional term and is not equivalent to that of the charged lepton even though they are produced in the same decay process.

The conservation law of the kinetic energy is violated in $S[\Gamma]$, and results to the unique finite-size correction expressed as $P^{(d)}$ to the electron mode. Pion does not decay to massless Fermion and anti-Fermion in the weak $(V - A) \times (V - A)$ interaction when the kinetic energy, momentum, and angular momentum are conserved, and cause the suppression of the electron mode. This conditions hold in $S[\infty]$ and $P^{(0)}$, but does not in $S[\Gamma]$ and $P^{(d)}$. Consequently the electron mode in $P^{(d)}$ is not suppressed. We study non-suppression of the electron mode and other implications derived from $P^{(d)}$, here. In Fig. 16, experiments of LSND [51] and the two neutrino experiment(TWN) [52] are compared with the diffraction components and the flavor oscillations. Theoretical values are obtained including geometries of the experiments. Since those of LSND and TWN are different, the theoretical value for the LSND are smaller than that for TWN. The experimental values plotted with crosses agree with the theoretical

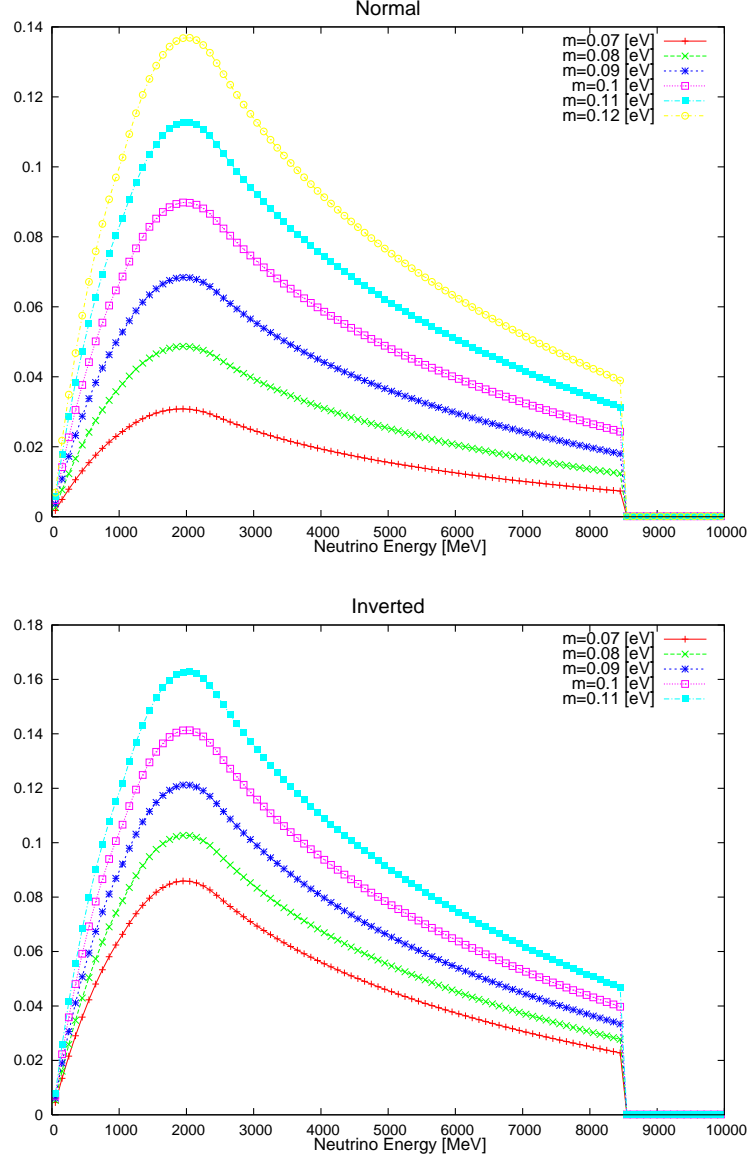


FIG. 19. Fraction of electron neutrino from a pion of 20 [GeV/c] in normal and inverted hierarchies at $L=100$ [m], distance=200 [m]. Pion's life time is included. The neutrino mass is 0.07(red-solid), 0.08(green cross), 0.09(purple cross), 0.10(pink-box), 0.11(bluebox), 0.12(yellow-cross) [eV/c²] [50].

values. The values from the flavor oscillations expected from the current parameters are also shown. The mass-squared differences and mixing angles from the recent ground experiments lead negligible values for both experiments. A sterile neutrino of the mass around 1 [eV/c²] is necessary to fit the data of LSND with the flavor oscillation. The agreements of the values from the neutrino diffraction in LSND and TWN suggest that it is unnecessary to introduce additional parameters.

In Fig. 17, the maximum possible fraction of the electron neutrino in a geometry of

T2K experiment is shown. The spreading of the pion beam is ignored in this Figure. Since the diffraction is sensitive to the pion beam spreading, the real value may become smaller than this figure. In lower energy region of the pion, the fraction becomes extremely small. Figure 18 shows electron neutrino spectra from the pion of life-time of this energy for the neutrino mass 0.08-0.12 of normal hierarchy and for the mass 0.07-0.11 of inverted hierarchy. The spectrum is sensitive to the absolute neutrino mass in this parameter regions. In lower energy region of the pion, the fraction becomes extremely small. Figure (19) shows the electron neutrino spectra including the pion's life-time at higher pion energy for the neutrino mass 0.08-0.12 [eV/c²] of normal hierarchy and for the mass 0.07-0.11 [eV/c²] of inverted hierarchy. The fraction becomes larger and the spectrum is sensitive to the absolute neutrino mass. Figure (20) shows the electron neutrino spectrum at lower energy.

1. *Electron(positron) enhancement*

The finite-size correction is small in the event that an electron or positron is detected if their wave packets are of nuclear sizes. That would become larger and non-negligible, if the wave packets for them of much larger than nuclear sizes are used. For a detector of having $\sigma_e \approx (10^{-8})^2$ [m²], the electron from a decay of pion has the finite size correction

$$\Gamma^{(d)} = \frac{m_\pi^2 \sigma_e}{4\pi} \left(1 - \frac{m_\mu^2}{m_\pi^2}\right)^2 \frac{E_\pi}{m_e^2 \Gamma} \Gamma, \quad (324)$$

in the high-energy region where the pion's life time is ignorable. In the energy region for the pion

$$\frac{E_\pi}{m_\pi c^2} > 10^5, \quad (325)$$

the life time is negligible at $c\Gamma \leq 4 \times 10^5$ [m], and $P^{(d)}$ gives a significant effect. An excess of positron from high energy positive pion would be observed.

D. Proton target anomaly

Magnitude of diffraction component depends upon the size of the nucleus which neutrino interacts with and is expressed by the wave packet size σ_ν . It becomes larger with the larger target. It is known and used in the text that nuclear size is proportional to $A^{\frac{2}{3}}$ and

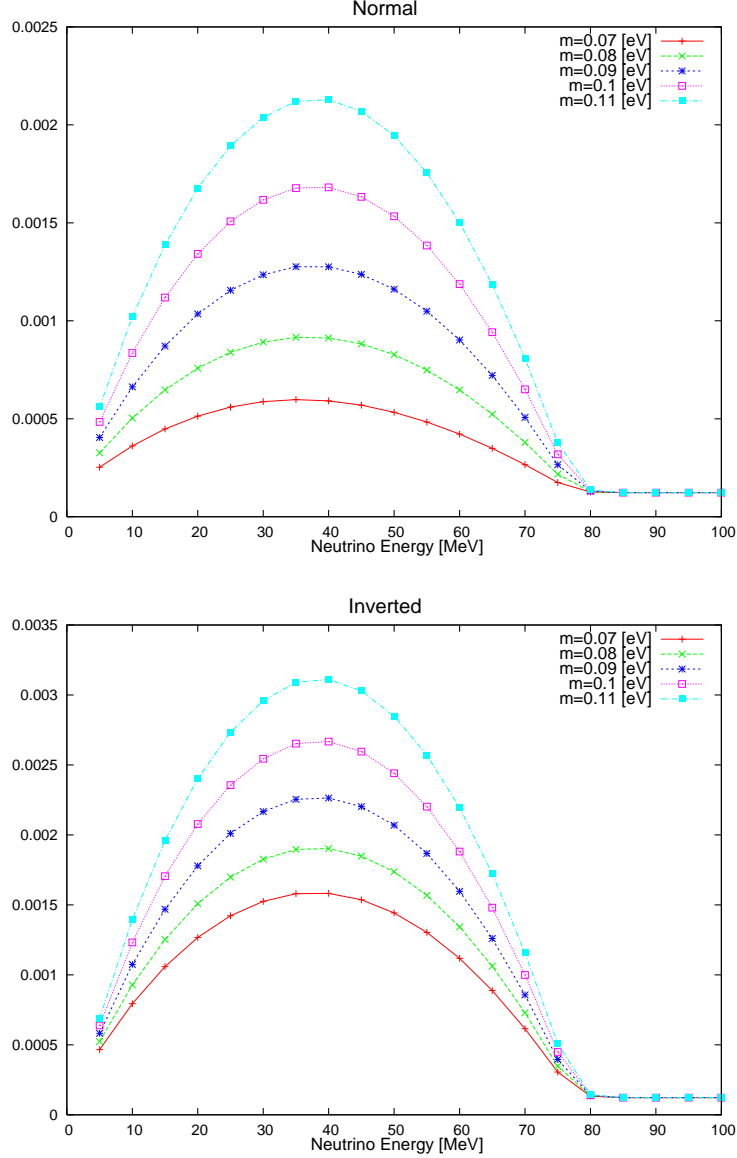


FIG. 20. Electron neutrino spectrum from a pion of 2 [GeV/c] in normal and inverted hierarchies at $L=110$ [m], distance=50 [m]. Pion's life time is included. The neutrino mass is 0.07(red-solid), 0.08(green cross), 0.09(purple cross), 0.10(pink-box), 0.11(bluebox), 0.12(yellow-cross) [eV/c²] [50].

the large A nuclear gives a large diffraction component, generally. Proton has a smallest intrinsic size. However a proton is expressed by a wave function of its position in matter. So the wave packet size is determined by a size of this wave function. Since a proton is the lightest nucleus, it has the largest size. We estimate this size using center of mass gravity effect between proton and electron. For the proton's mass m_p and the electron mass m_e , an

electron's coordinate $\vec{x}_{electron}$ and the proton coordinate \vec{x}_p are expressed as,

$$\vec{x}_{electron} = \vec{X} + \frac{m_p}{m_e + m_p} \vec{r} \approx \vec{X} + \left(1 + \frac{1}{2000}\right) \vec{r}, \quad (326)$$

$$\vec{x}_p = \vec{X} - \frac{m_e}{m_e + m_p} \vec{r} \approx \vec{X} - \frac{1}{2000} \vec{r}. \quad (327)$$

If the wave function of the atom is

$$\Psi(\vec{R})\varphi(\vec{r}), \quad (328)$$

and the function of the relative coordinate, $\varphi(\vec{r})$, is extended by an amount R_{atom} which is about 10^{-10} [m] then the proton is extended with a radius

$$R_p = \frac{1}{2000} R_{atom} \approx 5 \times 10^{-14} \text{ [m]}. \quad (329)$$

This value is much shorter than the atomic scale and is larger than one nucleon's size $1 \text{ [fm]} = 10^{-15} \text{ [m]}$ by factor 50. Thus proton in solid is extended to the size $\frac{1}{2000}$ of the atomic wave function, which is larger than the nuclear size of ^{16}O . Hence proton gives the important role in the neutrino diffraction. Its size may be in the range

$$l_{proton}(U) = 5 \times 10^{-14} - 10^{-13} \text{ [m]}. \quad (330)$$

An enhancement of diffraction contribution due to the proton is expected in

$$\bar{\nu} + p \rightarrow \mu^+ + \mathbf{X}, \quad \mathbf{X} = n, p\pi^-, n\pi^0 \text{ and others}. \quad (331)$$

E. Atmospheric neutrino

The neutrino flavor oscillation was found first with an atmospheric neutrino. Neutrinos are produced from decays of charged pions and muons in secondary cosmic rays. Since the matter density is low in atmosphere, these charged particles travel freely long distance. Thus neutrinos produced in decays of pions or muons show the diffraction phenomenon and the diffraction components are added to the neutrino fluxes. These neutrino events may be observed in detectors set in the ground, such as Super-KamiokaNDE(SK) if the absolute mass is a reasonable value. The minimum mass allowed from the mass-squared difference is about the value, $\sqrt{\delta m^2} \approx 10^{-2} \text{ [eV}/c^2]$. Then the length that the diffraction component is observed becomes $L_0 = \frac{2E_\nu c}{m_\nu^2} \approx 20 \text{ [km]}$ for $E_\nu = 1 \text{ [GeV]}$, which is longer than the height of troposphere. Hence the diffraction component could be observed with the angle-dependent

excess of the electron and muon neutrino fluxes. Since the diffraction components from pion decays are common to both neutrinos, their ratio is not sensitive to the diffraction. Instead of this ratio, a ratio of the neutrino flux to the flux of charged leptons is good to see the signal of the neutrino diffraction.

VIII. UNUSUAL PROPERTIES FROM $S[T]$

Unique properties of $S[T]$ expressed in Section 2, lead various unusual properties to observables.

A. Unitarity

Probability of the event that the neutrino is detected per unit time $P(L)$ decreases with the distance L . This behavior appears to suggest that the probability is not preserved and is inconsistent with the unitarity, if $S[\infty]$ is applied. However at T , the probability is derived from $S[T]$ that satisfies $S^\dagger[T]S[T] = 1$, Section 2.4, and is consistent with the unitarity. The probability at L is determined with S-matrix $S[T]$, $L = cT$ and has two components $P = P^{(0)} + P^{(d)}(L)$. Both terms are positive semi-definite and the latter is the finite-size correction that decrease with L . This behavior is a natural consequence of the wave nature of the states at finite T and is consistent with the unitarity. The unitarity leads that the life time of the pion becomes larger if the neutrino is detected at a finite T .

B. Lepton number non-conservation

The probability of the event that the neutrino is detected is different from that of the charged lepton even though they are produced in pair. They propagate with different velocities and different wave lengths along the light-cone. Consequently they have different retarded effects and are detected with different probabilities at finite T . The probabilities from $S[T]$ depend on boundary conditions, which differ in both cases, Eq. (79), and the two probabilities are different.

If the neutrino and charged lepton are observed simultaneously, they are expressed by $S[T]$ of one boundary condition, and the charged lepton shows the same behavior. Such an

experiment is not easy and has not been made.

The charged lepton has small finite-size corrections if the sizes of wave packets are almost the same. The sizes in detectors of ordinary experiments belong to this and the finite-size corrections are negligible, and the probability is computed with $S[\infty]$ using the plane waves. This situation has been studied well experimentally and agrees with the theoretical calculations obtained with $S[\infty]$.

Now the boundary conditions of the above two cases are different. One boundary condition leads unique probability and the different boundary conditions may lead different probabilities. The fact that those of the neutrino from $S[T]$ is different from those of the charged leptons from $S[\infty]$, is a natural consequence. It is meaningless to compare the probability for neutrino in the first case with that for the charged lepton in the second case, because they follow the different boundary conditions.

Decay probabilities computed at $T = \infty$ agree with the probability of the event that the decay products are detected at $T = \infty$. If the finite-size correction is finite in the neutrino and vanishes in the charged lepton, the probabilities of the events that they are detected become asymmetric, even though they are produced in pair. The fact that the probability for the neutrino at T is larger than that of the charged lepton does not mean the violation of the lepton number conservation. Because the neutrino propagates with almost the light speed, the probability of the event is enhanced in a similar manner as the retarded electric potential of a moving charged body.

C. Dependence on wave packet size

It is known that the total probability at $T = \infty$ does not depend on the wave packet size [42]. The result of the present paper Eq. (288) in fact shows that the asymptotic value, the first term in the right-hand side, is independent of the wave packet size. Now the finite-size correction, the second term in Eq. (288), is proportional to σ_ν . Since $S[T]$ is determined with the boundary condition Eqs. (32), (33), and (34) that depend on σ_ν , the finite-size correction depends on σ_ν . That increases with σ_ν and diverges at $\sigma_\nu = \infty$. The diverging correction at $\sigma_\nu = \infty$ is consistent, in fact, with the divergence of Eq. (31), and the fact that the total cross section diverges for the plane waves [45] obtained without the damping factor $e^{-\epsilon|t|}$. The latter divergence occurs because the denominator of the neutrino propagator

vanishes, which is connected with the boundary condition. The finite-size correction has the universal properties, despite of the σ_ν dependent behavior.

D. Non-conservation of kinetic energy

1. Violation of symmetries

$S[\text{T}]$ does not commute with the free Hamiltonian H_0 , and satisfies Eqs. (44) and (65). Particularly if the parent and decay products overlap, H_{int} has a finite expectation value and the kinetic energy is different from that of H . The kinetic energy is not conserved, despite the fact that the total energy is conserved. The transition probability from these states was computed analytically, and exhibits the diffraction in the finite-size correction.

The finite-size correction is not invariant under Lorentz transformation and the magnitude of the finite-size corrections depends on the systems.

2. Helicity suppression

Suppression of the branching ratio of electron mode over that of the muon mode is due to the helicity suppression, which is caused by conservation law of the kinetic energy and angular momentum. The helicity suppression hold in Γ of the decay of a pseudo-scalar particle to a neutrino and charged lepton caused by $V - A$ weak interaction. Now $S[\text{T}]$ violates the conservation law of the kinetic energy and the angular momentum. $P^{(d)}$ comes from the kinetic-energy non-conserving states, and is not suppressed in the electron mode. The finite-size corrections to the probabilities of the events that the electron neutrino are almost the same as those of the muon mode, and give the dominant contribution at small T . Thus when the neutrino is observed in suitable near-detector region, the electron neutrino is substantially enhanced.

3. Large finite-size correction

The finite-size correction vanishes with the use of $S[\infty]$ but becomes finite with $S[\text{T}]$. We study the amplitudes in tree level and identify the reason why $S[\text{T}]$ gives finite corrections.

$S[\infty]$ is Poincaré invariant and is expressed with Feynman diagrams in perturbative expansions. The energy and momentum of initial states are given and those of final and intermediate states are limited from exact conservation at each vertex. In $S[\infty]$, the states of infinite energies do not couple. The two point functions are short range and the light-cone singularity does not couple.

Now $S[T]$ is Poincaré non-invariant and final and intermediate states of unlimited kinetic energy and momentum can couple and produce the light-cone singularity. The light-cone singularity is the real function and extended to a large area and gives the universal finite-size correction to light particles. It is remarkable that the states of the ultraviolet region give the observable effect to the probability of the tree diagram.

The decay rate of the pion becomes different if the neutrino is detected in the region of the finite-size correction. The life time becomes shorter than the normal value. This phenomenon that the life time is modified by its interaction with matter is known in the literature as quantum Zeno effect. Neutrinos actually interact extremely weakly with matter, and a majority of neutrinos are passing freely without any interaction and are not affected by this effect. Consequently the majority of the pions are not affected by the finite-size effect and its life time is not modified and has the normal life time. Although the detected neutrino receives the large finite-size correction, its effect is negligibly small for observables of the pions.

E. Overlap of wave functions

The present diffraction of transition amplitude appears when the wave of parent overlap with the waves of daughters of varying kinetic energy. The neutrino is detected by the final states that are produced in the neutrino collision in the detector and its wave function is determined by the apparatus. Accordingly the diffraction pattern and the finite-size correction depend on the wave function that the neutrino interacts. This is a unique property of quantum physics. In classical physics, physical variables are observable and interference patterns do not depend on the apparatus.

The present phenomena appear always when the wave functions that retain the coherence overlap in wide area. Overlap of wave functions of various spatial sizes are presented in the following figures. The plane waves and small wave packet in particle decays are shown in

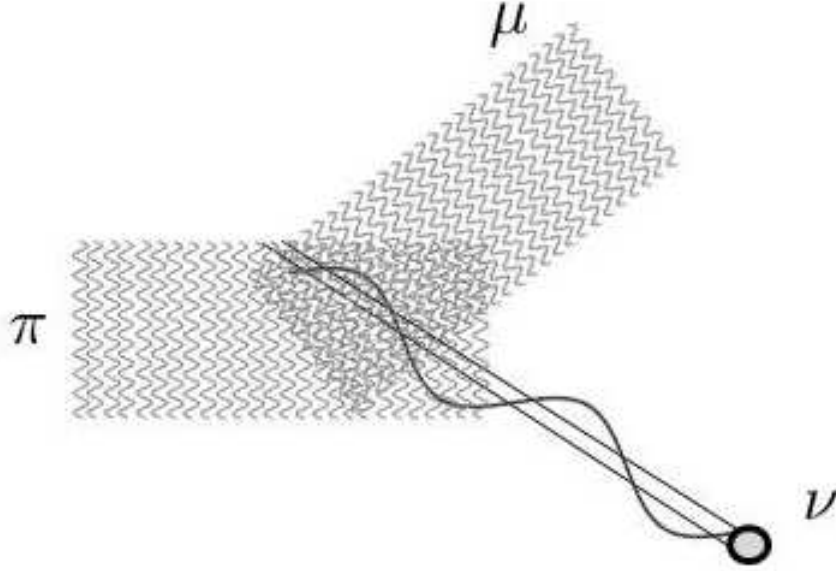


FIG. 21. Overlap of large waves of pion and muon and a small wave of a neutrino. They overlap in long area, and the rate is computed with $S[T]$ and has the large finite-size correction. The neutrino wave along the light-cone has a large wave length Eq. (332), and give the finite-size correction of macroscopic size.

Fig. (21). Short range fluctuations of the correlation functions overlap in the microscopic region and give the constant probabilities which agree with those at the asymptotic regions. Now the long range fluctuation expressed by the light-cone singularity in $S[T]$ extends to macroscopic area, and gives the long distance effects to light particles and gives the short distance effect to massive particle. The angular velocity ω along the light-cone is given as

$$\omega t = (E(\vec{p}) - c|\vec{p}|)t = \frac{m^2}{2|\vec{p}|}t, \quad (332)$$

and becomes extremely small for neutrino. Hence the probability decreases slowly as T_0/T , $T_0 = 2|\vec{p}|/m^2$. The light-cone singularity appears always in the many body correlation functions in tree levels, hence the finite-size corrections always appear in the tree levels. But the magnitude is inversely proportional to m^2 , and the corrections become significant only in light particles

Overlap of wave functions of other sizes are shown in Figs. (22) and (23), in configuration and momentum space. In Fig. (22) they overlap in small region and get contributions from

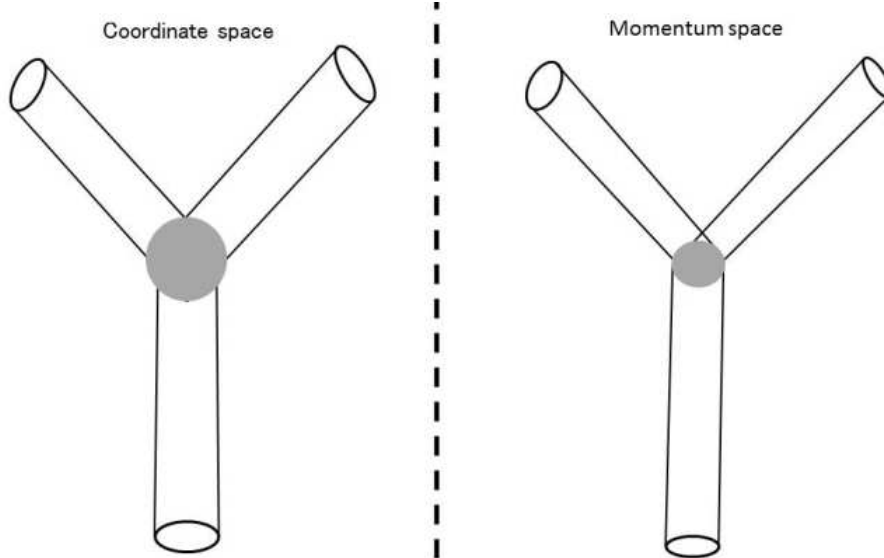


FIG. 22. Overlap of wave functions of finite sizes in momentum and coordinate. Wave functions overlap in small regions and the finite-size correction vanishes. $S[T]$ agrees with $S[\infty]$.

short-range fluctuations, and are studied with either $S[T]$ or $S[\infty]$ of the $e^{-\epsilon|t|}$ prescription. They give equivalent probabilities. In Fig. (23), the parent and daughters overlap in wide area in configuration space but they overlap in small region in momentum space. Accordingly the asymptotic values are treated with $S[\infty]$ with the damping factor $e^{-\epsilon|t|}$ or the value $\lim_{\sigma \rightarrow \infty} \left[\lim_{T \rightarrow \infty} P(T, \sigma) \right]$ obtained from the configuration of Fig. 22.

IX. SUMMARY AND IMPLICATIONS

The probability of the events that the final states are detected at T is computed with $S[T]$ that satisfies the boundary conditions at T . $S[T]$ was formulated and applied to the pion in nucleon collision and the neutrino in pion decay. The probability is modified from the asymptotic value ΓT and has the correction $P^{(d)}$. The correction violates the Poincaré symmetry of the Lagrangian and gives the large enhancement in the electron neutrino, which satisfies $\Gamma \approx 0$ by the helicity suppression. Due to $P^{(d)}$, the probability of the events for the neutrino is different from that for the charged particle. This deviation is caused by the mass difference between the neutrino and charged lepton, and by the large distance between the position of detection and that of production. The waves of light particle have the same

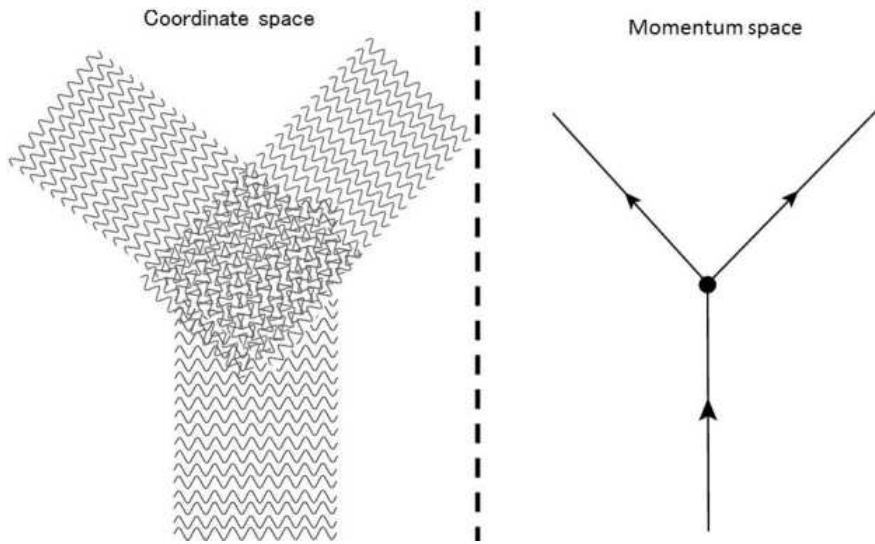


FIG. 23. Overlap of wave functions of large sizes in coordinate space becomes those of small sizes in momentum space. Wave functions overlap in small regions and $S[\infty]$ with the $i\epsilon$ prescription is applied.

velocity and cause the interference of waves to be constructive, but those of massive particle have varying velocity that depends on the momentum and cause the interference not to be constructive.

The probability amplitude at $T \leq \tau$ reveals the wave nature similar to but different from classical waves around a disorder or obstacle. The states in the overlapping region have non-constant kinetic energies, and show diffraction of waves. They modify the transition amplitude and probability and result in the finite-size corrections. The probability of the event that decay products are detected is decomposed to the normal term ΓT and the finite-size correction $P^{(d)}(\propto C_0(\sigma)\tilde{g}(T, \omega))$ that gives the $1/T$ correction. The correction has a universal form $\tilde{g}(T, \omega)$ of the magnitude proportional to $\frac{E_\nu}{m_\nu^2 T}$, which is extremely large and becomes observable with macroscopic experiments for a light particle.

$S[T]$ are formulated with wave packets. Γ does not depend on the wave packets but $P^{(d)}$ depends. Hence the wave packets can not be replaced with plane waves. Constructively added waves of the pion and lepton in the overlapping region form the light-cone singularity in the correlation function, and its overlap with the neutrino wave gives the large finite-size correction to the probability. $P^{(d)}$ appears in vacuum and is determined by the fundamental physical quantities of the Lagrangian. The origin, mechanism, characteristic features, and

implications are presented.

The modified rates in the pion decays were compared with previous neutrino experiments in Section 7. First, the slight energy dependence of the total νN cross sections at high-energy regions, which is hard to understand in the standard theory, was shown to agree with the excess of the effective neutrino flux due to the diffraction. The excesses of neutrino events will be observed in other reactions as well at macroscopic short distance regions. Theoretical calculations at distances of the order of a few hundred meters were computed and shown in Figures of Section 6. From these figures, the excesses are not large but are sizable magnitudes. Hence these excesses shall be observed in these distances. Actually fluxes measured in the near detectors of the long-baseline experiments of K2K [53] and MiniBooNE [54] may show excesses of about 10–20 percent of the Monte Carlo estimations. Monte Carlo estimations of the fluxes are obtained using naive decay probabilities and do not have the interference effects we presented in the present work. So the excesses of these experiments may be related with the excesses due to interferences. The excess is not clear in MINOS [55]. With more statistics, quantitative analysis might become possible to test the new universal term on the neutrino flux at the finite distance. If the mass is in the range from 0.1 [eV/ c^2] to 2 [eV/ c^2], the near detectors at T2K, MiniBooNE, MINOS and other experiments might be able to measure these signatures.

Second, the fraction of electron mode modified by $P^{(d)}$ was compared. Since the exact conservation law of kinetic-energy and momentum does not hold in the overlapping region, $P^{(d)}$ violates the helicity suppression. Thus the corrections preserve the universality of weak interaction, and are about the same for both modes. Consequently, the electron mode is enhanced drastically at a finite T. The theoretical value of the fraction of electron mode was compared with LSND and TWN, and agreements were obtained. Further confirmation of the diffraction component by observing the electron neutrino in pion decay will be made using modern version of LSND or similar experiments. T2K near detector is a possible place for that.

Third, anomalies in proton target and atmospheric neutrino were pointed out. They would supply also specific signature of the neutrino diffraction. The neutrino diffraction is sensitive to the absolute neutrino mass but is not so to other parameters such as pion and neutrino energies. Hence the observations of the neutrino diffraction is easy, and may give the absolute neutrino mass.

We summarize the reasons why the interference term of the long-distance behavior emerges in the neutrino but not in the charged lepton. The probability of the event that the decay product are detected at T, Eqs. (137) and (214), shows that their behaviors at large T are determined by the light-cone singularity of the correlation function $\Delta(\delta t, \delta \vec{x})$ and the wave function of detected particle. From relativistic invariance, the particle's momentum is unlimited and the singularity near $\lambda = c^2 \delta t^2 - \delta \vec{x}^2 = 0$, which is extended to large distance $|\delta \vec{x}| \rightarrow \infty$, emerges in $\Delta(\delta t, \delta \vec{x})$. The neutrino wave function along the light-cone region behaves as

$$\psi_\nu(\delta t, \delta \vec{x}) = \mathcal{F} \frac{e^{i(E_\nu \delta t - \vec{p}_\nu \cdot \delta \vec{x})}}{x} = \mathcal{F} \frac{e^{i \frac{m_\nu^2}{2E_\nu} \delta t}}{c \delta t}, \quad (333)$$

where \mathcal{F} has no dependence on the distance $|\vec{x}|$. Consequently the relation between the energy width δE and the time interval δt becomes

$$\delta t \delta \frac{m_\nu^2}{2E_\nu} = \delta t \delta E \times \frac{1}{2} \left(\frac{m_\nu}{E_\nu} \right)^2 \approx \hbar, \quad (334)$$

and

$$\delta t \delta E \approx 2 \left(\frac{E_\nu}{m_\nu} \right)^2 \hbar k. \quad (335)$$

The ratio $(E_\nu/m_\nu)^2$ is of order 10^{18} and δt becomes macroscopic even for the energy width δE of 100 [MeV]. Then $c \delta t$ becomes

$$c \delta t \approx 10^3 \text{ [m]}, \quad (336)$$

which is about the distance between the pion source and the near detector in fact. So the interference effect appears in this distance and is observable using the apparatus of much smaller size. Now the lepton wave function behaves in the same region as,

$$\psi_l(\delta t, \delta \vec{x}) = \mathcal{F} \frac{e^{i(E_l \delta t - \vec{p}_{l_e} \cdot \delta \vec{x})}}{x} = \mathcal{F} \frac{e^{i \frac{m_l^2}{2E_l} \delta t}}{c \delta t}, \quad (337)$$

where m_l is much larger than m_ν and $c \delta t$ is a microscopic size for charged leptons.

In time interval $T \leq l_0/c$, $P^{(d)}$ gives finite corrections, and the probability of the event that the neutrino is detected deviates from the probability of the event that the neutrino is produced. In another region $l_0/c \leq T, \tau_\pi$, the parent disappears and does not overlap with daughters. The decay products have the initial energy, and the neutrino behaves like a free isolated particle. The diffraction term vanishes and the probability of the event for

the detection is computable with $S[\infty]$ and agrees with the probability of the event for the production. At $T \gg \tau_\pi$, the corrections vanish, and the normal term remains. In this region, the flavor oscillations appear among the isolated neutrinos, and are detected at the position of much longer distance than those of the finite-size corrections. Thus both effects separate clearly, Fig. (16), and independent, and the flavor oscillation was not discussed in the present paper.

The amplitude and probability in the lowest order of interactions were studied, except some of the pion' life time, and effect of electroweak gauge theory was not included. They do not modify the long-distance effect of the paper that is due to the overlap of wave functions. The effects would appear to other light particles around overlapping regions, and give new insights to our understandings. We will study these problems and other large scale physical phenomena in subsequent papers.

ACKNOWLEDGEMENT

This work was partially supported by a Grant-in-Aid for Scientific Research (Grant No. 24340043). Authors thank Dr. Kobayashi, Dr. Nishikawa, Dr. Nakaya, and Dr. Maruyama for useful discussions on the near detector of T2K experiment, Dr. Asai, Dr. Kobayashi, Dr. Kawamoto, Dr. Komamiya, Dr. Minowa, Dr. Mori, and Dr. Yamada for useful discussions on interferences.

Appendix A: Wave packets sizes

A-I. Proton mean free path

We estimate the wave packet size of a proton first and those of a pion and a neutrino next, following a method of our previous works [5, 36].

A mean free path of a charged particle in matter is determined by its scattering rate with atoms by Coulomb interaction. An energy loss is also determined by the same cross section. Data on the energy loss are summarized well in particle data summary [22] and are used for the evaluation of the proton's mean free path.

The proton's energy loss rate at a momentum, 1 [GeV/c], for several metals such as Pb,

Fe, and others are

$$-\frac{dE}{dx} = 1 - 2 \text{ [MeVg}^{-1}\text{cm}^2], \quad (\text{A1})$$

hence we have the mean free path of the 1 [GeV/c] proton in the material of a density ρ ,

$$L_{\text{proton}} = \frac{E}{\frac{dE}{dx} \times \rho} = \frac{1 \text{ [GeV]}}{(1 - 2) \times 10 \text{ [MeV g}^{-1}\text{cm}^{-1}]} = 50 - 100 \text{ [cm]}. \quad (\text{A2})$$

At a lower energy of the order of 0.2 [GeV/c], the energy loss rate of the proton is about 10 [MeVg⁻¹cm²] and the mean free path is

$$L_{\text{proton}} = 10 \text{ [cm]}. \quad (\text{A3})$$

A wave which describes a proton maintains coherence in matter for a distance of the mean free path, hence this wave is approximately described by a wave packet that has a size of the mean free path. We use the mean free path for a wave packet size of the proton $\sqrt{\sigma}_{\text{proton}}$,

$$\sqrt{\sigma}_{\text{proton}} = L_{\text{proton}}. \quad (\text{A4})$$

When a proton of this size is emitted into the vacuum or to a dilute gas from matter, the wave keeps the same size. The proton that is moving freely has a constant size in vacuum or dilute gas. The size varies when the proton is accelerated. If the potential energy \mathcal{V} is added to the proton of momentum \vec{p}_{before} , then the final value of the momentum becomes \vec{p}_{after} and satisfies

$$\sqrt{\vec{p}_{\text{before}}^2 + m^2} + \mathcal{V} = \sqrt{\vec{p}_{\text{after}}^2 + m^2}. \quad (\text{A5})$$

From Eq. (A5) variants of the momentum satisfy

$$v_{\text{before}} \times |\delta\vec{p}_{\text{before}}| = v_{\text{after}} \times |\delta\vec{p}_{\text{after}}|, \quad (\text{A6})$$

$$v_{\text{before}} = \frac{|\vec{p}_{\text{before}}|}{\sqrt{\vec{p}_{\text{before}}^2 + m^2}}, \quad v_{\text{after}} = \frac{|\vec{p}_{\text{after}}|}{\sqrt{\vec{p}_{\text{after}}^2 + m^2}}. \quad (\text{A7})$$

Hence the size of a particle, $\sqrt{\sigma}_{\text{before}}$, which is proportional to the inverse of $|\delta\vec{p}_{\text{before}}|$, becomes $\sqrt{\sigma}_{\text{after}}$ after the acceleration from a velocity v_{before} to a velocity v_{after} . The wave packet size is determined by the velocity ratio,

$$\sqrt{\sigma}_{\text{after}} = \sqrt{\sigma}_{\text{before}} \times \frac{v_{\text{after}}}{v_{\text{before}}}. \quad (\text{A8})$$

The velocity is bounded by the light velocity c , and a velocity ratio from 1 [GeV/ c] to 10 [GeV/ c] is about 1.2 and that from 0.2 [GeV/ c] to 10 [GeV/ c] is about 5. Hence the proton of 10 [GeV/ c] regardless of the energy in matter has the mean free path

$$\sqrt{\sigma}_{\text{proton}} \approx 40 - 100 \text{ [cm]}, \quad (\text{A9})$$

in vacuum or dilute gas.

A-II. Pion wave packet

Wave packet size of pions which are produced by a proton collision with target nucleus is determined by the proton's initial size Eq. (A9) and a target size 10^{-15} [m], which is negligibly small. A pion is produced while the proton wave packet passes through the small target by the strong interaction, hence this pion has a size in temporal direction of the proton wave packet. Hence the size of pion wave packet, $\sqrt{\sigma}_{\text{pion}}$, is given from that of the proton, $\sqrt{\sigma}_{\text{proton}}$, in the form

$$\frac{\sqrt{\sigma}_{\text{proton}}}{v_{\text{proton}}} = \frac{\sqrt{\sigma}_{\text{pion}}}{v_{\text{pion}}}, \quad \sqrt{\sigma}_{\text{pion}} = \frac{v_{\text{pion}}}{v_{\text{proton}}} \sqrt{\sigma}_{\text{proton}} \approx \sqrt{\sigma}_{\text{proton}}. \quad (\text{A10})$$

In relativistic energy regions, particles have the light velocity. Consequently from Eq. (A9), pion's wave function of 1 [GeV/ c] or larger momentum has the size

$$\sqrt{\sigma}_{\text{pion}} \approx 40 - 100 \text{ [cm]}. \quad (\text{A11})$$

We use this value of Eq. (A11) as the size of the wave packet

$$\sqrt{\sigma}_{\pi} = \sqrt{\sigma}_{\text{pion}}. \quad (\text{A12})$$

In vacuum and dilute gas, pions of the size Eq. (A12) propagate freely. From Eqs. (A2), (A9) and (A11), the proton and pion have the sizes of the order of 50 – 100 [cm].

A-III. Neutrino on target: neutrino wave packet

A neutrino interacts with a nucleon or an electron in the detector which are constituent particles in bound atoms and are expressed with wave functions of finite sizes. So the neutrino wave function in the amplitude of event that the neutrino is detected has a size of nucleus or atom. The size of wave packet for the neutrino, therefore, is not determined with

a mean free path but with a size of the target in its detection process. They are either a size of a nucleons in a nucleus or that of an electron in an atom. Nucleus have sizes of the order of 10^{-15} [m] and electron's wave functions have sizes of the order of 10^{-11} [m]. So neutrino wave packet is either 10^{-11} [m] or 10^{-15} [m].

Interactions of muon neutrinos in detectors are

$$\nu_\mu + e^- \rightarrow e^- + \nu_\mu, \quad (A13)$$

$$\nu_\mu + e^- \rightarrow \mu^- + \nu_e, \quad (A14)$$

$$\nu_\mu + A \rightarrow \mu^- + (A + 1) + X, \quad (A15)$$

$$\nu_\mu + A \rightarrow \nu_\mu + A + X, \quad (A16)$$

hence the size of the neutrino wave packet $\sqrt{\sigma_\nu}$ in processes (A13) and (A14) is of the order of 10^{-11} , [m]

$$\sqrt{\sigma_\nu} = 10^{-11} \text{ [m]}, \quad (A17)$$

and the neutrino wave packet $\sqrt{\sigma_\nu}$ in processes (A15) and (A16) is of the order of 10^{-15} [m]

$$\sqrt{\sigma_\nu} = 10^{-15} \text{ [m]}. \quad (A18)$$

Interactions of electron neutrinos in detectors are

$$\nu_e + e^- \rightarrow e^- + \nu_e, \quad (A19)$$

$$\nu_e + A \rightarrow e^- + (A + 1) + X, \quad (A20)$$

$$\nu_e + A \rightarrow e + A + X. \quad (A21)$$

The neutrino wave packet $\sqrt{\sigma_\nu}$ in processes (A19) is of the order of 10^{-11} [m], Eq. (A17), and the neutrino wave packet $\sqrt{\sigma_\nu}$ in processes (A20) and (A21) is of the order of 10^{-15} [m], Eq. (A18). They are treated in the same way as the neutrino from the pion decay.

From Eqs. (A17) and (A18), the neutrino has the wave packet sizes of the order of 10^{-11} [m] or 10^{-15} [m].

For various nucleus the sizes are estimated from the nucleus size, $A^{2/3}/m_\pi^2$ as

$$\sigma_\nu = \begin{cases} 5.2/m_\pi^2; C, \\ 6.35/m_\pi^2; O, \\ 14.3/m_\pi^2; Fe, \\ 18.9/m_\pi^2; Pb. \end{cases} \quad (A22)$$

In the amplitude of the event that neutrinos is detected, the neutrino wave packet is determined by the size of nucleus in the detector. In this respect, the neutrino wave packet of the present work is different from some previous works of wave packets that are connected with flavor neutrino oscillations [38–45], where one particle properties of neutrino at productions are studied and the detection process was not considered.

A-IV. Charged particles on target: wave packets

Charged particles are detected from signals caused by their electromagnetic interactions with atoms in matter. The electromagnetic interactions are mediated by massless photons and the forces are long range and are much stronger than the weak interaction. Hence successive interactions with many atoms, which are correlated quantum mechanically each other, give signals. Thus the wave packet sizes of the charged particles would be much larger than the size of an atom. It would be reasonable to assume that the size is semi-microscopic, some number of the order of one times 10^{-10} [m]. This size might agree to those that have been considered before in textbooks [6–9]. Although these sizes are much larger than those of the neutrinos, their diffraction components are extremely small and negligible due to their large masses, and vanish at the macroscopic distance. Consequently the finite-size corrections may be negligible for charged particles. If a high-energy electron is detected with exceptionally large wave packet, an effect may appear.

-
- [1] H. Lehman, K. Symanzik, and W. Zimmermann, *Il Nuovo Cimento* (1955-1965). **1**, 205 (1955).
LSZ, text books on quantum fields theory [10, 11], and general arguments on scatterings [6–9] study the large wave packets which can be expressed without positions. In small wave packets used here, the positions are explicitly written.
 - [2] F. Low, *Phys. Rev.* **97**, 1392 (1955).
 - [3] K. Ishikawa and Y. Tobita, *Prog. Theor. Exp. Phys.* **2013**, 073B02 (2013).
 - [4] M. L. Goldberger and K. M. Watson, *Phys. Rev.* **136**, 1472 (1964).
 - [5] K. Ishikawa and T. Shimomura, *Prog. Theor. Phys.* **114**, 1201 (2005) [hep-ph/0508303].

- [6] M. L. Goldberger and K. M. Watson, *Collision Theory* (John Wiley & Sons, Inc. New York, 1965).
- [7] R. G. Newton, *Scattering Theory of Waves and Particles* (Springer-Verlag, New York, 1982).
- [8] J. R. Taylor, *Scattering Theory: The Quantum Theory of non-relativistic Collisions* (Dover Publications, New York, 2006).
- [9] T. Sasakawa, Prog. Theor. Phys. Suppl. **11**, 69 (1959).
- [10] See for instance, M. E. Peskin and D. V. Schroeder, *An Introduction to Quantum Field Theory*, Sect. 7.2, p. 222, Addison-Wesley Publishing Company, California, 1995; S. Weinberg, *The Quantum Theory of Fields I*, p. 109, Press Syndicate of the University of Cambridge, New York, 1996; M. Srednicki, *Quantum Field Theory*, p. 37, Cambridge University press, Cambridge, 2007.
- [11] See for instance, N. N. Bogolubov, et. al., *General Principles of Quantum Field Theory*, Kluwer Academic Publishers, Dordrecht (1990); R. Haag, *Local Quantum Physics*, Springer, Berlin (1992); H. Araki, *Mathematical Theory of Quantum Field*, Iwanami, Tokyo, 2002.
- [12] S. Sasaki, S. Oneda, and S. Ozaki, The Science Reports of the Tohoku University First series (Math., Phys., Chem., Astronomy) **XXXIII**, 77 (1949).
- [13] J. Steinberger, Phys. Rev. **76**, 1180,(1949).
- [14] M. Ruderman and R. Finkelstein, Phys. Rev. **76**, 1458 (1949).
- [15] H. L. Anderson, *et al.*, Phys. Rev. **119**, 2050 (1960).
- [16] J. Hosaka, *et al.*, Phys. Rev. **D74**, 032002 (2006) [arXiv:hep-ex/0604011].
- [17] S. Fukuda, *et al.*, Phys. Lett. **B539**, 179 (2002) [arXiv:hep-ex/0205075].
- [18] S. N. Ahmed, *et al.*, Phys. Rev. Lett. **92**, 181301 (2004) [arXiv:nucl-ex/0309004].
- [19] T. Araki, *et al.*, Phys. Rev. Lett. **94**, 081801 (2005) [arXiv:hep-ex/0406035].
- [20] E. A. Litvinovich, Phys. Atom. Nucl. **72**, 522 (2009); C. Arpesella, *et al.*, Phys. Rev. Lett. **101**, 091302 (2008) [arXiv:0805.3843].
- [21] E. Aliu, *et al.*, Phys. Rev. Lett. **94**, 081802 (2005) [arXiv:hep-ex/0411038].
- [22] J. Beringer, *et al.* [Particle Data Group], Phys. Rev. **D86**, 010001 (2012).
- [23] V. N. Aseev, *et al.*, Phys. Rev. **D84**, 112003 (2011) [arXiv:1108.5034[hep-ex]].
- [24] E. Komatsu, *et al.*, Astrophys. J. Suppl. **192**, 18 (2011) [arXiv:1001.4538[astro-ph.CO]].
- [25] J. D. Dollard, Commun. Math. Phys. **12**, 193 (1969).

- [26] M. Gell-Mann, *The Quark and the Jaguar: Adventures in the Simple and the Complex*, St. Martin's Griffin, London, 1995, ILL ed.
- [27] A. Tonomura, *et al.*, Ameri. J. Physics. **57** No2, 117 (1989).
- [28] S. Tomonaga, Prog. Theor. Phys., **1**, 27 (1946).
- [29] J. Schwinger, Phys. Rev. **74**, 1439 (1948).
- [30] L. I. Schiff, *Quantum Mechanics*, p. 197, McGRAW-HILL, New-York, 2003; L. D. Landau and E.M. Lifshitz, *Quantum Mechanics* p.157, Butterworth Heine Mann, New York, 2003.
- [31] P. A. M. Dirac, The Quantum Theory of the Emission and Absorption of Radiation. Pro. R. Soc. Lond. A 114, 243 (1927).
- [32] L. I. Schiff, *Quantum Mechanics*, p. 199, McGRAW-Hill Book COMPANY, Inc. New York, 1955.
- [33] R. Peierls, *Surprises in Theoretical Physics*, p. 121 (Princeton University Press, New Jersey, 1979)
- [34] C. Moller, DET DANSKE VID.SEL.MATH-PHY. XXIII, Nr.1,1
- [35] K. Wilson, in Proceedings of the Fifth International Symposium on Electron and Photon Interactions at High Energies, Ithaca, New York, 1971, p.115 (1971). See also N. N. Bogoliubov and D. V. Shirkov, *Introduction to the Theory of Quantized Fields* (John Wiley & Sons, Inc. New York, 1976).
- [36] K. Ishikawa and Y. Tobita, Prog. Theor. Phys. **122**, 1111 (2009) [arXiv:0906.3938[quant-ph]].
- [37] K. Ishikawa and Y. Tobita, [arXiv:0801.3124]; "Neutrino mass and mixing" in the 10th Inter. Symp. on "Origin of Matter and Evolution of Galaxies" AIP Conf. proc. 1016, 329 (2008).
- [38] B. Kayser, Phys. Rev. **D24**, 110 (1981); Nucl. Phys. **B19** (Proc. Suppl), 177 (1991).
- [39] C. Giunti, C. W. Kim, and U. W. Lee, Phys. Rev. **D44**, 3635 (1991).
- [40] S. Nussinov, Phys. Lett. **B63**, 201 (1976).
- [41] K. Kiers, S. Nussinov, and N. Weiss, Phys. Rev. **D53**, 537 (1996) [hep-ph/9506271].
- [42] L. Stodolsky, Phys. Rev. **D58**, 036006 (1998) [hep-ph/9802387].
- [43] H. J. Lipkin, Phys. Lett. **B642**, 366 (2006) [hep-ph/0505141].
- [44] E. K. Akhmedov, JHEP. **0709**, 116 (2007) [arXiv:0706.1216 [hep-ph]].
- [45] A. Asahara, K. Ishikawa, T. Shimomura, and T. Yabuki, Prog. Theor. Phys. **113**, 385 (2005) [hep-ph/0406141]; T. Yabuki and K. Ishikawa, Prog. Theor. Phys. **108**, 347 (2002).
- [46] P. Adamson, *et al.*, Phys. Rev. **D81**, 072002 (2010) [arXiv:0910.2201[hep-ex]].

- [47] Q. Wu, *et al.*, Phys. Lett. **B660**, 19 (2008) [arXiv:0711.1183 [hep-ex]].
- [48] A. A. Aguilar-Arevalo, *et al.*, Phys. Rev. **D81**, 092005 (2010) [arXiv:1002.2680[hep-ex]].
- [49] K. Abe *et al.*, Phys. Rev. Lett. **107**, 041801 (2001) [arXiv:1106.2822 [hep-ex]].
- [50] M. Antonello, *et al.*, arXiv:1203.3432 [physics].
- [51] C. Athanassopoulos, *et al.*, Phys. Rev. Lett. **75**, 2650 (1995) [nucl-ex/9504002]; **77**, 3082 (1996) [nucl-ex/9605003]; **81**, 1774 (1998) [nucl-ex/9709006].
- [52] G. Danby, *et al.*, Phys. Rev. Lett. **9**, 36 (1962).
- [53] M. H. Ahn, *et al.*, Phys. Rev. **D74**, 072003 (2006) [hep-ex/0606032].
- [54] A. A. Aguilar-Arevalo, *et al.*, Phys. Rev. **D79**, 072002 (2009) [arXiv:0806.1449 [hep-ex]].
- [55] P. Adamson, *et al.*, Phys. Rev. **D77**, 072002 (2008) [arXiv:0711.0769[hep-ex]].